U.PORTO
INSTITUTO DE CIÊNCIAS BIOMÉDICAS ABEL SALAZAR
UNIVERSIDADE DO PORTO

CHARACTERIZATION OF THE MECHANISM OF PROTEIN TRANSLOCATION ACROSS THE MAMMALIAN PEROXISOMAL MEMBRANE

MARTA CRISTINA OLIVEIRA DE FREITAS

Tese de Doutoramento em Ciências Biomédicas

MARTA CRISTINA OLIVEIRA DE FREITAS

CHARACTERIZATION OF THE MECHANISM OF PROTEIN TRANSLOCATION ACROSS THE MAMMALIAN PEROXISOMAL MEMBRANE

Tese de Candidatura ao grau de Doutor em Ciências Biomédicas, submetida ao Instituto de Ciências Biomédicas de Abel Salazar da Universidade do Porto.

Orientador – Prof. Doutor Jorge Eduardo da Silva Azevedo.

Categoria – Professor Catedrático

Afiliação – Instituto de Ciências Biomédicas Abel Salazar da Universidade do Porto.

Co-orientador – Doutora Maria Clara Pereira de Sá Miranda.

Categoria – Investigadora do Instituto de Biologia Molecular e Celular, Universidade do Porto.

Afiliação – Instituto de Biologia Molecular e Celular, Universidade do Porto.

Co-orientador – Doutora Andreia Filipa Ribeiro de Carvalho

Categoria – Investigadora do Instituto de Biologia Molecular e Celular, Universidade do Porto.

Afiliação – Instituto de Biologia Molecular e Celular, Universidade do Porto.

Aos meus pais…

TABLE OF CONTENTS

PRECEITOS LEGAIS

Nesta dissertação foram utilizados os resultados do trabalho publicado abaixo indicado. A autora desta dissertação declara que interveio na concepção e execução do trabalho experimental, na interpretação de resultados e na redacção dos resultados publicados, sob o nome de "**Freitas, M. O.**".

The published experimental results stated below were used in this thesis. The author of this thesis declares that she participated in the planning and execution of the experimental work, in the data interpretation, and in the preparation of the published results, under the name "**Freitas, M. O.**".

Freitas M. O., Francisco T., Rodrigues T. A., Alencastre I. S., Pinto M. P. , Grou C. P., Carvalho A. F., Fransen M., Sá-Miranda C., Azevedo J. E. (2011) PEX5 Protein Binds Monomeric Catalase Blocking Its Tetramerization And Releases It Upon Binding the N-terminal Domain of PEX14. *J Biol Chem.* 286(47):40509-19.

Este trabalho foi financiado pela Fundação para a Ciência e Tecnologia (FCT) através de uma bolsa de doutoramento (SFRH/BD/44285/2008), pelo programa PTDC/BIA-BCM/64771/2006, pelo Fundo Europeu de Desenvolvimento Regional (PTDC/BIA-BCM/118577/2010FCOMP-01-0124-FEDER-019731) e pelo European Union VI Framework program Grant LSHGCT-2004-512018, Peroxisomes in Health and Disease.

This work was supported by Fundação para a Ciência e Tecnologia through a PhD fellowship (SFRH/BD/44285/2008), by the PTDC/BIABCM/64771/2006 program, by the Fundo Europeu de Desenvolvimento Regional, Portugal (PTDC/BIA-BCM/118577/2010FCOMP-01-0124-FEDER-019731), and by the European Union VI Framework program Grant LSHG-CT-2004-512018, Peroxisomes in Health and Disease.

AGRADECIMENTOS/ACKNOWLEDGEMENTS

Gostaria de aproveitar para agradecer a quem esteve ao meu lado durante esta etapa.

Em primeiro lugar, agradeço ao Prof. Doutor Jorge Azevedo por tudo aquilo que me ensinou e pela sua orientação e disponibilidade. Este trabalho não seria possível sem a sua dedicação.

À Doutora Clara Sá Miranda agradeço pelo apoio e preocupação em proporcionar as melhores condições de trabalho possíveis.

À Doutora Andreia Carvalho pela sua co-orientação e apoio no laboratório.

Ao Doutor Marc Fransen, por toda a sua ajuda neste trabalho.

Agradeço à Fundação para a Ciência e Tecnologia (FCT), ao Fundo Europeu de Desenvolvimento Regional e ao European Union VI Framework program, Peroxisomes in Health and Disease pelo financiamento para este trabalho.

A todos os ex- e actuais membros do grupo OBF, com quem partilhei todos estes dias: à Inês, por todo o carinho e amizade; ao Tony, por me fazer pensar no futuro e destino do meu primeiro filho; ao Manel…ao Manelz, por fazer os comentários mais inesperados e cómicos num dia de trabalho; à Cláudia, por ser a melhor companheira de bancada que alguma vez terei, por todas as gargalhadas e por todas as tentativas de tomar conta do meu espaço. Aprendi muito convosco. Obrigada!

Agradeço também aos membros da UNILIPE, os vizinhos mais porreiros que a malta podia ter: Fátima, Ana Filipa, Rui, Daniel, Andrea e Lorena.

À Cátia, agradeço por comer tão lentamente que nos alarga sempre a hora de almoço.

Ao Paulo, agradeço as gargalhadas e cantorias pelo corredor…até mesmo os valentes sustos quando aparece sorrateiramente na sala de estudo.

À Sofia Guimarães, agradeço pela sua presença constante. Por me aturar desde o meu primeiro dia no IBMC e, mesmo estando na outra ponta do corredor, nunca deixou de estar presente na minha vida. Uma amizade para a vida. Obrigada por me ouvires, por todos os sorrisos e preocupações.

À Tânia e à Marisa…as minhas meninas!!! Obrigada por todos os momentos que passamos juntas, por todas as parvoíces e momentos mais sérios, pela vossa amizade. Sei que posso contar sempre convosco e que, sem dúvida, ter-vos conhecido foi dos maiores benefícios que estes anos me trouxeram.

Ao Nuno…sem palavras!!! Obrigada por seres o meu "mano" mais velho, por estares sempre do meu lado e vibrares comigo nos momentos bons e menos bons. A tua preocupação e apoio constantes foram muito importantes neste percurso.

Por fim, resta-me agradecer às duas pessoas mais importantes da minha vida…os meus pais. Obrigada pelos sorrisos a cada resultado, a cada conquista. Obrigada por estarem sempre do meu lado e por me apoiarem em tudo. Espero que sintam orgulho em mim e neste trabalho…o vosso apoio e contribuição foram muito importantes para toda esta etapa.

ABSTRACT / RESUMO

ABSTRACT

PEX5 interacts with *de novo* synthesized cargo-proteins in the cytosol, transports them to the peroxisomal membrane, and after release of the cargo into the matrix of the organelle is recycled back to the cytosol. The mechanism behind the interaction of PEX5 with cargoes remains poorly understood. Considering that matrix proteins are synthesized in the cytosol in the presence of PEX5, we asked whether or not PEX5 binds the monomeric forms of these proteins. We provide data on the interaction of PEX5 with catalase, a homotetrameric enzyme in its native state. PEX5 interacts with monomeric catalase inhibiting its tetramerization, a feature that requires both the N- and C-terminal halves of PEX5. Interestingly, the PEX5-catalase interaction is disrupted by the N-terminal domain of PEX14, a component of the docking/translocation machinery. One or two of the seven PEX14-binding diaromatic motifs present in the N-terminal half of PEX5 are probably involved in this phenomenon. These observations were extended to two other major matrix proteins, acyl-CoA oxidase 1 and urate oxidase, showing that the interaction with PEX5 also inhibits their oligomerization. Furthermore, we found that the monomeric version of these proteins is more efficiently imported into the organelle matrix. Taken together, these results strongly suggest that PEX5 sequesters the newly synthesized peroxisomal proteins *en route* to the organelle, resembling a chaperone. We propose that this binding mode prevents premature oligomerization/non-specific interactions of cargo proteins, leading to a more efficient peroxisomal import.

RESUMO

As proteínas da matriz peroxissomal são sintetizadas no citosol, onde posteriormente interactuam com o receptor PEX5. A PEX5 transporta estas proteínas para a membrana do organelo e, após libertação das mesmas para a matriz, é reciclada de volta ao citosol. O mecanismo de interacção do receptor PEX5 com as proteínas da matriz peroxissomal permanece por esclarecer. Tendo em consideração que as proteínas matriciais são sintetizadas no citosol na presença da PEX5, é lícito questionar se o receptor interactua ou não com a forma monomérica destas mesmas proteínas. Neste estudo fornecemos dados sobre a interacção da PEX5 com a catalase, uma enzima homotetramérica no seu estado nativo. A PEX5 interage com a catalase monomérica, inibindo a sua tetramerização, uma característica que requer ambos os domínios N- e C-terminais da PEX5. Na presença do domínio N-terminal da PEX14, um componente da maquinaria peroxissomal de docking/translocação, a PEX5 dissocia-se da catalase. Dos sete domínios de interacção com a PEX14 presentes no N-terminal da PEX5, apenas um ou dois parecem estar envolvidos neste evento. Estes resultados foram confirmados com duas outras proteínas abundantes da matriz peroxisomal, a acil-CoA oxidase 1 e a urato oxidase, mostrando que a PEX5 também inibe a sua oligomerização. Os nossos resultados mostram que a versão monomérica destas proteínas é mais eficientemente importada para a matriz do organelo. Em conjunto, estes resultados sugerem que a PEX5 sequestra as proteínas da matriz peroxissomal após a sua síntese, apresentando características de uma chaperone. Propomos que esta ligação previne a oligomerização e interacções não específicas prematuras das proteínas matriciais, levando a um importe peroxissomal mais eficiente.

ABBREVIATIONS

AAA	ATPases associated with diverse cellular activities
AOX	Acyl-CoA oxidase 1
At	*Arabidopsis thaliana*
ATP	Adenosine triphosphate
BSA	Bovine serum albumin
Cat	Catalase
cDNA	Complementar deoxyribonucleic acid
Ce	*Caenorhabditis elegans*
CG	Complementation group
CP	Cargo Protein
CoA	Coenzyme A
Cyt c	Cytochrome c
Cys11	Cysteine residue at position 11 of mammalian PEX5
DHAP	Dihydroxyacetone phosphate
Dr	*Danio rerio*
DTM	Docking/translocation machinery
DTT	Dithiothreitol
DUB	Deubiquitinating enzyme
E. coli	*Escherichia coli*
EDTA	Ethylenediaminetetraacetic acid
ER	Endoplasmic reticulum
E1	Ubiquitin-activating enzyme
E2	Ubiquitin-conjugating enzyme
E-64	N-(*trans*-epoxysuccinyl)-L-leucine 4-guanidinobutylamide
Fw	Forward Primer
GSH	Glutathione
HA	Hemaglutinin
Hb	Hemoglobin
Hs	*Homo sapiens*
IAA	Iodoacetamide
IgG	Immunoglobulin
IRD	Infantile Refsum disease
Kd	Dissociation constant
Ks	Rate of total peroxisomal matrix protein synthesis
LBP	L-bifunctional protein
MOPS	4-morpholinepropanesulfonic acid

mPTS	Membrane peroxisomal targeting sequence
MS	Mass spectrometry
NALD	Neonatal adrenoleukodystrophy
OA	Ovalbumin
ORF	Open Reading Frame
PAGE	Polyacrylamide gel electrophoresis
PBD	Peroxisomal biogenesis disorders
PCR	Polimerase Chain Reaction
PerCat	Peroxisomal Catalase
PEX	Peroxin
PIM	Peroxisomal import machinery
PK	Proteinase K
PMP	Peroxisomal membrane protein
PMSF	Phenylmethylsulfonyl fluoride
PNS	Postnuclear supernatant
PTS1	Peroxisomal targeting sequence type 1
PTS2	Peroxisomal targeting sequence type 2
RCDP1	Rhizomelic chondrodysplasia punctata type 1
REM	Receptor Export Module
RING	Really interesting new gene
Rv	Reverse Primer
S. cerevisiae	*Saccharomyces cerevisae*
SCP2	Sterol carrier protein 2
SDS	Sodium dodecylsulfate
SEC	Size-Exclusion Chromatography
SEM	Buffer containing sucrose, EDTA and MOPS
SH3	Src homology 3 domain
STI	Soybean trypsin inhibitor
$t_{1/2}$	Half-time
TCA	Trichloroacetic acid
TPR	Tetratricopeptide repeat
Tris	Tris(hidroximetil)aminomethane
Ub	Ubiquitin
Ub-PEX5	Monoubiquitinated PEX5 species
UOX	Urate oxidase
WD	Tryptophan-aspartate repeat
X-ALD	X-linked adrenoleukodistrophy
ZS	Zellweger syndrome

I. INTRODUCTION

1. Peroxisome Structure and Function

Peroxisomes are multifunctional organelles of eukaryotic cells. These structures were first described by Rhodin as microbodies [1], but in 1966 de Duve and Baudhuin discovered that they contained H_2O_2-producing oxidases and catalase, naming them peroxisomes [2]. Peroxisomes are ubiquitous and essential organelles delimited by a single membrane and, unlike mitochondria and chloroplasts, do not contain endogenous DNA [3-5], (Figure 1). This organelle may appear as elongated, tubular and reticular structures [3, 6-8]. One important feature of peroxisomes is their metabolic plasticity. Indeed, their number, morphology and function can vary widely depending on the organism, cell- or tissue-type and environmental conditions [3, 4, 9, 10].

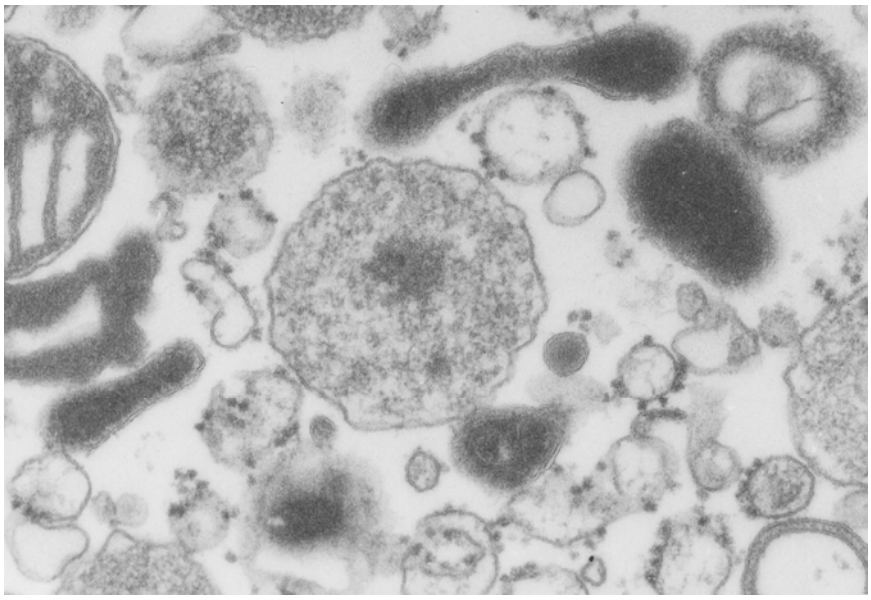

Figure 1: Peroxisomes. Electron micrograph of an organelle pellet from a rat liver post-nuclear supernatant, kindly taken by Prof. Dr. Manuel Teixeira da Silva (IBMC). P, peroxisome; the arrow indicates the urate oxidase paracrystalline structure; scale bar = 1μM.

Peroxisomes carry out several metabolic functions, being hydrogen peroxide metabolism [2, 11] and β-oxidation of fatty acids (long chain and very long chain) the main ones [12-14]. In animal cells they are also involved in several anabolic processes such as biosynthesis of plasmalogens and bile acids, catabolism of purines, polyamines and prostaglandins, α-oxidation of long chain and very long chain fatty acids and in the metabolism of some amino acids and glyoxylate [4, 15-21].

The functional diversity of peroxisomes is so extensive that in some organisms they are known by different names. For example, glyoxysomes are plant peroxisome-

like organelles containing enzymes responsible for the glyoxylate cycle [22-25]; glycosomes in trypanosomatids possess most of the enzymes of the glycolytic pathway [26-28]; and in filamentous ascomycete fungi (*e.g. Neurospora crassa*), the Woronin bodies are specialized peroxisomes that function to seal the septal pores in response to cellular damage [29].

2. Peroxisomal Disorders

Since peroxisomes are involved in numerous metabolic processes, it is not surprising that these organelles have an important and crucial role in human physiology. In fact, a number of distinct genetic diseases are associated with this organelle and are denominated peroxisomal disorders. These disorders have devastating consequences and are caused by the malfunction or even the absence of the peroxisome. Peroxisomal disorders are frequently divided into two groups: the single peroxisomal enzyme deficiencies and the peroxisomal biogenesis disorders [30-34].

The single peroxisomal enzyme deficiencies are characterized by defects in a single peroxisomal enzyme/transporter, affecting a specific metabolic pathway such as ether-phospholipid synthesis, α- or β-oxidation of fatty acids or glyoxylate detoxification (Table 1) (reviewed in [33]).

Table 1 – List of Single Peroxisomal Enzyme Deficiencies*.

Disorder	Deficient enzyme	Metabolic pathway affected
X-ALD	Adrenoleukodystrophy protein	Fatty acid β-oxidation
Acyl-CoA oxidase deficiency	Acyl-CoA oxidase 1	Fatty acid β-oxidation
D-bifunctional protein deficiency	D-bifunctional protein	Fatty acid β-oxidation
2-Methylacyl-CoA racemase deficiency	2-Methylacyl-CoA racemase	Fatty acid β-oxidation
Sterol carrier protein X deficiency	Sterol carrier protein X	Fatty acid β-oxidation
RCDP type 3	DHAP acyltransferase	Fatty acid β-oxidation
RCDP type 2	Alkyl-DHAP synthase	Ether-phospholipids synthesis
Refsum disease	Phytanoyl-CoA hydroxylase	Fatty acid α-oxidation
Hyperoxaluria type 1	Alanine:glyoxylate aminotransferase	Glyoxylate detoxification
Acatalasaemia	Catalase	H_2O_2 metabolism

* Adapted from [33]. X-ALD, X-linked adrenoleukodystrophy; RCDP, rhizomelic chondrodysplasia punctata; CoA, coenzyme A; DHAP, dihydroxyacetone phosphate.

Peroxisomal Biogenesis Disorders (PBDs) are characterized by mutations in one of the many genes involved in proper peroxisome biogenesis, either in the membrane biogenesis, the matrix protein import pathway or division and proliferation [35, 36]. PBDs reflect a series of abnormalities due to the low number and size of peroxisomes or even the absence of normal organelles [10]. In cells of many PBD patients it is often possible to detect the so-called peroxisome "ghosts" [37]. These structures represent organelles with a normal repertoire of membrane proteins but possessing little or no matrix content [37]. Presently, the *PEX* genes responsible for PBDs are all known (Table 2). The association between the 13 genes and these disorders was possible due to cell fusion experiments using primary cultures of fibroblasts from PBD patients and also complementation analysis by transfection of fibroblasts with plasmids encoding different PEX proteins to restore peroxisome assembly [38-40].

Table 2 – *PEX* gene affected and clinical phenotypes*.

Gene	Clinical phenotypes
PEX1	ZS, NALD, IRD
PEX2	ZS, IRD
PEX3	ZS
PEX5	ZS, NALD
PEX6	ZS, NALD, IRD
PEX7	RCDP type 1
PEX10	ZS, NALD
PEX11β	Mild ZS
PEX12	ZS, NALD, IRD
PEX13	ZS, NALD
PEX14	ZS
PEX16	ZS
PEX19	ZS
PEX26	ZS, NALD, IRD

* Adapted from [40]. ZS, Zellweger syndrome; NALD, neonatal adrenoleukodystrophy; IRD, infantile Refsum disease; RCDP, rhizomelic chondrodysplasia punctata.

The PBDs group includes disorders of the Zellweger spectrum and Rhizomelic Chondrodysplasia Punctata (RCDP) type 1 [32, 34]. The Zellweger spectrum includes the Zellweger syndrome (ZS), the neonatal adrenoleukodystrophy (NALD) and infantile Refsum disease (IRD), and these disorders have some overlapping symptoms such as liver disease, retinopathy and variable neurodevelopmental delay. One major difference between the three conditions regards the survival and phenotype severity of patients. The ZS is the most severe, with patients rarely surviving the first year, and

IRD is the milder one, with patients living over 30 years [30, 32]. In RCDP type 1 only some metabolic functions are lost, differing from the Zellweger spectrum in its biochemical and molecular basis and clinical presentation. In fact, this disease is characterized by mutations in only one gene that encodes PEX7, whereas the Zellweger spectrum is caused by mutations in any of the remaining *PEX* genes [32, 41].

3. Peroxisome Biogenesis

As refered earlier, peroxisomes have no DNA and therefore peroxisomal proteins are encoded by nuclear DNA, synthesized on cytosolic ribosomes and post-translationally targeted to the organelle [3, 42-44].

Identification of *PEX* genes started with studies in *Saccharomyces cerevisiae* and were applied to a variety of organisms such as *Pichia pastoris*, *Hansenula polymorpha* and *Yarrowia lipolytica* [45-50]. These studies allowed the identification of the majority of known peroxisome biogenesis-associated genes. The mammalian homologs were then identified by homology probing approaches [51]. Over 30 peroxins have been identified among several organisms [52, 53], but only sixteen were reported in mammals (Table 3) [54]. Most of these proteins are conserved between species but depending on the organism some specific roles were embraced by a single peroxin [53, 54].

Peroxisomal biogenesis is generally divided into three processes: peroxisome membrane biogenesis, import of matrix proteins into the organelle and peroxisome proliferation. A brief description of each of these processes is provided below.

3.1 Peroxisomal Membrane Biogenesis

The origin of the peroxisomal membrane is a subject of some controversy in the field [55, 56]. Several studies support a model in which peroxisomes are regarded as autonomous organelles deriving from pre-existing ones by growth and division [57-59]. The phospholipid requirements are fulfilled by the endoplasmic reticulum (ER) [55]. However, some authors claim that the ER is involved in the *de novo* formation and maintenance of peroxisomes, producing vesicles (protoperoxisomes) that eventually mature into peroxisomes or fuse with pre-existing organelles [57].

Targeting of newly synthesized peroxisomal intrinsic membrane proteins (PMPs) to the organelle requires signals, designated membrane peroxisomal targeting signals (mPTS), which are characterized by a cluster of basic aminoacids and a

transmembrane domain anchoring the protein to the peroxisomal membrane [60, 61]. These signals are quite different from the ones in proteins to be imported into the matrix of the organelle (see section 3.3).

Table 3 – Proteins implicated in peroxisomal biogenesis (peroxins).

Peroxin	Organisms	Localization	Domains	Proposed function
PEX1	M, P, F, Y	membrane (cytosol)	AAA ATPase	Matrix protein import, export of PEX5
PEX2	M, P, F, Y	membrane	Zinc RING finger	Matrix protein import
PEX3	M, P, F, Y	membrane		Membrane biogenesis, PMP import
PEX4	P, F, Y	membrane (cytosol)	E2 Ubiquitin-conjugating enzyme	Matrix protein import, ubiquitination of PEX5
PEX5[a]	M, P, F, Y	cytosol/membrane	Natively unfolded domain, TPRs	Matrix protein import, PTS1 (and PTS2 in M, P) receptor
PEX6	M, P, F, Y	membrane (cytosol)	AAA ATPase	Matrix protein import, export of PEX5
PEX7	M, P, F, Y	cytosol/membrane	WD repeats	Matrix protein import, PTS2 receptor
PEX8	F, Y	membrane (matrix)		Matrix protein import
PEX9	Yl	(ORF misidentified,	antisense sequence of	PEX26)
PEX10	M, P, F, Y	membrane	Zinc RING finger	Matrix protein import
PEX11[b]	M, P, F, Y	membrane		Division and proliferation
PEX12	M, P, F, Y	membrane	Zinc RING finger	Matrix protein import
PEX13	M, P, F, Y	membrane	SH3	Matrix protein import
PEX14	M, P, F, Y	membrane	Coiled-coil	Matrix protein import
PEX15	Sc	membrane		Matrix protein import, PEX1/PEX6 anchor
PEX16	M, P, F, Yl	membrane		Membrane biogenesis
PEX17	Y	membrane	Coiled-coil	Matrix protein import
PEX18	Sc	cytosol/membrane		Matrix protein import, PTS2 import
PEX19	M, P, F, Y	cytosol/membrane	Farnesylation motif	Membrane biogenesis, PMP import
PEX20	F, Y	cytosol/membrane		Matrix protein import, PTS2 import
PEX21	Sc	cytosol/membrane		Matrix protein import, PTS2 import
PEX22	P, F, Y	membrane		Matrix protein import, PEX4 anchor
PEX23	F, Y	membrane	Dysferlin	Proliferation
PEX24	F, Y	membrane		Proliferation
PEX25	Y	membrane		Proliferation
PEX26	M, F, Y[c]	membrane		Matrix protein import, PEX1/PEX6 anchor
PEX27	Sc	membrane		Proliferation
PEX28	Sc	membrane		Proliferation (PEX24 ortholog)
PEX29	Y	membrane		Proliferation
PEX30	Sc	membrane	Dysferlin	Proliferation (PEX23 ortholog)
PEX31	Sc	membrane	Dysferlin	Proliferation
PEX32	Y	membrane	Dysferlin	Proliferation

M, mammals; P, plants; F, filamentous fungi, Y, yeasts, Yl, *Yarrowia lipolytica* only; Sc, *Saccharomyces cerevisiae* only; [a]Mammals contain two main isoforms, PEX5S and PEX5L, the later harbouring a PEX7-binding site; [b]Mammalian cells contain three *PEX11* genes encoding PEX11α, PEX11β and PEX11γ; [c]PEX26 is absent in Sc and related yeasts. PEX1, PEX4 and PEX6 are peripheral membrane proteins facing the cytosol. PEX8 is a peripheral membrane protein facing the peroxisomal matrix. Colour coding is according to the involvement of peroxins in peroxisomal biogenesis pathways, *i.e.*, membrane assembly (**violet**), import of matrix proteins (**blue**) and growth and division (**green**). AAA ATPase, ATPase associated with several cellular activities; RING, Really interesting new gene; WD, Tryptophan-aspartate motif; TPRs, tetratricopeptide repeats; SH3, Src-homology 3 domain; ORF, open reading frame.

Membrane biogenesis in mammals and other organisms requires three peroxins: the intrinsic membrane proteins, PEX3 and PEX16, and a cytosolic/membrane protein, PEX19 [62, 63]. Most PMPs interact with their receptor PEX19 in the cytosol during or right after their translation, guaranteeing an import-competent status. Therefore, PEX19 acts as a chaperone for membrane proteins probably by protecting their hydrophobic domains [64-69]. PEX3 is the docking protein at the peroxisomal membrane for the PEX19-PMP complexes [70-72] and may also promote the insertion of PMPs into the peroxisomal membrane [73]. As for PEX16, its role remains poorly understood [63] but some authors state that PEX16 promotes the peroxisomal growth from the ER [74, 75].

3.2 Peroxisome proliferation

Peroxisomes are organelles characterized by their metabolic plasticity, being able to adjust to different physiological requirements [76, 77]. In mammals, the PEX11 family is involved in peroxisome proliferation and comprises three proteins: PEX11α, PEX11β and PEX11γ [7, 78, 79]. Loss of these proteins will lead to a reduction in peroxisomal number and presence of large peroxisomes [40, 80].

Peroxisome proliferation involves growth, elongation and a final step of division (reviewed in [81]). PEX11 is responsible for peroxisome elongation while the final membrane fission is performed by a dynamin-like protein (DLP1) [57, 58]. DLP1 anchors at the peroxisomal membrane through Fis1, a C-tail anchored protein [82]. These last two proteins, required for peroxisome proliferation, are also involved in mitochondria division [83].

3.3 Peroxisome matrix protein import

Peroxisomal matrix is the place of higher protein concentration in eukaryotic cells [84]. More than 50 different enzymes can be found in the matrix of the organelle [3, 21]. Similarly to the membrane biogenesis, the matrix protein import involves targeting sequences, cytosolic receptors and a membrane machinery to promote the internalization of these proteins.

Regarding the targeting signals, peroxisomal matrix proteins are sorted via one of two pathways. The majority of proteins present a Peroxisomal Targeting Signal type 1 (PTS1), a C-terminal tripeptide with the consensus sequence (S/A/C) – (K/R/H) –

(L/M) [85-87]. However, residues upstream from the PTS1 signal can also influence the interaction between the receptor and the cargo protein [87, 88]. PEX5 is the receptor for PTS1-containing proteins and the PTS1 recognition site is at its C-terminal half [89-92]. The second PTS signal (PTS2) is a N-terminal degenerate nonapeptide consisting of the consensus sequence (R/K) – (L/V/I) – $(X)_5$ – (H/Q) – (L/A). Only a small number of proteins possess a PTS2 signal and after internalization it is cleaved from the matrix protein [93-95]. PEX7 is the receptor for these PTS2 proteins [96, 97] but accessory proteins are needed to assist the delivery of these cargoes to the peroxisome [93, 98]. These proteins are species-specific: PEX18/PEX21 in *S. cerevisiae* [99] and PEX20 in the majority of yeast and fungi [100, 101]. In mammals and plants, PEX7 uses PEX5 itself for the targeting of PTS2-proteins to the peroxisome [102-104].

3.3.1 – PEX5

PEX5 was initially identified in *P. pastoris* and subsequently found in all peroxisome-containing organisms (revised in [4]). In mammals, two isoforms are found due to alternative splicing of the *PEX5* transcript: a large isoform, PEX5L, and a small one, PEX5S. PEX5L comprises 639 amino acids while the smaller isoform lacks an internal sequence of 37 amino acids, encoded by exon 8 [91, 105, 106]. This small region comprises the domain that interacts with PEX7, the PTS2 receptor, but this interaction is only observed in plants and mammals [102-105, 107, 108].

PEX5 can be divided in two distinct domains based on structural/functional data: the N-terminal and the C-terminal halves (Figure 2). A highly conserved C-terminal domain can be found when aligning PEX5 sequences, while the N-terminal half reveals low conservation between several organisms (Figure 3).

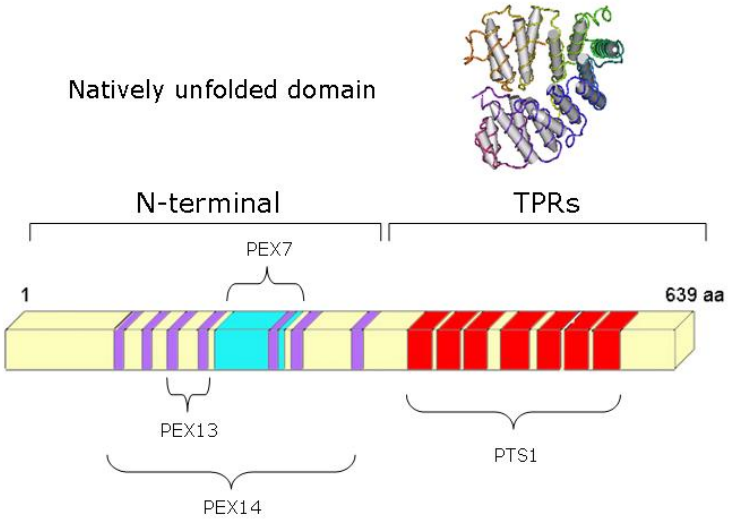

Figure 2: PEX5. Schematic presentation of the domain structure of human PEX5L and interaction sites for known components of the peroxisomal import machinery. The purple bars indicate the diaromatic motifs (WxxxF/Y PEX14 binding sites). The blue area indicates the extra 37 aminoacid encoded by exon 8 which contains the PEX7 binding site and is absent in the small isoform of PEX5. The red boxes represent the TPR domains. TPR, tetratricopeptide repeats.

The N-terminal half of PEX5 is a natively unfolded domain [109]. PEX5, being a monomeric protein, displays a flexible N-terminal half, being characterized by an unusually large Stokes radius and a small sedimentation coefficient [110]. Natively unfolded proteins/domains are frequently involved in protein-protein interactions with multiple partners [111]. Indeed, the N-terminal domain of PEX5 is characterized by the existence of several domains of interaction with other peroxins. Seven pentapeptide diaromatic motifs WXXXF/Y are present in this PEX5 domain and are responsible for the interaction with PEX14 and PEX13, two members of the Docking/Translocation Machinery (DTM) [112-119]. As previously mentioned, the N-terminal half of PEX5 harbours the PEX7 interaction site. Besides binding to PEX7, some observations also show that the N-terminal half of PEX5 also interacts with some cargo proteins [120, 121]. The C-terminal domain of PEX5 contains seven tetratricopeptide repeats (TPRs) with a highly conserved structure, consisting of two clusters, TPRs 1-3 and TPRs 5-7, connected by a flexible hinge comprising TPR4. These TPRs are involved in the interaction with PTS1-containing proteins. This property was confirmed with studies showing PEX5 interacting with SKL-containing peptides or a PTS1 cargo protein (Figure 4) [122-126]. When PEX5 interacts with a PTS1 protein, a ring-like structure is formed by the two TPR clusters with the PTS1 peptide occupying the center of this ring-like structure. In the absence of a cargo protein there is a slight opening of the ring-like structure.

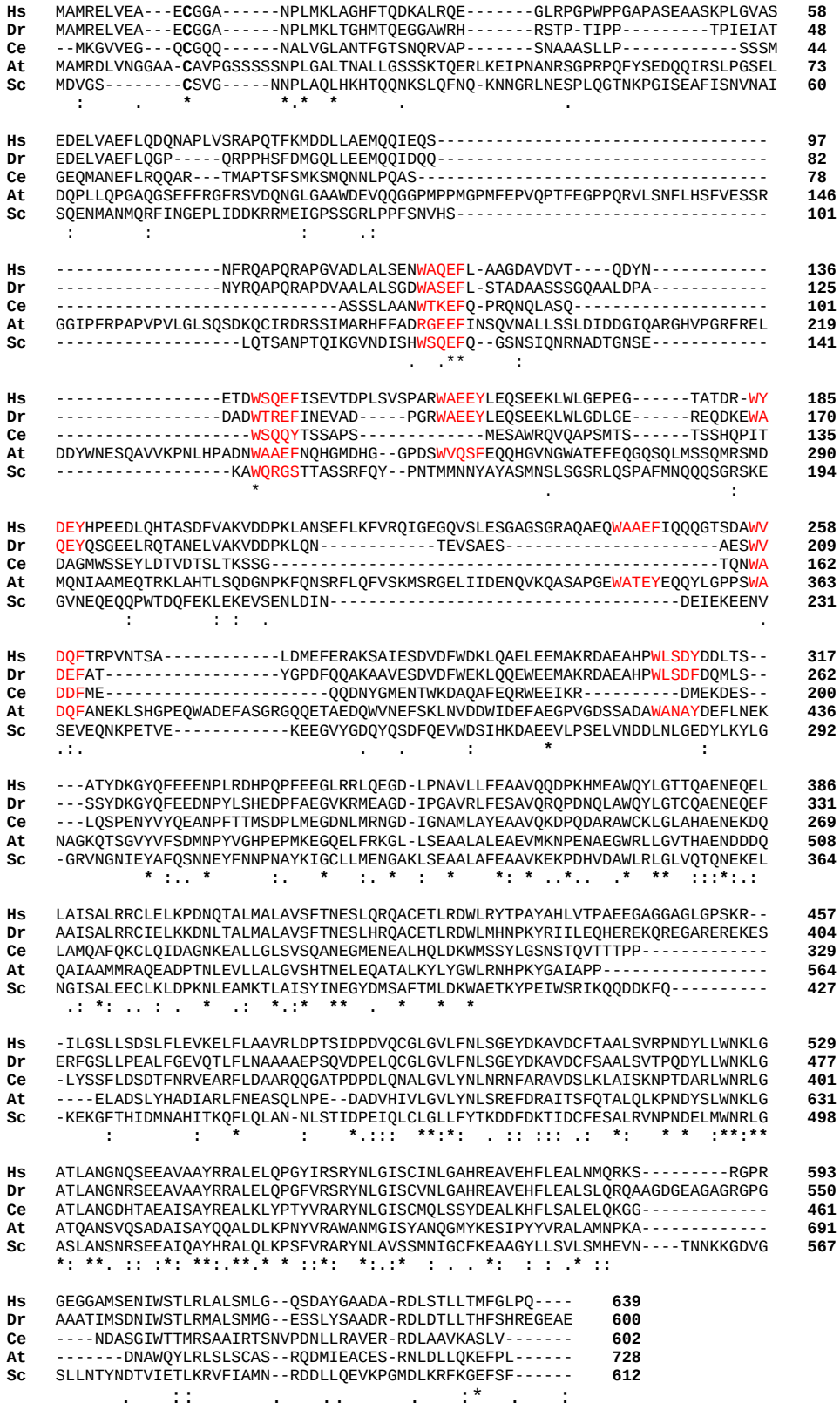

Figure 3: Sequence alignment of PEX5 proteins (ClustalW2, www.ebi.ac.uk). The long isoform of human (Hs) PEX5 is aligned with homolog proteins from *Danio rerio* (*Dr*), *Caenorhabditis elegans* (*Ce*), *Arabidopsis thaliana* (*At*) and *Saccharomyces cerevisae* (*Sc*). Red colour marks the WXXXF/Y diaromatic motifs located at PEX5 N-terminal half.

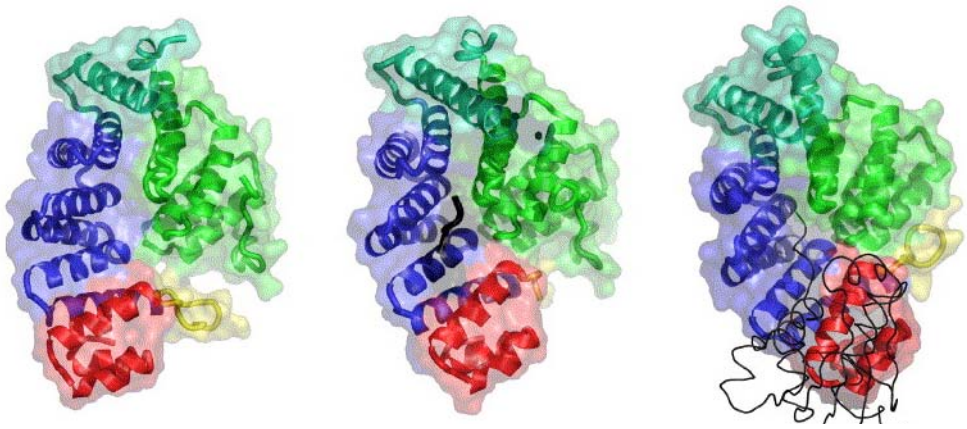

Figure 4: Structures of the C-terminal half of PEX5 (PEX5(C)). The structures were obtained in the absence of a ligand (left, [123]) in the presence of the consensus PTS1 peptide YQSKL (Protein Data Base accession number 1FCH) (central, [122]) or in the presence of the functional PTS1 cargo protein SCP2 (right, [123])**.** Colour coding: TPR segments 1–3, **light green**; TPR4 segment, **dark green**; TPR segments 5–7, **blue**; loop connecting the TPR segment and the C-terminal helical bundle, **yellow**; C-terminal α-helical bundle, **red**; PTS1 ligands, black. Adapted from [123].

3.3.2 – The Cycling Receptor Model

PEX5 presents a dual subcellular localization. Elegant studies demonstrated that PEX5 can accumulate at the peroxisomal membrane when temperature and ATP levels are experimentally decreased [127]. Moreover, the peroxisomal accumulation of PEX5 is completely reversible suggesting that PEX5 can undergoe multiple cycles of association/dissociation. Knowing that PEX5 recognizes and binds cargo proteins, it was proposed that this protein is a cycling receptor [127]. According to this model, matrix proteins are recognized by PEX5 in the cytosol, are directed to the peroxisomal membrane, translocated to the matrix of the organelle and finally PEX5 is recycled back into the cytosol.

Understanding how the peroxisomal import machinery works requires knowledge on the arquitecture of its components. Over the years, numerous studies have addressed this issue. Using biochemical (*e.g.*, pull-down assays, immunoprecipitation experiments and protein purification techniques) and genetic approaches (*e.g.*, yeast two-hybrid) it was possible to build models on the structure of the Peroxisomal Import Machinery (PIM) (Figure 5) [128-132]. In mammals, this machinery comprises: 1) a membrane-embedded DTM that includes PEX14, PEX13 and the Really Interesting New Gene (RING)-finger peroxins PEX2, PEX10 and PEX12; and 2) a Receptor Export Module (REM) that includes the two ATPases

Associated with diverse Activities (AAA) peroxins, PEX1 and PEX6, and their membrane anchor, PEX26. Besides these peroxins, the PIM also includes ubiquitin, an ubiquitin-activating enzyme (E1) and an ubiquitin-conjugating enzyme (E2).

	Proteins	Properties
Receptors and Co-receptors	PEX5	Cytosolic/ peroxisomal NUD/TPRs
	PEX7	Cytosolic/ peroxisomal WD repeats
	PEX18/ PEX20/ PEX21	Cytosolic/ peroxisomal
Docking /Translocation Module	PEX2	Intrinsic RING
	PEX10	Intrinsic RING
	PEX12	Intrinsic RING
	PEX13	Intrinsic SH3
	PEX14	Intrinsic Coiled-coil
	PEX8	Extrinsic (matrix)
	PEX17	Intrinsic Coiled-coil
Ubiquitin-conjugating enzymes		Cytosolic E2
	PEX4	Extrinsic (cytosolic) E2
	PEX22	Intrinsic
Receptor Export Module	PEX1	Extrinsic/ cytosolic AAA ATPase
	PEX6	Extrinsic/ cytosolic AAA ATPase
	PEX26/ PEX15	Intrinsic

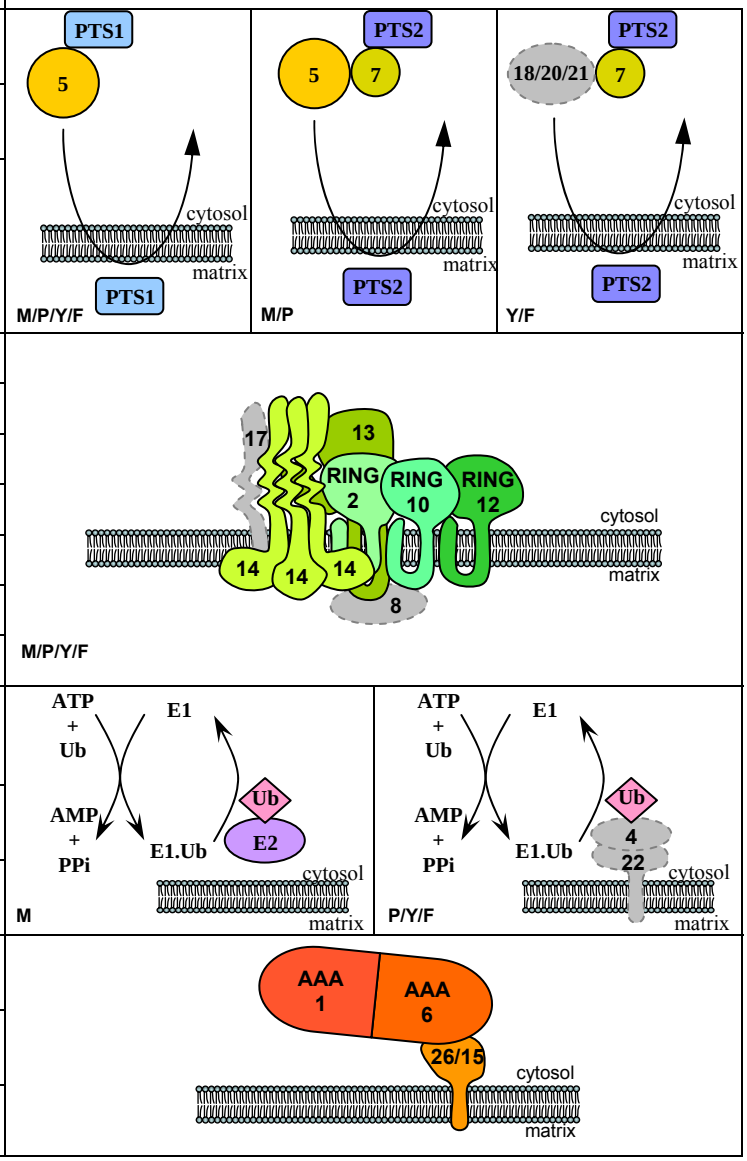

Figure 5: Components of the peroxisomal import machinery (PIM). Peroxins absent in mammals (*M*) are depicted in gray. Receptors and co-receptors of cargo proteins are represented. The docking/translocation module comprises mostly transmembrane proteins. PEX8 and PEX17 have been found only in lower eukaryotes [53, 54]. The first two reactions of the ubiquitin-conjugating cascade involved in the peroxisomal protein import pathway are shown. Note that in mammals the E2 component is a cytosolic protein whereas in plants, yeasts and fungi the E2 PEX4 is bound to the organelle membrane via PEX22. The precise identity of the final component of this cascade, ie, the ubiquitin-ligase catalyzing mono-ubiquitination of PEX5 remains unknown but it may be any of the 3 RING peroxins of the DTM or combinations of them. The receptor export module comprises AAA peroxins PEX1 and PEX6 and one intrinsic membrane protein anchor [133, 134], PEX26 in mammals and other organisms, and PEX15 in some yeasts. PEX26 and PEX15 are unrelated at the primary structure level [53]. Their plant functional counterpart is presently unknown [135]. Adapted from [136].

Using an *in vitro* import system, our laboratory has provided valuable data regarding the mammalian PEX5-mediated peroxisomal protein import pathway. This system is based in the incubation of radiolabeled PEX5 or a PTS2-containing protein with a rat liver post-nuclear supernatant (PNS) under appropriate experimental conditions. A protease-protection assay is then performed to evaluate the specificity of the process, since non-peroxisomal PEX5 or non-imported cargo protein are susceptible to proteolytic cleavage. The model presented in Figure 6 accommodates all the data gathered so far regarding this pathway. The model comprises several steps (numbered 0-4) as detailed below.

First, soluble PEX5 (stage 0) binds to cargo proteins in the cytosol yielding stage 1a PEX5. It is possible that this interaction somehow changes the conformation of PEX5 because the receptor only engages the next steps (i.e., interaction with the DTM) if cargo proteins are available [137]. The cytosolic cargo-loaded PEX5 then interacts with the DTM yielding stage 1b. There are some data suggesting that the docking site for the complex at the peroxisomal membrane is PEX13 and/or PEX14 although convincing data for these possibilities are still lacking [138, 139]. Once at the peroxisomal membrane, cargo-loaded PEX5 becomes inserted into the DTM (stage 2), acquiring a transmembrane topology with a small N-terminal domain exposed to cytosol and protease accessible [140], whereas the bulky fraction of PEX5 polypeptide chain can only be accessed by the matrix of the organelle [140]. Strikingly, the transition between stage 1b and stage 2 PEX5 is an ATP-independent process [137, 141, 142]. Next, the DTM-embedded PEX5 is monoubiquitinated at a conserved N-terminal cysteine residue (Ub-PEX5, stage 3, completely protease-resistant) [143, 144]. The evidence supporting the importance of the cysteine residue is several fold: deletion of the 17 amino acid domain containing this cysteine, its alkylation or its substitution by a serine or alanine results in PEX5 proteins still functional in the docking and membrane insertion steps but export-incompetent [142, 144, 145]. Monoubiquitination is a mandatory event for the export of PEX5, an event that is ATP-dependent [144]. PEX1/PEX6 endorse this export step, where Ubiquitin-PEX5 (Ub-PEX5) is recognized and extracted from the peroxisomal membrane back into the cytosol, yielding a soluble Ub-PEX5 conjugate (stage 4) [134, 146]. Finally, the ubiquitin moiety is removed from the Ub-PEX5 conjugate, a process that possibly occurs by a combination of enzymatic and non-enzymatic mechanisms [147, 148]. In mammals, it was recently shown that USP9X is by far the most active deubiquitinase (DUB) acting on Ub-PEX5 [149].

All the data mentioned so far was obtained using a PEX5-centered *in vitro* import system. However, this approach gave us no information about the cargo insertion into the DTM and its release into the organelle matrix. Recent findings from

our laboratory came to elucidate these matters. Indeed, using a PTS2-centered *in vitro* import system [150], it was possible to conclude that PTS2-cargo insertion into the DTM occurs at the stage 1b-to-stage 2 transition, as previously hypothesized [151] and that the release of the reporter protein to the organelle matrix occurs before ubiquitination of PEX5.

4. – Oligomeric matrix protein import

Peroxisomes can be distinguished from other organelles by their ability to import proteins in their oligomeric state (reviewed in [3]). However, this has been a controversial subject during the past years. On one hand, some work has been published stating that protein oligomerization occurs after import into the peroxisome: Lazarow and de Duve showed that catalase was imported as a monomer [152, 153] and the same was observed in cucumber glyoxysomes for malate synthethase import [154]; finally alcohol oxidase octomerization was shown to occur during or right after import to the peroxisomes [155-157]. On the other hand, several authors claim that peroxisomes have the ability to import proteins in their native state. It was shown that a peroxisomal protein lacking a PTS1 signal can form a complex with a PTS1-containing protein and enter the organelle. This phenomenon is designated “piggy-back” import.

The first evidences supporting this idea came from studies where a N-terminal truncated version of thiolase, lacking the PTS2 signal, was found to be imported in complex with a full-length version of itself [158]. Another example comes from the work with chloramphenicol acetyltransferase. Those authors proposed that subunits of this protein, lacking the PTS1 signal, were able to form heterotrimers with subunits containing a PTS1 in the cytosol and be targeted to the peroxisome [159]. The same phenomenon was reported for other proteins like Mdh3 from *S. cerevisiae* [85], isocitrate lyases of some plants [160] and enoyl-CoA isomerases Dci1p and Eci1p from *S. cerevisiae* [161]. In a different experimental setting, Walton and collaborators microinjected mammalian cells with gold particles (with a diameter ranging from 4-9 nm) coated with human serum albumin conjugated with a PTS1 signal [162]. They observed that these particles could be imported into the peroxisomal matrix.

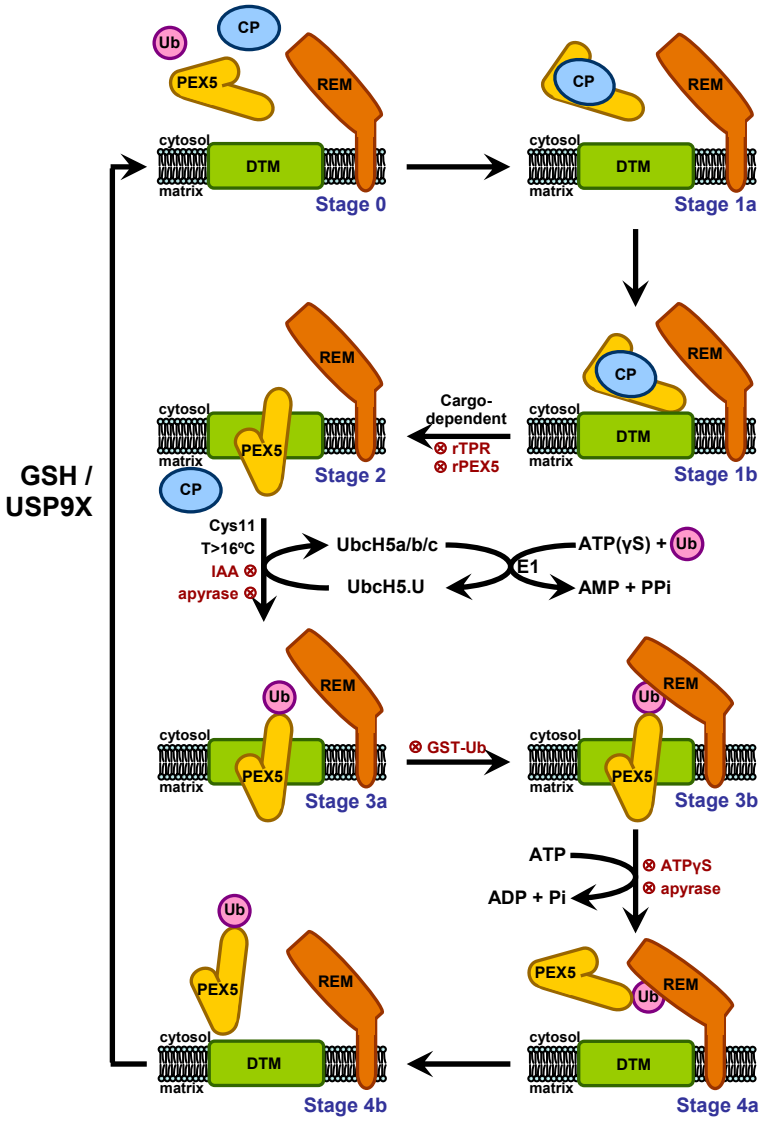

Figure 6: The PEX5-mediated peroxisomal protein import pathway in mammals. The matrix protein import pathway comprises five major steps (numbered 0-4). *Stage 0*, cytosolic cargo-free PEX5 (protease accessible). *Stage 1*, cytosolic PEX5-cargo protein complex (protease accessible). *Stage 2*, PEX5 embedded in the peroxisomal docking/translocation machinery (*DTM*) (only 2 kDa of PEX5 N-terminus are accessible to exogenously added Proteinase K). *Stage 3*, DTM-embedded monoubiquitinated PEX5 at Cys11 (protease protected). *Stage 4*, protease accessible monoubiquitinated PEX5. ⊗,indicates reagents that block the pathway at specific steps; CP, cargo protein; Ub, ubiquitin; IAA, iodoacetamide; rTPR, recombinant protein comprising the PTS1-binding domain of PEX5; rPEX5, recombinant full-length PEX5; REM, receptor export module. Adapted from [150].

These observations come together to illustrate the ability of peroxisomes to import: 1) proteins in their native state, 2) oligomeric proteins and 3) large structures ([158, 159], reviewed in [3]). However, the import kinetics of a given cargo protein has never been truly studied. In fact, there is only one study where this issue was

considered. Goodman and co-workers showed that the import kinetics of the trimeric chloramphenicol acetyltransferase is strangely slow, taking hours to occur [159], in contrast with the import of authentic peroxisomal proteins which, for all cases analyzed so far, occurs in minutes [152, 153, 155, 163]. The import of oligomeric proteins shows that the DTM is quite flexible, which is expected since it allows the import of monomeric proteins with different sizes, like glutathione S-transferase kappa 1 (25 kDa) or Lon-protease (105 kDa). Neverthless, it remains to be clarified if the import of oligomeric proteins represents a *bona fide* mechanism used under normal physiological conditions or simply a residual activity of the peroxisome import machinery.

II. AIMS

Understanding the PEX5-mediated protein import pathway requires knowledge on how this peroxin binds cargoes in the cytosol and releases them in the peroxisomal matrix.

The aims of the work were:

- to characterize the interaction of PEX5 with cargo proteins using a biologically relevant experimental set-up;

- to determine whether the PEX5-cargo protein interaction can be disrupted by some DTM components;

- to characterize the peroxisomal import efficiency of a cargo protein in its monomeric and oligomeric state.

III. EXPERIMENTAL PROCEDURES

1. Primer list

Table 4: Primers used in DNA manipulations

Protein	Primers	
PEX5ΔN110	Fw - GAGCGCGCCATATGGCAGACTTGGCCTTGTCT	
	Rv* - GCGTAATTAAGCTTGGCTGCAGGTC	
PEX5ΔN147	Fw - GAGCGCGCCATATGGTTACAGACCCCTTGTCTG	
PEX5ΔN196	Fw - GAGCGCGCCATATGACGGCCAGTGACTTTGTG	
PEX5ΔN267	Fw - GAGCGCGCCATATGTCTGCCCTTGATATGGA	
PEX5ΔN290	Fw - GAGCGCGCCATATGTTGCAGGCAGAGTTGGA	
PEX5ΔN267-M7 ; PEX5-M7	W308A	Fw - GCTGAGGCCCACCCCGCTCTTTCTGACTATGAT
		Rv - ATCATAGTCAGAAAGAGCGGGGTGGGCCTCAGC
	Y312A	Fw - CCGCTCTTTCTGACGCTGATGACCTTACG
		Rv - CGTAAGGTCATCAGCGTCAGAAAGAGCGG
PEX5M6,7**	W257A	Fw - TACATCAGATGCCGCGGTTGACCAGTTCAC
		Rv - GTGAACTGGTCAACCGCGGCATCTGATGTA
	F261A	Fw - CCGCGGTTGACCAGGCCACAAGACCAGTAA
		Rv - TTACTGGTCTTGTGGCCTGGTCAACCGCGG
PEX5 (*Mus musculus*)	Fw - GCGAACTGCATATGGCAATGCGGGAGCTGG	
	Rv - GCGGTCGACTCACTGGGGCAGGCCAAACAT	
Catalase	Fw - GGTCTAGAGCCACCATGGCTGACAGCC	
	Rv - GGTACCCCTCACAGATTTGCCTTCT	
CatΔKANL	Fw - ACTTGGCGGCAAGGGAGTAGGCAAATCTGTGA	
	Rv - TCACAGATTTGCCTACTCCCTTGCCGCCAAGT	
CatED	Fw - CGGCAAGGGAGGAGGACTAACTGTGAGGTACCGA	
	Rv - TCGGTACCTCACAGTTAGTCCTCCTCCCTTGCCG	
AOX	Fw - GCTAATTCTAGAGCCACCATGAATCCCGATCTG	
	Rv - CGCCGTGGTACCTAGCATCAAAGCTTCGACTG	
UOX	Fw - GCAGCATCTAGAGCCACCATGGCCCATTACC	
	Rv - CGCGCGGGTACCTTTCACAGCCTGGAAGGCA	
2HA-UOX	Fw - GCGCCGTCTAGAGCCCATTACCATGACAACT	
	Rv - CGCGCGGGTACCTTTCACAGCCTGGAAGGCA	

* The same reverse primer was used for PEX5ΔN110, PEX5ΔN147, PEX5ΔN196, PEX5ΔN267 and PEX5ΔN290.

** This plasmid encoding PEX5-M7 was used as the template for this mutagenesis.

Cat, catalase; AOX, acyl-CoA oxidase; UOX, urate oxidase; Fw, forward primer; Rv, reverse primer.

2. Production and expression of recombinant proteins

The recombinant large isoform of human PEX5 [91, 105], a protein comprising the first 324 amino acid residues of PEX5 (ΔC1PEX5), a protein containing amino acid residues 315-639 of PEX5 (TPRs), PEX5 containing the missense mutation N526K (PEX5N526K), a protein comprising the first 80 amino acid residues of human PEX14 (NDPEX14) and full-length PEX19 (PEX19) were obtained as previously described [64, 109, 110, 145, 164].

The following His-tagged truncated versions of human PEX5 were also produced: PEX5ΔN110 (amino acid residues 111-639 of PEX5), PEX5ΔN147 (amino acid residues 148-639 of PEX5), PEX5ΔN196 (amino acid residues 197-639 of PEX5), PEX5ΔN267 (amino acid residues 268-639 of PEX5) and PEX5ΔN290 (amino acid residues 291-639 of PEX5). The cDNAs encoding these proteins were obtained by PCR using the primers listed in Table 4, and the pQE30-PEX5 [110] construct as template. The amplified DNA fragments were then digested with NdeI and SalI and cloned into the NdeI/SalI digested pET-28c vector (Novagen). Expression of these truncated versions of PEX5 was performed in the BL21 (DE3) strain of *Escherichia coli* (*E. coli*).

The QuickChange® Site-Directed Mutagenesis Kit (Stratagene) was used to replace tryptophan and phenylanaline/tyrosine residues by alanines in diaromatic motifs of PEX5 (see primers in Table 4). The three proteins obtained in this way are: PEX5ΔN267-M7 and PEX5-M7, proteins with a mutated 7th diaromatic motif; and PEX5-M6,7, a protein possessing both the 6th and 7th diaromatic mutated. Expression of these mutated versions of PEX5 was performed in the BL21 (DE3) strain of *E. coli*.

In order to obtain the His-tagged mouse PEX5, its cDNA was amplified from a commercially available clone (clone MMM1013-7510385, Open Biosystems) using the primers listed in Table 4, digested with NdeI and SalI and cloned into the NdeI/SalI digested pET-28c vector. Expression of this protein was performed in the BL21 (DE3) strain of *E. coli*.

All plasmids were sequence verified. Purification of all PEX5 proteins was performed as described [110].

3. Plasmids for the synthesis of ^{35}S-radiolabeled proteins

The cDNAs encoding full-length human catalase (Cat) (clone IMAGE ID 5551309, Open Biosystems), full-length mouse acyl-CoA oxidase (AOX) (clone IMAGE ID 5704873,Open Biosystems) and full-length mouse urate oxidase (UOX) (clone IMAGE ID 5136328,Open Biosystems) were amplified by PCR using the primers listed

in Table 4. The amplified sequences were digested with XbaI and KpnI and cloned into the XbaI/KpnI digested pGEM-4® vector (Promega), originating pGEM-4-Cat, pGEM-4-AOX and pGEM-4-UOX, respectively.

The plasmid pGEM-4-Cat was used as template to produce two other plasmids, one encoding a catalase lacking its last four C-terminal amino acid residues, the PTS1 signal (CatΔKANL), and the other encoding a catalase in which these four residues were replaced by a glutamate and aspartate sequence (CatED). These plasmids were obtained using the QuickChange® Site-Directed Mutagenesis Kit (Stratagene) and the primer pairs described in Table 4.

The plasmid pGEM-4-2HA-AOX was kindly provided by Dr. Marc Fransen from the Katholieke Universiteit of Leuven.

A tag containing two hemaglutinin (HA) sequences (2HA-tag) was obtained by annealing of the following primers: 5'- AG CTT ACC ATG GGC TAC CCC TAT GAT GTG CCC GAT TAC GCC TAC CCA TAC GAC GTC CCA GAC TAC GCT T - 3' and 5'-CT AGA AGC GTA GTC TGG GAC GTC GTA TGG GTA GGC GTA ATC GGG CAC ATC ATA GGG GTA GCC CAT GGT A - 3'. This linker was cloned into the HindIII/XbaI digested pGEM-4® vector, originating the pGEM-4-2HA plasmid. The UOX cDNA was amplified from the commercial clone referred above using the primers listed in Table 4, digested with XbaI and KpnI and inserted into the previously digested pGEM-4-2HA vector. The final product (pGEM-4-2HA-UOX) encodes for a UOX with a 2HA-tag at its N-terminus.

4. Synthesis of ^{35}S-radiolabeled proteins

^{35}S-labeled proteins were synthesized using the TNT® T7 Quick Coupled Transcription/Translation kit (Promega) in the presence of [^{35}S] methionine (specific activity >1000 Ci/mmol; PerkinElmer) following the standard conditions of the manufacturer. Unless otherwise indicated, protein synthesis was allowed to proceed for 55 min and was then blocked with 0.5 mM of cycloheximide (final concentration). Chase incubations were performed at 30 ºC for the specified periods of time. Chase reactions performed in the presence of recombinant proteins typically contained 6 µl of the translation mixture in a final volume of 10 µl.

5. Native Polyacrylamide Gel Electrophoresis

Proteins were incubated in 10 µl of 50 mM Tris-HCl, pH 8.0, 2 mM DTT for 5 min at room temperature. After addition of 1 µl of 0.17% (w/v) bromophenol blue, 50% (w/v) sucrose, the samples were loaded into Tris nondenaturating discontinuous 8%

polyacrylamide gels [165]. The gels were run at 250 V at 4 °C, for 1 hour (unless indicated otherwise), blotted onto nitrocellulose membranes, stained with Ponceau S and exposed to an x-ray film.

6. Size-Exclusion Chromatography

^{35}S-labeled proteins (50 µl of *in vitro* transcription/translation reactions) or mixtures containing recombinant proteins and ^{35}S-labeled proteins were diluted to 250 µl with 50 mM Tris-HCl, pH 7.5, 150 mM NaCl, 1 mM EDTA-NaOH pH 8.0, 1 mM DTT and injected into a Superose 12 10/300 GL column (GE Healthcare; loop volume 200 µl) running with the same buffer at 0.5 ml/min. The column was calibrated with the following globular proteins: ferritin (440 kDa), bovine serum albumin (66 kDa), and soybean trypsin inhibitor (21.5 kDa). Fractions of 500 µl were collected, subjected to trichloroacetic acid (TCA) precipitation, and one third of each sample was analyzed by SDS-PAGE. The gels were blotted onto nitrocellulose membranes, stained with Ponceau S and exposed to an x-ray film.

Soluble mouse liver peroxisomal matrix proteins were obtained by sonicating purified peroxisomes (prepared as in Ref. [166]) in 50 mM Tris-HCl, pH 7.5, 150 mM NaCl, 1 mM EDTA-NaOH pH 8.0, 1 mM DTT and 1:500 (v/v) mammalian protease inhibitor mixture (Sigma) and centrifuging for 30 min at 100,000 x g. Two-hundred micrograms of soluble proteins, supplemented or not with 300 µg of recombinant mouse PEX5, were injected into the size-exclusion column, as above. Aliquots of 25 µl from each fraction were analyzed by SDS-PAGE/western blotting with antibodies directed to catalase (catalogue number RDICATALASEabr; Research Diagnostics, Inc) and L-bifunctional protein [167].

7. Sucrose Gradient Centrifugation

Fifty microliters of *in vitro* transcription/translation reactions were incubated in 200 µl of buffer A (50 mM Tris-HCl, pH 7.5, 150 mM NaCl, 1 mM EDTA-NaOH pH 7.4, 1 mM DTT) for 10 min at 37 °C. Thirty micrograms of bovine immunoglobulins G (IgGs) (156 kDa), bovine serum albumin (BSA) (66 kDa) and chicken ovalbumin (OA) (45 kDa) were added to the samples as internal standards. These mixtures were then applied onto the top of a continuous 5%-30% (w/v) sucrose gradient in buffer A. After centrifugation at 39,000 rpm for 29 h at 4 °C in a SW41 swing-out rotor (Beckman), 14 fractions of 0.8 ml were collected from the bottom of the tube. One fifth of the fractions was subjected to trichloroacetic acid precipitation and analyzed by SDS-PAGE. The

gels were blotted onto nitrocellulose membranes, stained with Ponceau S and exposed to an x-ray film.

8. Immunoprecipitations

^{35}S-labeled proteins were diluted to 500 µl with 50 mM Tris-HCl, pH 8.0, 150 mM NaCl, 1 mM EDTA-NaOH pH 7.4, 10% (w/v) glycerol, 0.1% (w/v) Triton X-100, 0.025% of BSA and 1:500 (v/v) mammalian protease inhibitor mixture (Sigma) and subjected to immunoprecipitation using 30 µl of anti-HA antibody agarose beads (Sigma) for 3 h at 4 ºC. Beads were washed three times with the same buffer without BSA and mammalian protease inhibitor mixture. The immunoprecipitated proteins were eluted with gel loading buffer supplemented with 100 mM DTT and subjected to SDS-PAGE. The gels were blotted onto nitrocellulose membranes, stained with Ponceau S and exposed to an x-ray film.

9. *In vitro* import reactions

Rat liver post-nuclear supernatant (PNS) was prepared in buffer containing 0.25 M sucrose, 20 mM MOPS-KOH, pH 7.4, 1 mM EDTA-NaOH, pH 7.4, 2 µg/ml N-(trans-epoxysuccinyl)-l-leucine 4-guanidinobutylamide (E-64) (SEM buffer) as described before [140]. Where indicated, the reactions were supplemented with 10 ng or 50 ng of PEX5/PEX5N526K, 0.3 µM of TPRs/TPRsN526K or 10 µM of NDPEX14/PEX19.

In a typical import reaction, 400 µg of rat liver PNS protein and 1 µl of a rabbit reticulocyte lysate containing ^{35}S-labeled AOX or UOX were used. Incubation was for 45 min at 37 °C in 100 µl of import buffer (0.25 M sucrose, 50 mM KCl, 20 mM MOPS-KOH, pH 7.4, 3 mM $MgCl_2$, 20 µM methionine, 2 µg/ml E-64, and 2 mM GSH, pH 7.2) containing 3 mM ATP. Recombinant proteins were added to some reactions, as indicated. Protease treatment of import reactions was performed on ice for 40 min using 400 µg/ml Proteinase K (PK) (final concentration). After inactivation of the protease with 500 µg/ml phenylmethylsulfonyl fluoride (PMSF) for 2 min on ice, the organelle suspensions were diluted to 1 ml with SEMK (SEM buffer containing 50 mM KCl) and isolated by centrifugation. The samples were subjected to trichloroacetic acid precipitation and analyzed by SDS-PAGE/Autoradiography.

10. Density gradient centrifugation analysis

A 4-fold scale-up of a standard import reaction was used. After PK treatment and inactivation of the protease, the complete import mixture was diluted to 1.5 ml with

SEM buffer and analyzed by Nycodenz step gradient (1.5 ml of 45% (w/v), 6 ml of 30% (w/v), 2 ml of 25% (w/v), and 2 ml of 20% (w/v) Nycodenz in 5 mM MOPS-KOH, pH 7.2, and 1 mM EDTA-NaOH, pH 7.2). The tubes were centrifuged in a vertical rotor (STEPSAVER™ 65V13; Sorvall®) at 25,000 rpm for 2 h at 4°C. Fourteen equal fractions were collected from the bottom of the gradient, and a 250-µl aliquot of each fraction was subjected to trichloroacetic acid precipitation and SDS-PAGE. First the membranes were exposed to an x-ray film and then blotted with several antibodies. The antibodies directed to catalase (catalogue number RDI-CATALASEabr; Research Diagnostics, Inc.), KDEL (catalogue number ab12223; Abcam), and cytochrome *c* (catalogue number 556433; BD Pharmingen) were purchased. Rabbit and mouse antibodies were detected on Western blots using alkaline phosphatase-conjugated anti-rabbit and anti-mouse antibodies (Sigma).

11. Miscellaneous

The concentration of PEX5 in rat liver cytosol (0.75 µM) was calculated from the following data: total amount of PEX5 in liver, 4 ng/µg of total peroxisomal protein; percentage of PEX5 in cytosol, 85% [131]; peroxisomes, 2.5% (w/w) of total liver protein [168]; protein content of liver, 260 mg/g [169]; one gram of liver corresponds to 0.94 ml of which 44.4% is cytosol [170]. The weighted average molecular mass of monomeric rat liver peroxisomal proteins was estimated from the densitometric analysis of a Coomassie-stained SDS-gel loaded with a highly pure peroxisomal preparation [166]. Peak areas were divided by the corresponding apparent molecular masses and expressed as percentage of total moles. The weighted average of these values is 49 kDa. For newly synthesized peroxisomal proteins, this value may be slightly underestimated because protein maturation processes that occur in the matrix of the organelle (*e.g.*, the cleavage of the 75 kDa acyl-CoA oxidase into the 53 and 22 kDa subunits; [171]) were not taken into account. Mole percentage for catalase (13 mole %) was calculated considering the mass percentage of the protein in rat liver peroxisomes, 15% [172], the weighted average molecular mass of rat liver peroxisomal proteins (49 kDa), the theoretical molecular mass of catalase (60 kDa), and the mass percentage of matrix proteins in total rat liver peroxisomes, 92% [166]. The amount of total peroxisomal matrix proteins in nmol/gram of rat liver was calculated from the above referred data. A value of 122 nmol/g of liver was obtained.

Because “all the major protein components of the peroxisome have the same rate of turnover” (half-life of 1.3-1.5 days; [173, 174]) one can estimate the rate of total peroxisomal matrix protein synthesis (K_s) as 30 pmol/min/g of liver. The rate of

synthesis for a particular protein is K_s times its mole fraction in the peroxisomal matrix. For catalase (0.13 mole fraction) this corresponds to 3.9 pmol/min/g of liver, a value similar to the one reported previously (3.87 pmol/min/g of liver; [172]). The steady-state concentration of newly synthesized peroxisomal matrix proteins in the cytosol ([P]cyt) can be estimated from the expression: $[P]_{cyt} = K_s \times 1.443 \times t_{1/2}$, where $[P]_{cyt}$ is in pmol/g of liver and $t_{1/2}$ is the cytosolic half-life of the protein in min (see [152]). According to Lazarow and colleagues [153, 175] several peroxisomal proteins display cytosolic half-lives of about seven minutes (see Figure 5 in Ref. [175]). Two outliers were noted by those authors: one was catalase, a protein presenting a cytosolic half-life of 14 min; the other was urate oxidase, a protein that after 4 min of chase was already completely found in peroxisomes, an observation suggesting that its cytosolic half-life is 2 min or less. We assume that all peroxisomal matrix proteins present a similar kinetic behavior, i.e., that on average their cytosolic half-lives is 7-8 min. The total concentration of newly synthesized peroxisomal proteins in the cytosol is thus 0.73-0.83 μM, with monomeric catalase contributing with 0.19 μM.

IV. RESULTS

1. Characterization of the PEX5-cargo protein interaction

Presently, most of what we know regarding the interaction of PEX5 with cargo proteins comes from studies involving either PTS1-containing peptides or already folded peroxisomal matrix proteins. Although useful data have been obtained using these strategies, the fact remains that these studies do not reflect the *in vivo* situation. Indeed, in vivo, peroxisomal matrix proteins are synthesized in the cytosol in the presence of PEX5, a fact that may influence their folding/oligomerization processes and, therefore, their biogenesis pathway. For this reason, we decided to study the interaction of PEX5 with cargo proteins in a system that mimics the biological relevant situation. We selected catalase for our initial studies. Catalase, one of the most abundant peroxisomal matrix proteins, is a heme-containing enzyme containing four 60 kDa subunits, each possessing a non-canonical PTS1 (KANL) at its C-terminus [176-180]. The reason behind our choice is related to the controversy around the oligomeric state of catalase accepted by the PIM. Indeed, some authors have shown that catalase is imported still in its monomeric state, whereas other researchers propose that import occurs only after oligomerization in the cytosol [152, 153, 181-185].

1.1 – *In vitro* tetramerization of ^{35}S-Catalase

We started by synthesizing the radiolabeled human catalase for 90 min using the rabbit reticulocyte lysate-based *in vitro* transcription/translation system. By native-PAGE analysis we observed three distinct populations of ^{35}S-catalase (Figure 7A, lane -). Strikingly, when catalase is synthesized in the presence of 1 μM of recombinant PEX5, a physiological relevant concentration (see Discussion), two of these populations are no longer detected. Apparently, the presence of PEX5 during synthesis of catalase blocks some event.

To determine the nature of the three populations, we performed a pulse-chase analysis where catalase was synthesized for 55 min, cycloheximide was added to arrest protein synthesis and the reaction was further incubated for 4 h. By native-PAGE analysis (Figure 7B) we observed that after 55 min of synthesis (lane 55') the main product was the faster migrating population, which is converted into the slower one during the 4 h chase (lane 240'). The intermediary population remains constant during the experiment, probably representing an oligomerization intermediate, the dimeric form of catalase (see below).

To better understand the properties of each catalase population observed, we performed a sedimentation analysis with catalase synthesized for just 55 min or chased for four hours. This analysis showed that the faster migrating population corresponds to a specie displaying properties of a 60 kDa globular protein, whereas the slower migrating population behaves as a 200-250 kDa protein (data not shown). These findings indicate that the faster migrating catalase population represents the monomeric form of catalase (mCat). The 200-250 kDa species might represent either tetrameric catalase (tCat) or a complex between catalase and some protein(s) from the *in vitro* transcription/translation system (*e.g.*, a chaperone).

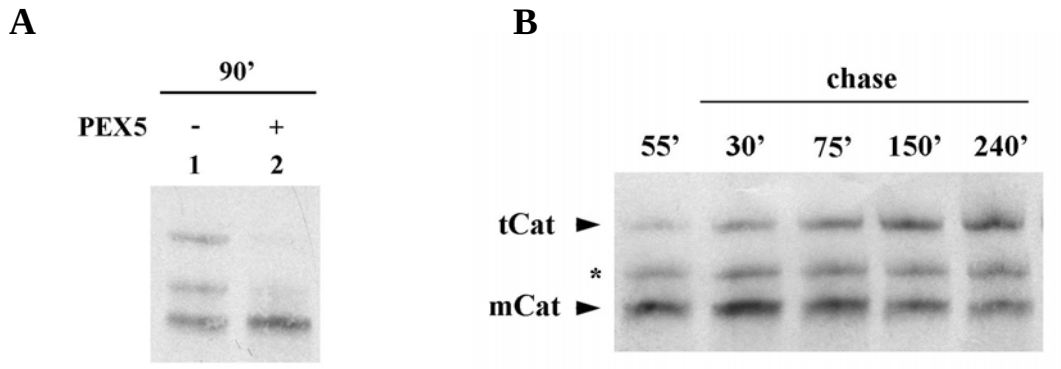

Figure 7: ^{35}S-catalase populations after *in vitro* synthesis. A) Human catalase was synthesized in vitro in a rabbit reticulocyte lysate for 90 min at 30 ºC in the absence or presence of 1 µM human PEX5, as indicated, and analyzed by native-PAGE/autoradiography. B) ^{35}S-labeled catalase was synthesized for 55 min. After adding cycloheximide, an aliquot was removed and frozen in liquid N_2 (lane 55`). The remainder of the reaction was then incubated at 30 ºC and aliquots were removed and frozen at the indicated time points. The samples were subjected to native-PAGE/autoradiography. mCat and tCat correspond to the monomeric and tetrameric forms of catalase; the band labeled with an asterisk probably represents dimeric catalase.

To discriminate between these two possibilities, we produced an acidic mutant version of catalase (CatED), which migrates faster than the normal protein in native gels. If, in fact, the slower migrating form corresponds to the tetrameric catalase, one should be able to form heterotetramers with CatED, containing 1, 2 or 3 molecules of the normal protein; all these heterotetramers should migrate in these gels between the homotetramers of the parental molecules. On the other hand, if the slower migrating band corresponds to a complex containing catalase and some other protein(s), then the band pattern of the protein mixture should just correspond to the sum of the

patterns obtained with each of the two catalase versions individually. Both catalase and CatED were synthesized for 55 min (lanes 1 and 2) and then subjected to a 4 h-chase incubation, either individually (lanes 3 and 5) or combined (lane 4). Figure 8 shows the results of this experiment. Heterotetramers were indeed detected in the samples where the two catalase species were incubated together for 4 h. Thus, the slower migrating catalase species represents tetrameric catalase.

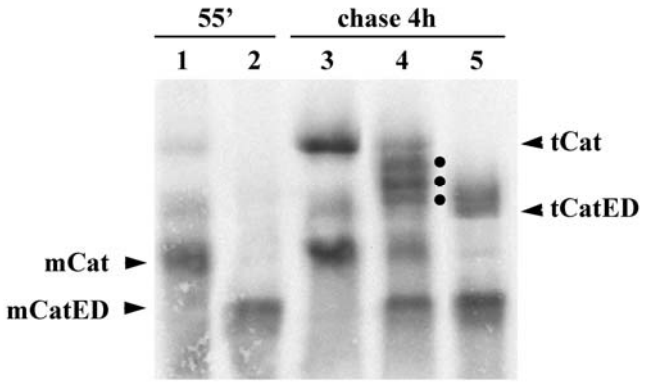

Figure 8: ^{35}S-catalase tetramerizes *in vitro*. Catalase and a mutant version of it possessing two acidic amino acid residues at the C-terminus (CatED) were synthesized *in vitro* for 55 min and supplemented with cycloheximide (lanes 1 and 2, respectively). Aliquots of each reaction were then combined and incubated for 4 h at 30 ºC (lane 4) or incubated individually under the same conditions (lanes 3 and 5 for catalase and CatED, respectively), and subjected to native PAGE/autoradiography. Note that this gel was run for 2.5 hours to improve separation of tetramers. Longer electrophoretic runs also result in more diffuse bands. The dots in lane 4 indicate the three expected heterotetramers. mCatED and tCatED indicate the monomeric and tetrameric forms of CatED, respectively.

1.2 – PEX5 binds monomeric Catalase

The results presented above suggest that PEX5 interferes with catalase tetramerization. To better understand this phenomenon, we decided to characterize the interaction of PEX5 with mCat and tCat. For this purpose, we synthesized catalase for 55 min to obtain mainly monomeric catalase and performed another reaction that was chased for 4 h, this one containing a mixture of monomer and tetramer. Each reaction was then subjected to SEC to purify mCat and tCat. The isolated proteins were incubated in the presence of PEX5, to allow the formation of a complex, or buffer alone, as a negative control, and subjected to a second SEC.

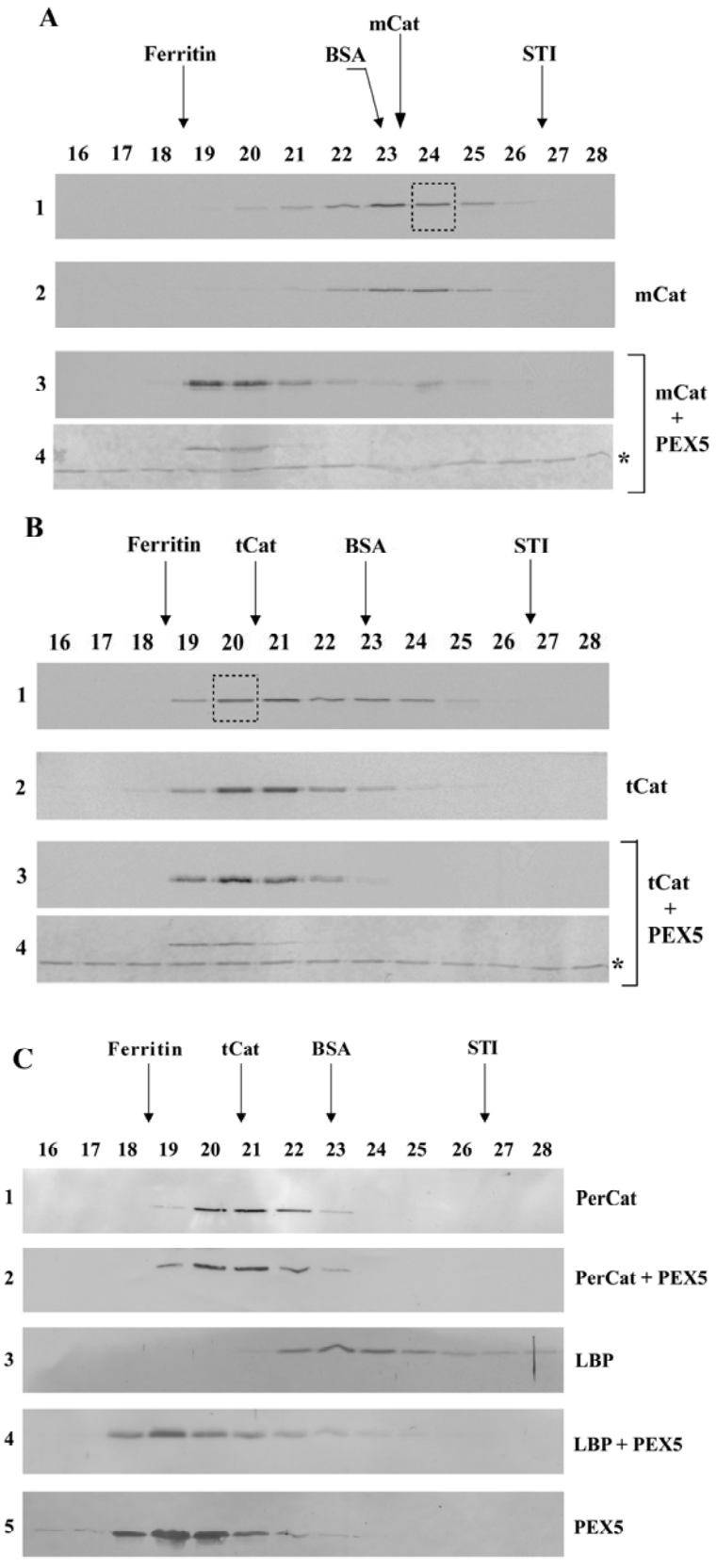

Figure 9: PEX5 binds monomeric catalase. A) ^{35}S-labeled catalase was synthesized *in vitro* for 55 min and subjected to SEC. Radiolabeled mCat eluting in fraction 24 of this chromatography (panel 1; boxed lane) was then subjected to a second SEC either alone (panel 2) or after receiving 1 µM recombinant PEX5 (panels 3 and 4). Fractions were collected, and subjected to SDS-PAGE/western-blotting. Autoradiographs (panels 1-3) and the Ponceau S-stained membrane showing PEX5 (panel 4) are presented. No recombinant PEX5 or ^{35}S-labeled catalase were detected in the void volume of this column (fractions 14-15; not shown). The asterisk marks bovine serum albumin added to chromatography fractions before precipitation to control protein recoveries. B) ^{35}S-labeled catalase, synthesized *in vitro* for 55 min and incubated for 4 h at 30 ºC in the presence of cycloheximide, was subjected to SEC. Radiolabeled tCat eluting in fraction 20 (panel 1; boxed lane) was then subjected to a second SEC either alone (panel 2) or after receiving 1 µM recombinant PEX5 (panels 3 and 4). Fractions were processed as described above. Autoradiographs (panels 1-3) and the Ponceau S-stained membrane (panel 4) are presented. C) Soluble proteins from mouse liver peroxisomes were incubated either with recombinant PEX5 or buffer alone and subjected to SEC. Fractions were subjected to SDS-PAGE/western-blotting using antibodies directed to catalase (PerCat) or L-bifunctional protein (LBP). Immunoblots (panels 1-4) and a Ponceau S-stained membrane showing PEX5 (panel 5) are presented. Note that PEX5, a monomeric 70 kDa protein in solution, displays an abnormal behavior upon SEC because a major fraction of its polypeptide chain is natively unfolded.

As shown in Figure 9, mCat (fraction 24) purified by SEC behaves as a monomer when subjected to a second SEC (panel 2). In contrast, in the presence of PEX5 the elution profile of mCat changes, with the radiolabeled protein co-eluting with recombinant PEX5 (panels 3 and 4). Thus, PEX5 interacts with mCat.

In Figure 9B, we present the results obtained with tCat, present in fraction 20 of the first SEC. In this case, the elution profiles in the presence or absence of PEX5 are almost identical suggesting that the interaction between these two proteins is very weak at best (panels 2 to 4). It is noteworthy that tCat is kept under near-equilibrium with recombinant PEX5 during SEC since both proteins co-elute. This should facilitate the formation of a complex between the two proteins.

To extend these observations, we performed the same type of analysis with mouse liver peroxisomal matrix proteins (Figure 9C). After incubation with recombinant PEX5 or buffer alone, peroxisomal matrix proteins were subjected to SEC. The elution profile of mouse catalase in the presence or absence of recombinant PEX5 remains the same (panels 1 and 2). In contrast, the majority of L-bifunctional protein (LBP), a 78 kDa monomeric protein in its native state, co-elutes with PEX5, showing that a complex between these two proteins was formed (panels 3 and 4). Taken together, our results strongly suggest that PEX5 binds stronger to mCat than to tCat.

1.3 – Characterization of the PEX5-mCat interaction

To better understand the PEX5-mCat interaction we performed pulse-chase analysis by incubating *in vitro* synthesized catalase with different recombinant proteins. As shown in Figure 10A, PEX5 at 1 μM blocks catalase tetramerization, as expected. Such an effect is not observed when the 4h incubation is performed in the presence of PEX5(N526K), a mutant PEX5 containing a single missense mutation in the PTS1-binding domain that abolishes its activity. By titrating the PEX5 concentration necessary to produce an effect in catalase tetramerization, we determined that its inhibitory effect is quite strong, with an IC_{50} of about 100 nM (Figure 10B).

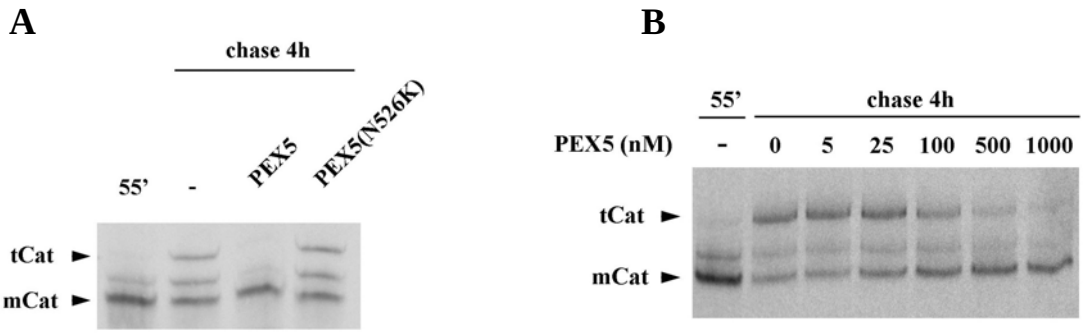

Figure 10: PEX5 inhibits catalase tetramerization. A) ^{35}S-labeled catalase was synthesized *in vitro* for 55 min (lane 55') and chased for 4 h in the absence (lane -) or presence of 1 μM of the indicated recombinant proteins. B) Same as in A) but using the indicated concentrations of PEX5. Samples were analyzed by native-PAGE/autoradiography.

Next, we asked whether the weak PTS1-signal of catalase (KANL) was important for PEX5-catalase interaction. Hence, we produced a mutant version of catalase lacking the PTS1 sequence (CatΔKANL) and performed a pulse-chase analysis, in the presence or absence of 1 μM of recombinant PEX5. As shown in Figure 11, PEX5 is no longer able to inhibit CatΔKANL tetramerization, demonstrating that PEX5 inhibition of catalase tetramerization requires the PTS1 signal of catalase.

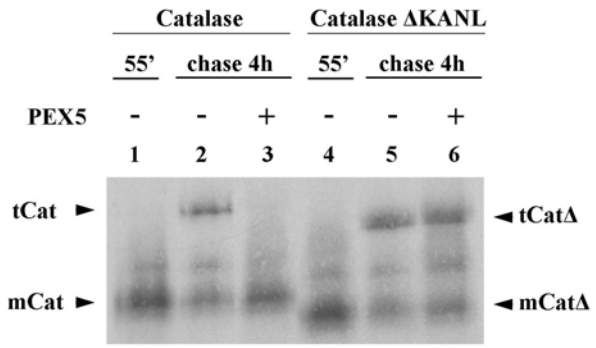

Figure 11: The PTS1 of catalase is required for the interaction with PEX5. Catalase (lanes 1-3) and a truncated version of it lacking the PTS1 signal (catalaseΔKANL; lanes 4-6) were synthesized for 55 min, and chased in the absence (lanes 2 and 5) or presence of 1 μM PEX5 (lanes 3 and 6). Samples were analyzed by native-PAGE/autoradiography. Note that the gel was run for 2.5 hours. mCat and tCat, monomeric and tetrameric versions of catalase, respectively; mCatΔ and tCatΔ, monomeric and tetrameric forms of catalaseΔKANL, respectively.

To better characterize the interaction of PEX5 with mCat we have also performed pulse-chase analyses using full-length PEX5 or PEX5 truncated proteins comprising its N-terminal half (ΔC1PEX5) or its C-terminal half (TPRs) (Figure 12A). As

expected, in the presence of PEX5 no tetramerization is observed (lane 3). The two domains of PEX5 alone do not display the capacity to inhibit catalase tetramerization (lanes 4 and 5), not even when mixed in the same reaction at 1 μM each (lane 6). This last result suggests that the two domains of PEX5 have to be in the same molecule (*i.e.*, they have to be in a *cis* configuration) to display an inhibitory effect in catalase tetramerization at this concentration.

To test this hypothesis, we performed additional tetramerization assays but this time using 200-fold larger concentrations of TPRs and ΔC1PEX5 in the chase incubations. As a negative control we used PEX19, a protein involved in a different aspect of peroxisomal biogenesis. As shown in Figure 12B, TPRs have a strong inhibitory effect on catalase tetramerization at this high concentration while ΔC1PEX5 has a weak but reproducible effect (n=5). These results show that both domains of PEX5 interact with mCat, an interaction that is particularly strong when the two domains reside in the same molecule.

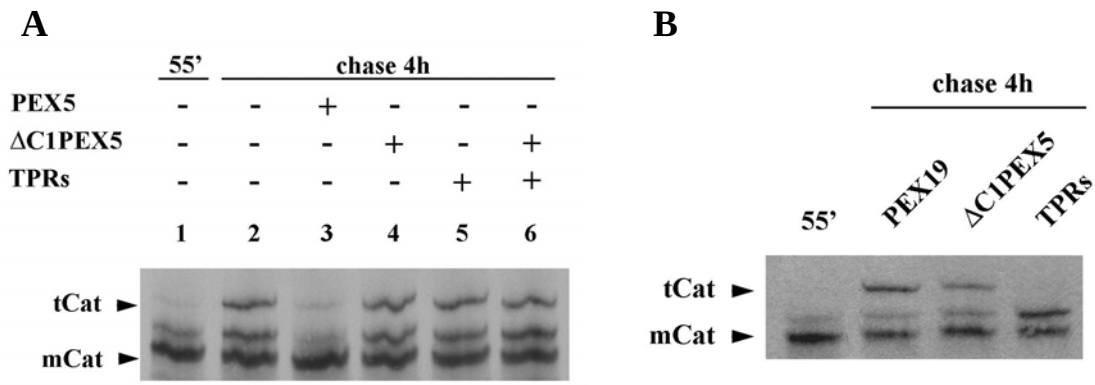

Figure 12: Full-length PEX5 is required to inhibit catalase tetramerization. A) ^{35}S-labeled catalase was synthesized *in vitro* for 55 min (lane 1) and chased in the absence (lane 2) or presence of 1 μM of the indicated recombinant proteins (lanes 3-6). ΔC1PEX5 and TPRs, recombinant proteins comprising the N-terminal and C-terminal half of PEX5, respectively. B) Same as in A) but using 200 μM of the indicated recombinant proteins. Samples were analyzed by native-PAGE/autoradiography.

1.4 – The N-terminal domain of PEX14 disrupts the mCat-PEX5 interaction

As referred in the Introduction section, PEX5 binds newly synthesized peroxisomal proteins in the cytosol, and after docking at the DTM, PEX5 then promotes their translocation across the membrane. Somewhere during or after this event, PEX5 has to release the cargo protein into the organelle matrix. Previous work in yeast suggested that PEX8, a DTM component, might perform this task [186]. However,

mammals do not possess a PEX8 ortholog and therefore the triggering mechanism of this last event is unknown. One can assume that in mammals a DTM component could also be involved in this event. PEX14, an intrinsic membrane protein possessing a single putative transmembrane domain, would be a good candidate. PEX14 has two thirds of its polypeptide chain exposed to the cytosol, whereas its N-terminal third is either embedded in the peroxisomal membrane or exposed to the matrix of the organelle [187, 188]. It is also known that the N-terminal domain of PEX14 (NDPEX14) interacts with seven diaromatic motifs present in the N-terminal half of PEX5 [112-114].

Considering all of these properties, we asked if NDPEX14 affects the PEX5-mCat interaction. In order to address this hypothesis, we used SEC to purify mCat, as before (Figure 13, panel 1) and incubated the radiolabeled protein with 1 μM of recombinant PEX5 to allow the formation of a PEX5-mCat complex. Then, the complex was either incubated with buffer alone or with 15 μM of NDPEX14 and subjected to a second SEC. As observed in Figure 13, in the presence of NDPEX14 (panels 4 and 5), the elution volume of PEX5 decreases indicating that a PEX5-NDPEX14 complex was formed. Importantly, the majority of the mCat elutes now as a monomeric protein, indicating that the complex between PEX5 and mCat was disrupted.

To better understand the interaction between PEX5 and NDPEX14 and its effect in the PEX5-mCat interaction, we produced the following truncated versions of recombinant PEX5 (Figure 14): PEX5ΔN110 (amino acid residues 111-639 of PEX5), PEX5ΔN147 (amino acid residues 148-639 of PEX5) lacking diaromatic motifs 1 and 2, PEX5ΔN196 (amino acid residues 197-639 of PEX5) lacking diaromatic motifs 1 to 4, and PEX5ΔN267 (amino acid residues 268-639 of PEX5) and PEX5ΔN290 (amino acid residues 291-639 of PEX5), both lacking diaromatic motifs 1 to 6.

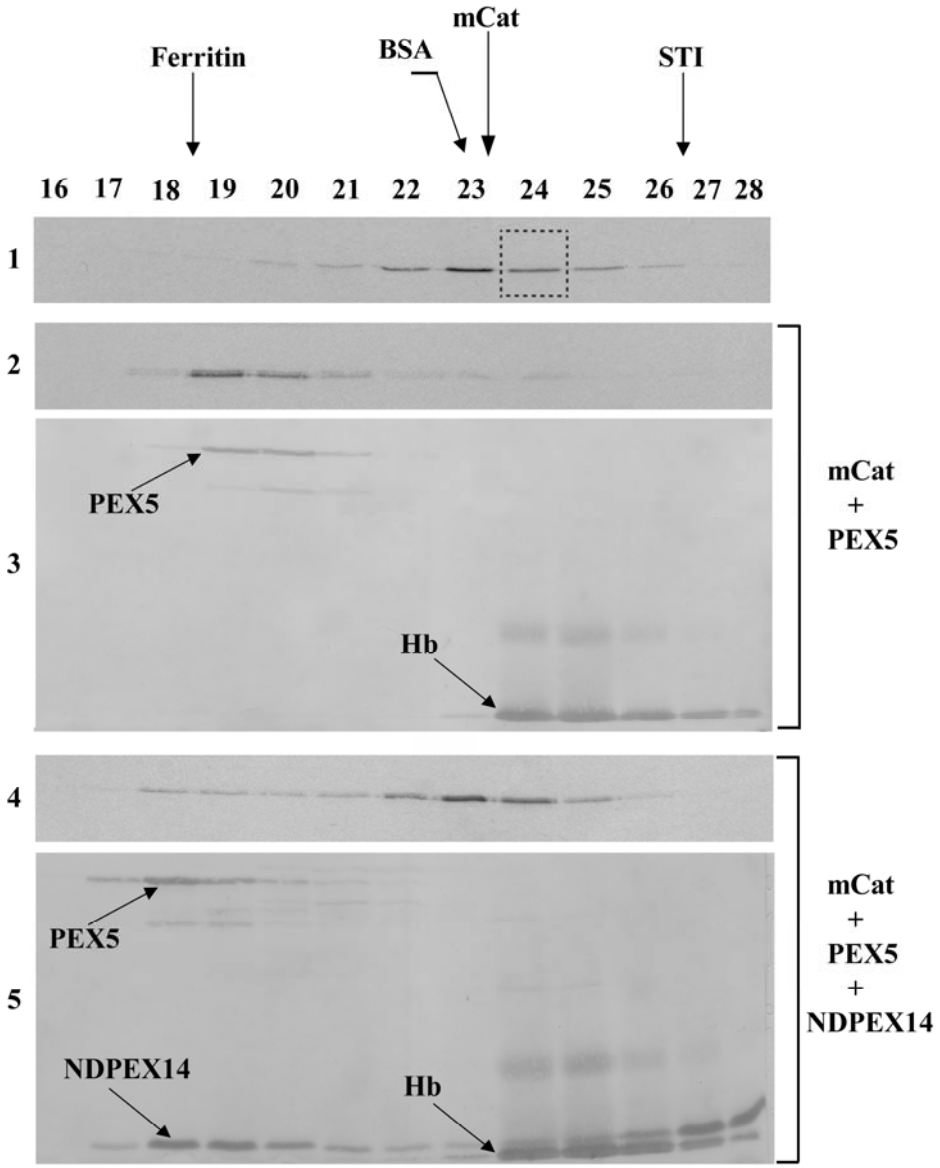

Figure 13: The N-terminal domain of PEX14 disrupts the mCat-PEX5 interaction. ^{35}S-labeled mCat was purified by SEC (panel 1; fraction 24), supplemented with 1 µM recombinant PEX5 and incubated for 30 min at room temperature to generate the PEX5-mCat protein complex. Half of this sample was analyzed directly by SEC (panels 2 and 3). The other half received recombinant NDPEX14 (15 µM) 30 min before chromatography (panels 4 and 5). Fractions were subjected to SDS-PAGE and blotted onto a nitrocellulose membrane. Autoradiographs (panels 1, 2 and 4) and the Ponceau S-stained membranes (panels 3 and 5) are presented. Hb, hemoglobin from the reticulocyte lysate that co-purified with mCat in the first SEC; BSA, bovine serum albumin; STI, Soybean trypsin inhibitor.

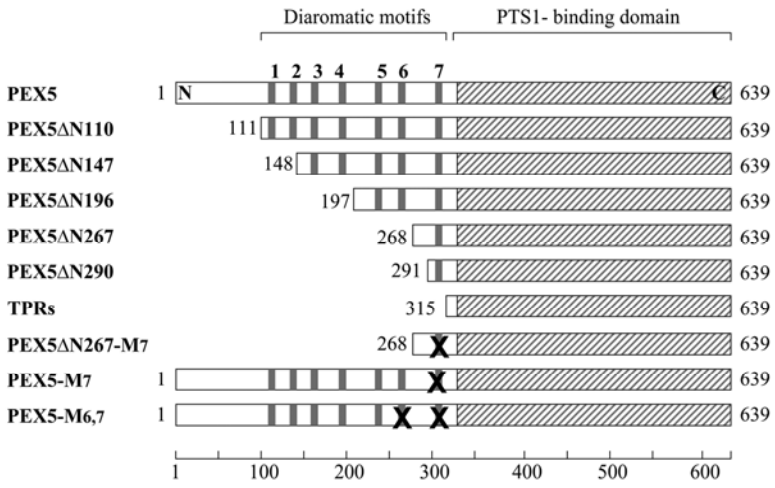

Figure 14: Schematic representation of recombinant PEX5 proteins. The diaromatic motifs in the N-terminal half of PEX5 are numbered 1 to 7. Replacement of tryptophan and phenylalanine/tyrosine residues by alanines in these motifs is indicated by X.

We first assessed the solubility of these proteins and their capacity to interact with NDPEX14. As shown in Figure 15, all proteins analyzed behave as single monodisperse species. In addition, with the exception of TPRs (a protein lacking diaromatic motifs) all truncated PEX5 proteins interact with NDPEX14, as expected.

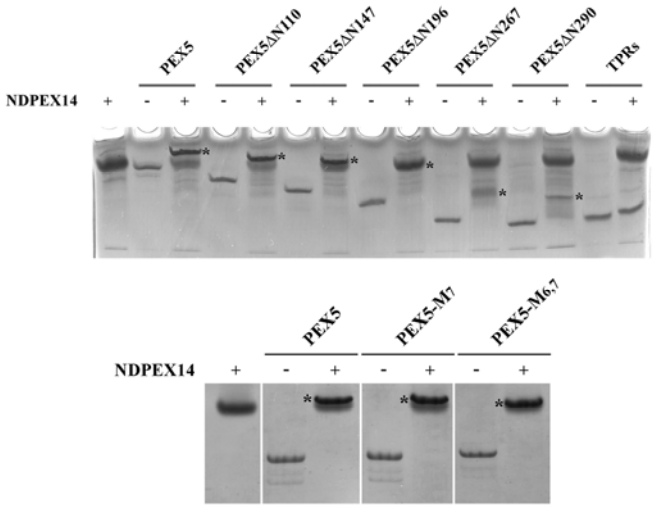

Figure 15: Native-PAGE analysis of recombinant PEX5 proteins. Native-PAGE analysis of the indicated PEX5 proteins (3 µg each) in the absence or presence of recombinant NDPEX14 (12 µg per lane). The asterisks mark the complexes between the recombinant PEX5 proteins and NDPEX14. Coomassie blue-stained gels are shown.

We then assessed the ability of these recombinant PEX5 truncated forms to inhibit catalase tetramerization in the absence or presence of NDPEX14 by native-PAGE analysis. As shown in Figure 16A, PEX5ΔN110, PEX5ΔN147 and PEX5ΔN196 have a similar effect in catalase tetramerization as the full-length protein. In the presence of NDPEX14 this effect was abolished, in a similar way to what has been already observed when using PEX5. PEX5ΔN267, has a partial inhibitory effect in catalase tetramerization but in the presence of NDPEX14 this effect was also abolished. Finally, PEX5ΔN290 has no effect in catalase tetramerization. Taken together these results show that the smallest molecule of PEX5 that still retains the capacity to inhibit catalase tetramerization at low concentration (1 μM) is PEX5ΔN196 and that the region between amino acids 197 and 290 of PEX5 is important in the mCat-PEX5 interaction. In addition, binding of NDPEX14 to PEX5ΔN267 is sufficient to disrupt its interaction with mCat, suggesting that the single diaromatic motif (7^{th}) present in PEX5ΔN267 is important to this interaction.

Knowing this, we produced another version of recombinant PEX5 where we mutated the only diaromatic motif present in PEX5ΔN267. The tryptophan and tyrosine residues were replaced by alanines, to block the binding of NPEX14 [113], resulting in PEX5ΔN267-M7 (Figure 14). Using the same approach to address catalase tetramerization, one observed that this protein no longer inhibits catalase tetramerization (Figure 16B). We assumed that these mutations may have caused some structural/conformational alterations in PEX5. So, we produced a full-length version of PEX5 possessing the same mutation, PEX5-M7 (Figure 14), and tested it in the same assay. Interestingly, as shown in Figure 16C, PEX5-M7 has the same inhibitory effect in catalase tetramerization as PEX5, an effect which is also neutralized by NDPEX14. These results suggest that other regions of PEX5 might compensate for the absence of the 7^{th} diaromatic motif and that at least one of the remaining 6 diaromatic motifs present in PEX5-M7 is involved in the NDPEX14-induced disruption of the mCat-PEX5 interaction.

To identify additional diaromatic motifs involved in the NDPEX14-induced inactivation of PEX5 we produced a full-length version of PEX5 mutated in both the 6^{th} and the 7^{th} diaromatic motifs, PEX5-M6,7 (Figure 14). Using the same approach, we observed that PEX5-M6,7 has a less potent inhibitory effect in catalase tetramerization comparing to PEX5 (Figure 16C). Moreover, NDPEX14 is no longer capable of disrupting the mCat-PEX5-M6,7 interaction. These results suggest that binding of NDPEX14 to the 6^{th} (and probably the 7^{th}) diaromatic motif of PEX5 disrupts mCat-PEX5 interaction.

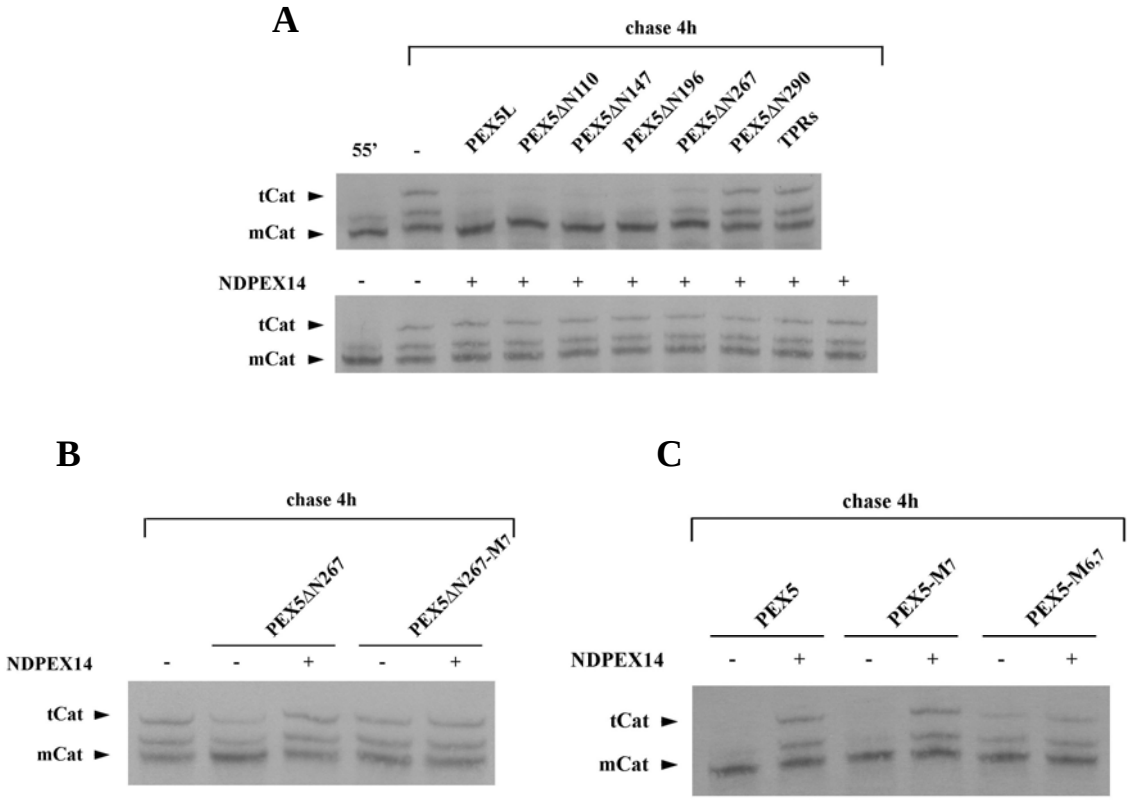

Figure 16: PEX5 diaromatic motifs involved in the NDPEX14-induced disruption of the mCat-PEX5 interaction. A-C) ^{35}S-labeled catalase was synthesized *in vitro* for 55 min (lane 55') and chased for 4 h in the absence (lane -) or presence of 1 µM of the indicated recombinant PEX5 proteins alone or together with NDPEX14 (30 µM). Samples were analyzed by native-PAGE/autoradiography.

2. The interaction of monomeric/oligomeric proteins with the PIM

The data presented in the previous section revealed that PEX5 interacts strongly with monomeric catalase, blocking its tetramerization. Because the amount of cytosolic PEX5 in a cell is probably sufficient to bind mCat and all the other newly synthesized proteins that are *en route* to the organelle (see Discussion), those results raised the interesting possibility that monomeric proteins are the preferred substrate for the PIM, at least at the PEX5 level. Obviously, it could also be that the data on the PEX5-catalase interaction reflects some particularity of this cargo protein and not a general property of peroxisomal matrix proteins. Thus, we decided to characterize the interaction of PEX5 with other cargo proteins. We selected for this task peroxisomal matrix proteins having canonical PTS1 sequences which bind to PEX5 in a much stronger manner than the KANL sequence of catalase [189]. We reasoned that with these cargo proteins we might be able to characterize their import into the organelle. Such an assumption turned out to be correct as described below.

2.1 – ^{35}S-AOX dimerizes *in vitro* and its dimerization is inhibited by PEX5

We first focused our attention in Acyl-CoA oxidase 1 (here after referred to as AOX). AOX is a homodimeric protein in its native state (2 x 72 kDa) with a canonical PTS1 (SKL) at its C-terminal [190, 191].

To determine if dimerization of ^{35}S-AOX occurs *in vitro* and whether this event can be inhibited by PEX5, we synthesized AOX for 30 min, added cycloheximide to stop further protein synthesis, collected a sample and performed a 4 h chase in the presence or absence of 1 μM recombinant PEX5. Due to its alkaline isoelectric point, AOX cannot be analyzed by native-PAGE as catalase. Therefore, AOX samples were analyzed by centrifugation in sucrose gradients.

Four gradients were analyzed: two having a control protein along the gradient to analyze the oligomeric state of AOX (30 min and 4 h chase, in the absence of PEX5, panel 1 and 2); and the other two having 1 μM recombinant PEX5 along the gradient to compare the profile of the 4 h-chased AOX in the presence and absence of PEX5 and simultaneously its interaction with the recombinant protein (panel 3 and 4). As shown in Figure 17, after 30 min of synthesis (panel 1) the AOX population observed displays the behaviour of a 70 kDa globular protein, thus suggesting that AOX is in a monomeric state (mAOX). After a 4 h chase, in the absence of PEX5, we detected a population behaving as a 150 kDa protein (lane 9, panel 2), probably representing the dimeric

form of AOX (dAOX). When the samples were analyzed in a gradient containing recombinant PEX5, we observed that both mAOX and dAOX were shifted towards the bottom of the gradient (panel 3), suggesting that both mAOX and dAOX interact with PEX5. When the 4 h chase is performed in the presence of 1 µM PEX5 (panel 4), the dAOX population is no longer observed, suggesting that PEX5 inhibits AOX dimerization as observed before for catalase.

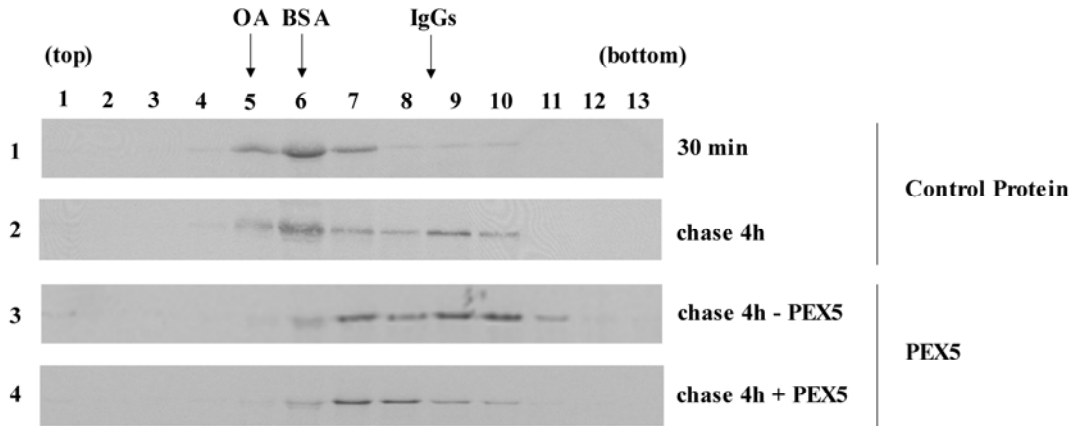

Figure 17: Sucrose gradient sedimentation analysis of ^{35}S-AOX populations. A 30 min reaction and a 4h-chase in the presence or absence of 1 µM of recombinant PEX5 were loaded onto the top of sucrose gradients, supplemented either with a control protein or PEX5. After centrifugation, the fractions were collected from the bottom of the tube, subjected to SDS-PAGE and blotted onto nitrocellulose membranes. Autoradiographs are shown. BSA, bovine serum albumin; OA, ovalbumin; IgGs, immunoglobulins G.

To determine if the second population observed in the sucrose gradients indeed corresponds to dAOX, two different strategies were used. In the first, we used protease assays to monitor the proteolytic profiles of mAOX and dAOX. We performed a titration of PK and also a time-course analysis. As shown in Figure 18A, ^{35}S-mAOX is highly susceptible to PK digestion, even at low concentration of the protease. In contrast, ^{35}S-dAOX has an intrinsic resistance (fragment of 51 kDa) (arrow) to PK digestion even at high concentrations of the protease. Also, when using the maximum concentration of PK (400 µg/ml), mAOX is completely digested just after 5 min of incubation, while dAOX remains resistant even after 40 min of digestion (Figure 18B).

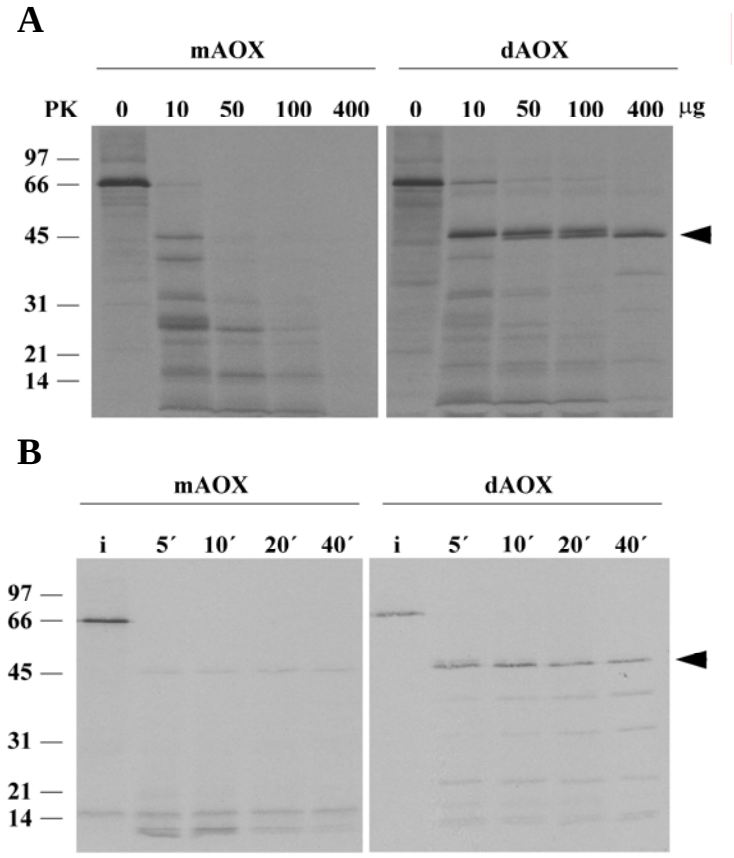

Figure 18: dAOX is intrinsically resistant to protease treatment. A) mAOX and dAOX were isolated from a sucrose gradient, incubated with different concentrations of PK for 40 min. B) mAOX and dAOX were isolated from a sucrose gradient, incubated with 400 µg of PK and different aliquots were removed at the indicated time points. After protease inactivation, all samples were subjected to trichloroacetic acid precipitation and analyzed by SDS-PAGE. Autoradiographs are shown. Numbers on the left indicate the standard molecular weights; i, 5% input.

We performed the same analysis comparing the behaviour of ^{35}S-dAOX with that of native AOX from mouse liver peroxisomes. We performed a PK treatment of purified mouse liver peroxisomes in the presence of Triton X-100 to solubilize the peroxisomal membrane. All samples were analyzed by SDS-PAGE and the membranes were blotted with antibodies against the 51 kDa and the 21 kDa fragments of AOX. As shown in Figure 19, ^{35}S-dAOX displays the same proteolytic profile as the native AOX, as assessed using the antibody against the 51 kDa fragment. The 53 kDa fragment is originated after AOX processing inside the peroxisome, and thus is not present in ^{35}S-dAOX, while the 51 kDa fragment is originated after PK treatment and is the result of intrinsic resistance of the AOX dimer to the protease.

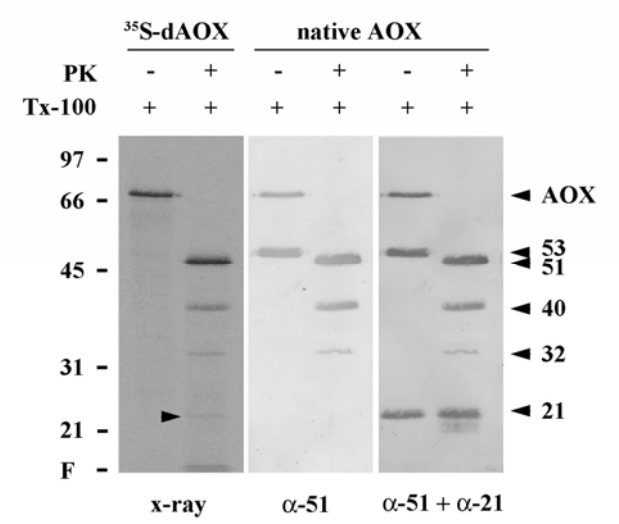

Figure 19: ^{35}S-dAOX behaves as native AOX in protease treatment. ^{35}S-dAOX and native AOX (from purified mouse liver peroxisomes) were subjected to protease treatment in the presence of Triton X-100. Following PK inactivation, the samples were subjected to trichloroacetic acid precipitation and analyzed by SDS-PAGE. For dAOX the autoradiograph is shown and for native AOX immunoblotting against the 51 kDa and 21 kDa fragments of AOX is shown. Numbers on the left indicate the standard molecular weights; F, front of the gel.

Western-blot analisys using the anti-21 kDa fragment antibody, reveals that this domain of native AOX is protease resistant. We were able to detect a similar fragment in the PK-treated ^{35}S-dAOX (arrow head in left panel). The low intensity of this fragment in the autoradiograph can be explained by the fact that only one of the 18 methionines present in AOX is present in this domain of the protein. The finding that ^{35}S-dAOX (but not ^{35}S-mAOX) behaves as native AOX from mouse liver upon protease treatment suggests that the two proteins have similar structures.

In the second strategy, we produced a tagged version of AOX with a 2HA-tag added to its N-terminus (HA-AOX). Then, both HA-AOX and AOX were synthesized individually or together in the presence or absence of 1 μM recombinant PEX5. After the addition of cycloheximide, all samples were subjected to a 4 h chase to allow dimerization to occur. In this experimental setting, if AOX is indeed able to dimerize *in vitro*, one should be able to detect heterodimers comprising HA-AOX and the untagged AOX. As shown in Figure 20, when an immunoprecipitation using an anti-HA antibody was performed using a mixture of the individual proteins, no AOX was co-immunoprecipitated with HA-AOX. However, when proteins are co-synthesized in the absence of PEX5, a fraction of AOX was co-immunoprecipitated with HA-AOX. In agreement with the results obtained for catalase, when the co-synthesis of HA-AOX and AOX is performed in the presence of PEX5 no oligomerization was detected.

Taken together these findings suggest that PEX5 interacts with mAOX, blocking its dimerization.

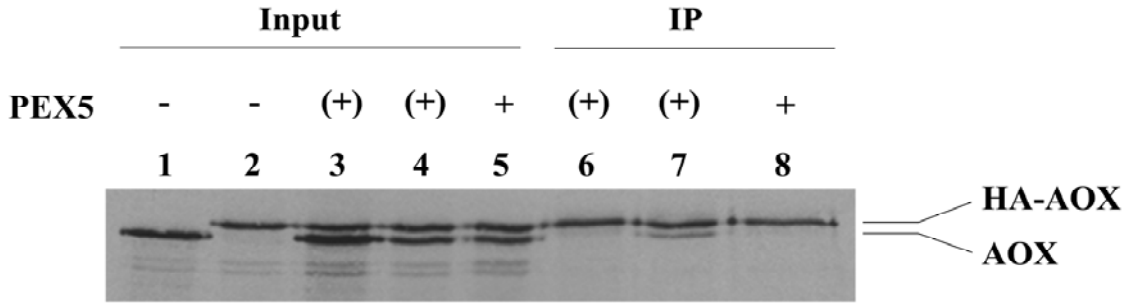

Figure 20: ^{35}S-AOX dimerizes *in vitro*. AOX and HA-AOX were synthesized individually (lanes 1 and 2) and co-translationally in the absence or presence of 1μM of recombinant PEX5 (lanes 4 and 5, respectively) and subjected to a 4 h-chase. A mixture of the two proteins synthesized individually can be observed in lane 3. The samples (lanes 3 to 5) were subjected to immunoprecipitation using an anti-HA antibody agarose beads. The immunoprecipitated proteins (lanes 6 to 8) were washed, eluted from the beads and analyzed by SDS-PAGE. Autoradiograph is shown. -, no PEX5 during synthesis; +, 1 μM PEX5 during synthesis; (+), addition of equivalent amount of PEX5 before the immunoprecipitation.

2.2 – mAOX is a better substrate than dAOX for the peroxisomal matrix protein import machinery

As shown above, we were able to develop a procedure to obtain purified ^{35}S-mAOX and ^{35}S-dAOX. The availability of these two forms of AOX gave us the opportunity to compare the import efficiencies of a cargo protein in its monomeric and oligomeric state. Obviously, we first determined whether or not we could import ^{35}S-AOX using an *in vitro* import system. We performed an *in vitro* import reaction using a rabbit reticulocyte system containing both mAOX and dAOX. The import reaction was performed in the presence of PEX5 and/or other recombinant proteins: PEX5(N526K), NDPEX14, and PEX19 (1-124), a truncated version of PEX19, a protein involved in other aspect of peroxisome biogenesis. As shown in Figure 21, ^{35}S-AOX import is increased in the presence of recombinant PEX5 and, as expected, not in the presence of recombinant PEX5(N526K). When NDPEX14 is added to the reaction there is a significant decrease in the levels of imported AOX. This indicates that NDPEX14 interacts with both endogenous and recombinant PEX5, thus blocking AOX import. Noteworthy, these results show the clear difference between the 53 kDa fragment that is originated from processing of mAOX after import into the organelle (upper arrow) and the 51 kDa fragment that is originated from the intrinsic resistance of dAOX to PK

(lower arrow). The latter is present in all lanes with the same intensity, independently of import conditions, while the 53 kDa fragment is specific of mAOX import and presents a similar behaviour as the full-length AOX.

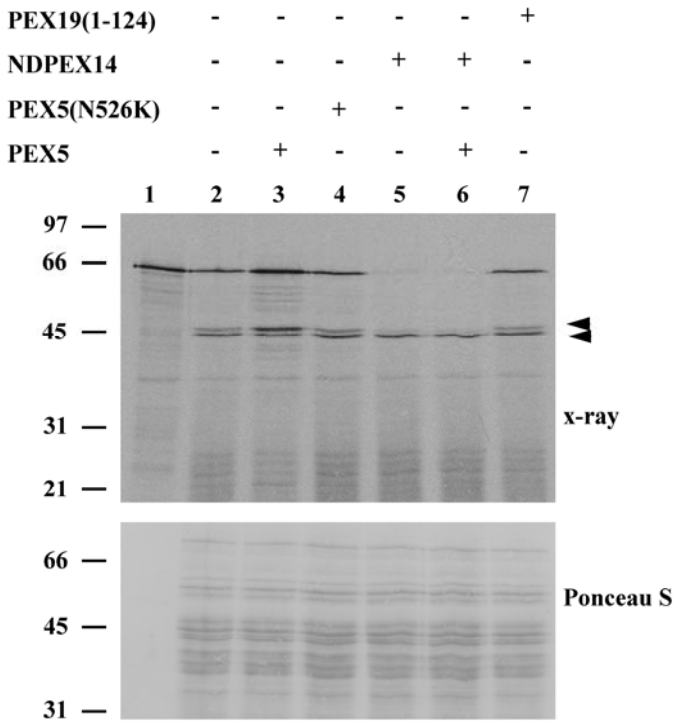

Figure 21: Specificity of the AOX import into the peroxisomes. A rat liver PNS fraction was incubated with a ^{35}S-labeled mixture of mAOX and dAOX in import buffer containing ATP in the absence (lane 2) or presence of recombinant PEX5 (lane 3), PEX5(N526K) (lane 4), NDPEX14 (lane 5), PEX5 and NDPEX14 (lane 6) and PEX19(1-124) (lane 7). After PK treatment, the organelles were isolated by centrifugation, subjected to SDS-PAGE, and blotted onto a nitrocellulose membrane. The Ponceau S-stained membrane (lower panel) and its autoradiograph (upper panel) are shown. Numbers on the left indicate the standard molecular weights.

After confirming that ^{35}S-AOX can be imported using an *in vitro* import system, we performed import reactions using either the mAOX or the dAOX isolated from sucrose gradients. All reactions were performed in the presence of 10 ng of recombinant PEX5, as we found that this amount of PEX5 increases the import yield of AOX by a factor of two (Figure 21, lane 3). Two other recombinant proteins were also used in import assays to assess the specificity of these import reactions. These were TPRs to compete with PEX5 for cargo binding and so to inhibit the import reaction [109] and TPRs(N526K), mutant version of TPRs unable to bind to the PTS1 signal, as a control. Following import, the reactions were divided into two halves. One was subjected to PK treatment whereas the other was left untreated. As shown in Figure

22, in the absence of PK treatment there is no significant difference between the 3 conditions (PEX5, TPRs and TPRsN526K) and between mAOX and dAOX. This is not the case after PK treatment. In the presence of PEX5 we observed that a reasonable amount of mAOX was imported (it is resistant to PK treatment) and that this import is specific since it was inhibited by TPRs and not by TPRs(N526K) (lanes 5 and 6). The same was not observed for dAOX. In this case, we found that most radiolabeled AOX found in organelle pellets (lanes 7-9) was not protected from PK, indicating that most dAOX sedimenting with organelles is simply adsorbed at their surface. Furthermore, although a small fraction of dAOX resisted to PK treatment (lanes 10-12), most of this protease-resistant material was insensitive to the presence of TPRs in the reaction. Thus, we are not sure that this protease-resistant species really represents imported protein.

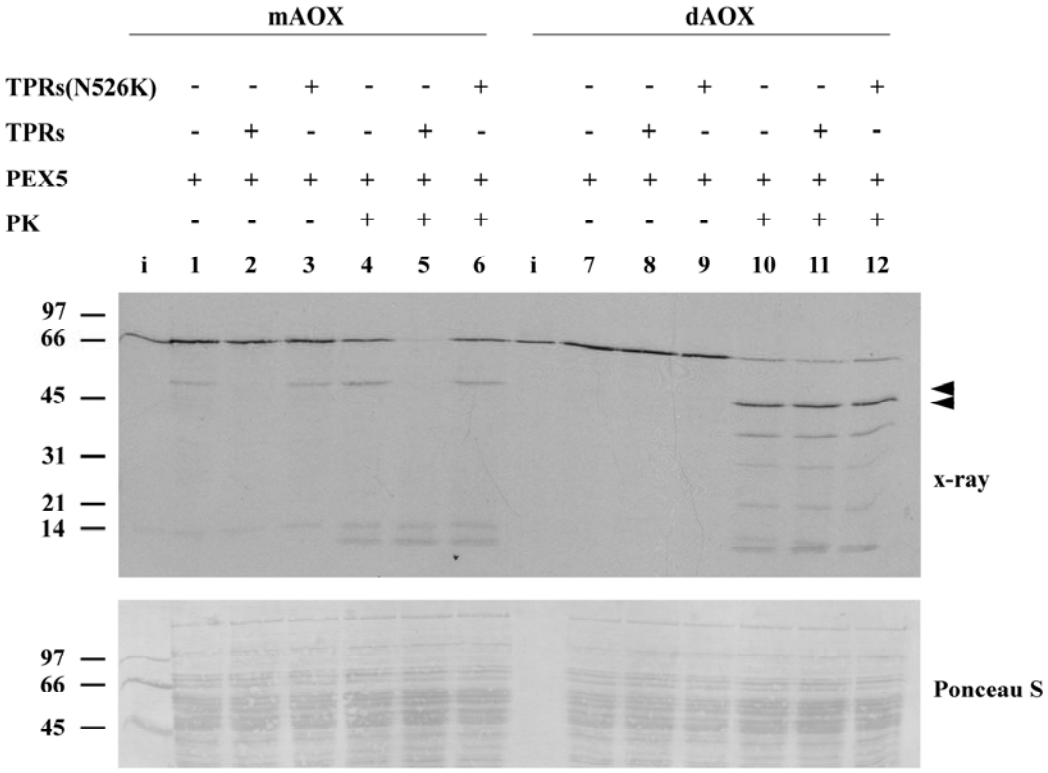

Figure 22: mAOX and dAOX import into peroxisomes. A rat liver PNS fraction was incubated either with ^{35}S-labeled mAOX or dAOX in import buffer containing ATP, in the presence of recombinant PEX5, TPRs or TPRs(N526K). After PK treatment, the organelles were isolated by centrifugation, subjected to SDS-PAGE, and blotted onto a nitrocellulose membrane. The Ponceau S-stained membrane (lower panel) and its autoradiograph (upper panel) are shown. Numbers on the left indicate the standard molecular weights; i, 5% input.

In order to understand if the mAOX is being specifically imported into the peroxisomal compartment, we subjected import reactions programmed with ^{35}S-mAOX

and ^{35}S-dAOX to Nycodenz gradient centrifugation. The gradients were then fractionated and equal volumes of each fraction were analyzed by SDS-PAGE. As shown in Figure 23, catalase, a peroxisomal matrix protein displays a dual behaviour. One fraction is recovered in fractions 2 and 3 (bottom) of the gradient and represents a population of highly pure peroxisomes, and the other peaks at fractions 11 to 14 representing protein that leaked from peroxisomes during PNS preparation/manipulation. In the gradient were mAOX was analyzed, the full-length AOX has a distribution profile similar to catalase, indicating that ^{35}S-AOX was specifically imported into the peroxisomes. Regarding the gradient containing dAOX, we can observe that the majority of the protein was not imported into peroxisomes, being distributed through the top half of the gradient in the form of the 51 kDa fragment resistant to the PK treatment. Taken together these results strongly suggest that mAOX is a better substrate for the peroxisomal import machinery than dAOX.

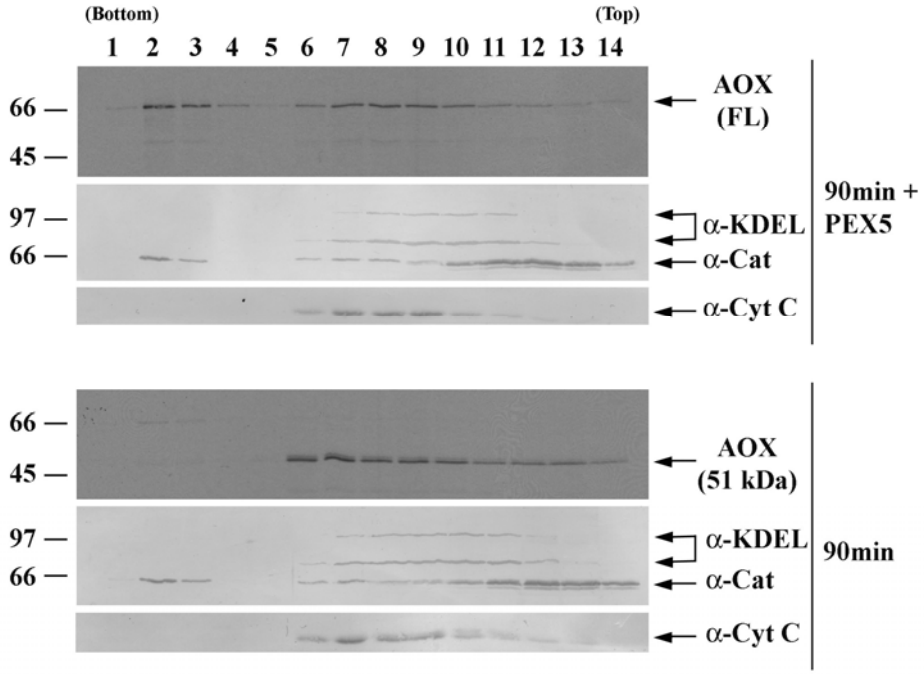

Figure 23: ^{35}S-mAOX is specifically imported into peroxisomes. A PEX5-supplemented PNS fraction was incubated with ^{35}S-labeled AOX in import buffer containing ATP for 45 min. After PK treatment and inactivation of the protease, the complete import mixture was diluted with SEM buffer and subjected to Nycodenz gradient centrifugation. The gradient was then fractionated from the bottom (lane 1) to the top (lane 14), and equal aliquots from each fraction were subjected to SDS-PAGE and Western blotting. The nitrocellulose membrane was exposed to an x-ray film to detect the ^{35}S-labeled protein (x-ray panels) and afterward probed with the following antisera: anti-KDEL (KDEL; recognizes GRP72 and GRP98, two endoplasmic reticulum proteins), anti-cytochrome c (Cyt c; a mitochondrial marker) and anti-catalase (CAT; a peroxisomal enzyme). Note that catalase remaining at the top of the gradient results from leakage of peroxisomes. Numbers on the left indicate the standard molecular weights.

2.3 – PEX5 inhibits UOX tetramerization and mUOX is the preferred substrate for the PIM

We decided to extend our work to another abundant protein of the peroxisomal matrix: urate oxidase (hereafter referred to as UOX). UOX is a protein with four 34 kDa subunits with a canonical PTS1 (SRL) at their C-terminus [7, 10]. We started by synthesizing radiolabeled UOX for 45 min, using the rabbit reticulocyte lysate-based *in vitro* transcription-translation system. After synthesis arrest with cycloheximide, a sample was collected and a 4 h chase was performed. Like AOX, UOX has an alkaline isoelectric point and cannot be analyzed by native-PAGE. The samples were analyzed by centrifugation in sucrose gradients. As shown in Figure 24, after 45 min of synthesis the population observed behaves as a 35 kDa globular protein, suggesting that UOX is in a monomeric state (mUOX). After a 4 h chase, a second population is observed and it behaves as a 150 kDa protein, being probably the tetrameric form of UOX (tUOX).

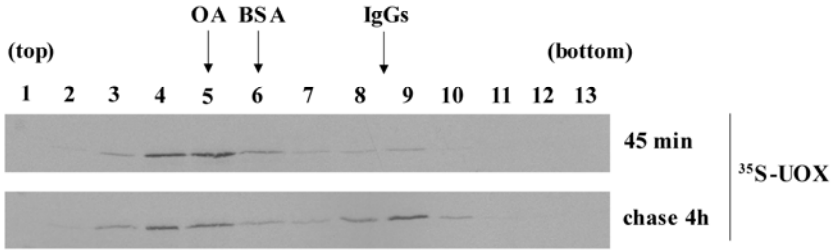

Figure 24: Sucrose gradient sedimentation analysis of ^{35}S-UOX populations. A 45 min reaction and a 4 h-chase in the absence of any recombinant protein were loaded onto the top of sucrose gradients. After centrifugation, the fractions were collected from the bottom of the tube, subjected to SDS-PAGE and blotted onto nitrocellulose membranes. Autoradiographs are shown. BSA, bovine serum albumin; OA, ovalbumin; IgGs, immunoglobulins G.

To determine if the second population observed in the sucrose gradients corresponds to tUOX, we monitored the proteolytic profile of mUOX and tUOX by performing protease assays. Both mUOX and tUOX were isolated from sucrose gradients and incubated with 400 µg of PK. Aliquots were collected at different time points and analyzed by SDS-PAGE. As shown in Figure 25, mUOX is completely susceptible to protease treatment while tUOX is mainly resistant to proteolysis yielding a diffuse double band, displaying an apparent molecular mass almost identical to the one of the intact UOX.

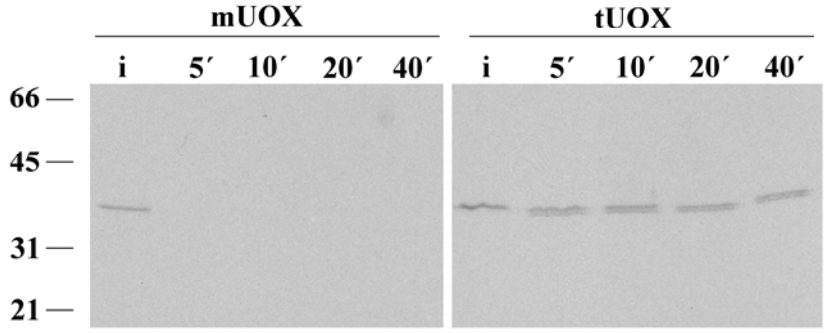

Figure 25: tUOX is resistant to protease treatment. mUOX and tUOX were isolated from a sucrose density gradient centrifugation, incubated with 400 µg of PK and different aliquots were withdrawn at the indicated time points. After inactivation of the protease, all samples were subjected to trichloroacetic acid precipitation and analyzed by SDS-PAGE. Autoradiographs are shown. Numbers on the left indicate the standard molecular weights.

Next, we produced a tagged version of UOX, with a 2HA-tag added to the N-terminal (HA-UOX). We synthesized both untagged UOX and HA-UOX individually or together in the presence or absence of 1 µM recombinant PEX5. After synthesis arrest with cycloheximide, a 4 h chase was performed to allow oligomerization to occur. As described for AOX, we performed an immunoprecipitation using an anti-HA antibody. As shown in Figure 26, when the immunoprecipitation was performed with a mixture of the individual proteins, no UOX was co-precipitated with HA-UOX. Oligomers were detected only when both UOX and HA-UOX were co-synthesized in the absence of PEX5. In the presence of PEX5, UOX oligomerization was no longer detected.

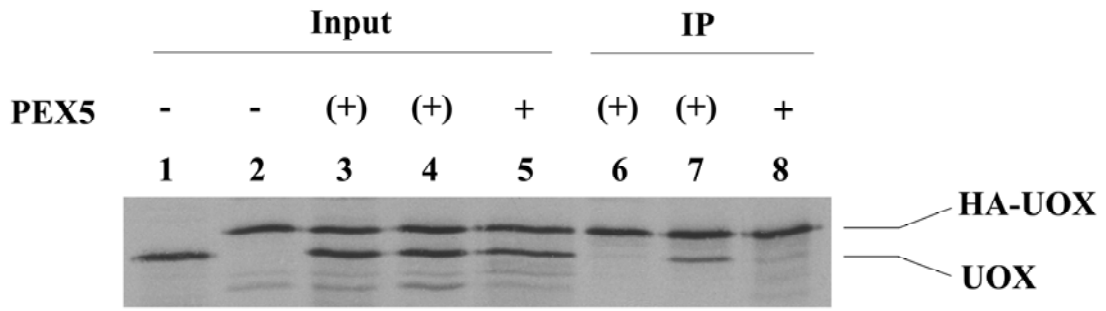

Figure 26: ^{35}S-UOX tetramerizes *in vitro*. UOX and HA-UOX were synthesized individually (lanes 1 and 2) and in a co-translation reaction in the absence or presence of 1µM of recombinant PEX5 (lanes 4 and 5, respectively) and subjected to a 4 h chase. A mixture of the two proteins synthesized individually can be observed in lane 3. The samples (lanes 3 to 5) were subjected to immunoprecipitation using an anti-HA antibody agarose beads. The immunoprecipitated proteins (lanes 6 to 8) were washed, eluted from the beads and analyzed by SDS-PAGE. Autoradiograph is shown. -, no PEX5 during synthesis; +, 1 µM PEX5 during synthesis; (+), addition of equivalent amount of PEX5 before the immunoprecipitation.

Having both mUOX and tUOX isolated from sucrose gradients, we were able to compare the import efficiencies of these proteins by performing *in vitro* import reactions. All reactions were performed in the presence of 50 ng of PEX5 to increase import yield. As described for AOX, TPRs and TPRs(N526K) were added to the reactions when needed. Following import, the reactions were divided into two halves. One was subjected to PK treatment whereas the other was left untreated. As shown in Figure 27, in the absence of PK treatment there is no significant difference between the 3 conditions (PEX5, TPRs and TPRsN526K) and between mUOX and tUOX. After PK treatment, in the presence of PEX5 we observed a small amount of mUOX that presents PK resistance, indicating that it is was imported (lane 4). This import is specific since it was inhibit by TPRs and not by TPRs(N526K) (lanes 5 and 6). For tUOX the same result was not observed. Taken together these results show that, like AOX, PEX5-UOX interaction inhibits its tetramerization and that mUOX is the preferred substrate for the matrix protein import machinery.

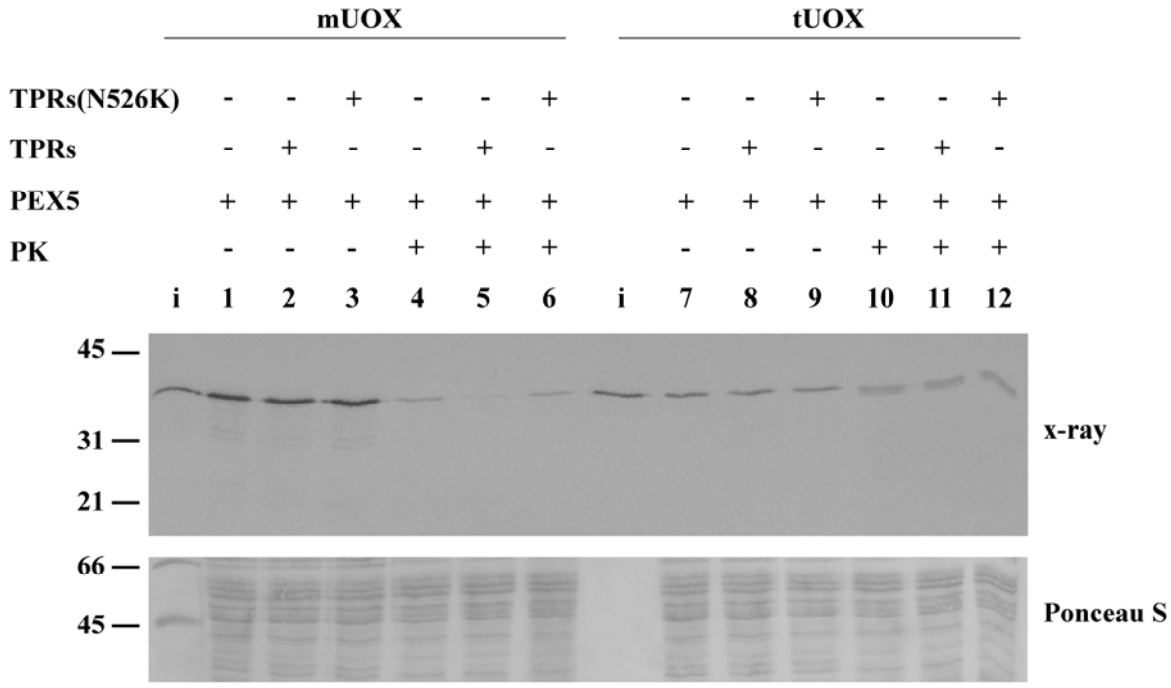

Figure 27: mUOX and tUOX import into peroxisomes. A rat liver PNS fraction was incubated with ^{35}S-labeled mUOX or tUOX, individually, in import buffer containing ATP, in the presence of recombinant PEX5, TPRs or TPRs(N526K). After PK treatment, the organelles were isolated by centrifugation, subjected to SDS-PAGE, and blotted onto a nitrocellulose membrane. The Ponceau S-stained membrane (lower panel) and its autoradiograph (upper panel) are shown. Numbers on the left indicate the standard molecular weights; i, 5% input.

V. DISCUSSION

In this work we used an *in vitro* approach to characterize the PEX5-cargo protein interaction. As previously mentioned, whether PEX5 binds to monomeric or oligomeric versions of the matrix proteins was still a controversial subject. Our results show that, at least for three very abundant peroxisomal matrix proteins (cat, AOX and UOX), PEX5 binding to the monomeric version of these proteins inhibits their oligomerization. This PEX5 characteristic was best addressed using catalase. The proposed mechanism for the catalase assembly pathway consists of three steps: 1) apo-monomers + heme → holomonomers; 2) holomonomers → holodimers; 3) holodimers → holotetramers (reviewed in [192]). Our results suggest that in the presence of PEX5 step 2 no longer occurs.

When evaluating the affinity of PEX5 for both mCat and tCat, we found that the PEX5-mCat interaction is favored. In this work we show that not only the C-terminal but also the N-terminal half of PEX5 has a role in PEX5-mCat interaction, specially since the inhibitory effect in catalase tetramerization is increased when both domains are in the same molecule. In the literature, we can find several data suggesting that the interaction of the N-terminal half of PEX5 with catalase is also observed in other organisms. In yeast, Kragler and co-workers showed that catalase possesses not only the PTS signal at its C-terminal but also another peroxisomal targeting information at its N-terminal [120]. In plants, it was observed that the last four residues of cottonseed catalase are sufficient to target a reporter protein to the peroxisome [193]. These residues are conserved in pumpkin catalase. However, this protein was also shown to interact with the N-terminal half of PEX5 [121]. Taken together, the results suggest that PEX5 possesses more than one catalase-interacting domain.

In order to corroborate these observations, we also addressed this issue using two other major matrix proteins, AOX and UOX. Our results show that PEX5 also inhibits their oligomerization. This PEX5 property is only relevant if the amount of cytosolic PEX5 in a cell is enough to sequester all newly synthesized peroxisomal proteins *en route* to the organelle. We estimated that the cytosolic concentration of PEX5 in rat hepatocytes is 0.75 μM and that the concentration of newly synthesized peroxisomal proteins is in a range of 0.73 – 0.83 μM (see Miscelaneous in “Experimental Procedures”). Taken together our experimental results and these estimated values, we proposed that PEX5 binds peroxisomal matrix proteins immediately after their synthesis keeping them in a monomeric state.

Next, we evaluated which was the best substrate to the matrix protein import machinery. The work performed with AOX and UOX suggests that the monomer is the preferred substrate for the PIM. The results presented here thus corroborate and extend the observations of Lazarow and de Duve [152, 153]. Indeed, using pulse-

chase analysis, these authors were able to show that the major pathway for catalase import involved the translocation of monomeric catalase across the peroxisomal membrane. Two other studies suggest that the monomeric version of a given protein is imported into the organelle: malate synthase in cucumber glyoxysomes [154] and alcohol oxidase in the methylotrophic yeast *Candida boidinii* [155].

Many studies have shown that peroxisomes can import already oligomerized proteins. However, those studies were conducted under protein over-expression conditions, frequently using very strong promoters to drive expression of the protein being analyzed [158, 161, 184, 194]. It is therefore possible that the observed import of oligomerized proteins is the result of an artificial situation in which PEX5 or other components of the PIM become stoichiometrically limiting. Despite these limitations, many authors proposed that only already folded proteins can be imported into the organelle [185]. According to those authors, the “proff-of-concept” for this model comes from the work of Danpure and co-workers on alanine-glyoxylate aminotransferase (AGT) [195, 196]. Indeed, it was proposed that AGT has to dimerize in the cytosol before import. The data behind this idea comes from the observation that mutations that affect dimerization of AGT result in the degradation or mistargeting of the protein, leading to the mistargeting of the protein to the mitochondria. This results in the hereditary kidney-stone disease primary hyperoxaluria type 1. Unfortunately, those authors never considered the possibility that mutations affecting the dimerization of AGT may also affect the structure of monomeric AGT, and thus, the interactions of these mutant proteins with cytosolic chaperones and PEX5 itself.

Another caveat of the studies mentioned above regards import kinetics of oligomerized cargo proteins. In fact, only the work performed with chloramphenicol acetyltransferase (CAT) by Goodman and co-workers addressed this important question [159]. In that work, the import of trimeric CAT, measured by immunoelectron microscopy and organellar fractionation, was shown to occur over several hours, in contrast with the import of other peroxisomal proteins [152, 153, 155]. In our work, we compare the import efficiency of monomeric and oligomeric versions of two peroxisomal matrix proteins. Even though we cannot exclude that peroxisomes can import already folded proteins, our results strongly suggest that the monomers are the preferred substrate for the peroxisomal import machinery.

The strong binding of PEX5 to the monomeric version of peroxisomal matrix proteins, inhibiting their oligomerization, resembles the properties of a chaperone protein. In this regard, it is interesting to note that this capacity of PEX5 of inhibiting cargo proteins oligomerization evokes the properties of a family of bacterial chaperones functioning in type III secretion systems. The type III secretion pathway is

used by several pathogenic bacteria to deliver proteins to the eukaryotic cells with which they interact. The proteins that will be secreted are synthesized in the cytosol, where they have to be stabilized and separated from other interaction partners to be kept in a secretion-competent state. Chaperones, without any energetic requirement, have an important role by associating in the cytosol with these proteins before their secretion. There are several types of chaperones in this secretion system, some them possessing TPR motifs ([197, 198] and reviewed in [199]). The interaction between these chaperones and the proteins is crucial for the secretion itself since it prevents premature or incorrect interactions. A parallelism can thus be established with PEX5 and peroxisomal matrix proteins, i.e., PEX5 prevents the interaction between the monomers of a given protein until they reach the matrix of the organelle.

PEX14, a central component of the DTM, was seen for many years as a protein involved only in the docking of the receptor at the peroxisomal membrane [19]. However, several observations showed that this protein also has a role in the translocation of cargo proteins across the membrane of the organelle [139, 200]. Our results show that the N-terminal domain of human PEX14 disrupts the PEX5-mCat interaction. Data reported earlier for *Leishmania donovani* PEX5 showed that its affinity for a PTS1 protein is decreased in the presence of PEX14 [201]. Taken together, these results suggest another function for this membrane protein, a role in the release of cargoes from DTM-embedded PEX5 into the peroxisomal matrix (Figure 28).

From the seven diaromatic motifs present in human PEX5, only one or two have a major role in the NDPEX14-induced disruption of the mCat-PEX5 interaction. Previous data showed that diaromatic motifs 2–4 of PEX5 are required for catalase import in vivo [112]. Taken together, these results suggest that several interactions are occurring in a sequential manner between the N-terminal domain of peroxisomal PEX14 and the diaromatic motifs present in PEX5 and may serve two different purposes. According to this hypothetical model, the first set of interactions may contribute to the docking/insertion of the PEX5-cargo protein complex into the DTM; subsequently, binding of additional PEX14 molecules to the 6th (and probably 7th) diaromatic motif(s) of PEX5 would trigger the release of the cargo protein into the peroxisomal matrix.

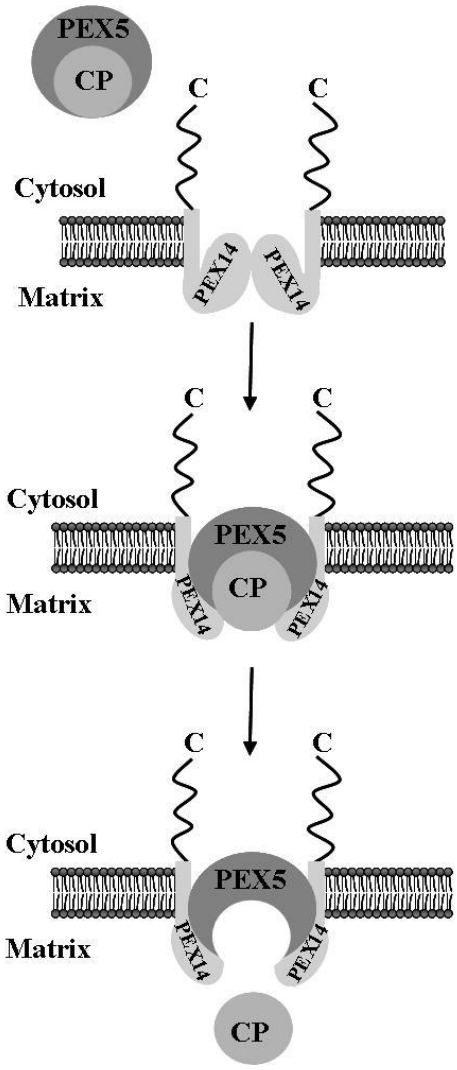

Figure 28: Role of PEX14 in the release of cargo proteins into the peroxisomal matrix. A newly synthesized cargo protein (CP) is recognized by PEX5 in the cytosol. This protein complex then docks at, and becomes inserted into the peroxisomal DTM of which only PEX14 is shown for simplicity. The DTM component(s) providing the docking site for the PEX5-cargo protein complex have not been unambiguously identified yet. As discussed elsewhere, two strong candidates for this role are PEX13 [138] and PEX14 itself [202, 203]. Note that PEX13 may also participate in the cargo-release step [112]. The multiple interactions of PEX5 with the N-terminal domain of the several PEX14 molecules present in the DTM ultimately trigger the release of the cargo into the peroxisomal matrix.

VI. CONCLUDING REMARKS

In this work we have demonstrated that:

- PEX5 interacts with the monomeric version of three matrix proteins (Cat, AOX and UOX) and inhibits their oligomerization;

- The N-terminal of PEX5 has a role in cargo-binding;

- NDPEX14 disrupts the mCat-PEX5 interaction, through the binding to the 6th (and probably the 7th) diaromatic motif of PEX5;

- mAOX and mUOX are the preferred substrates for the peroxisomal import machinery.

Numerous data have been gathered concerning the matrix protein import pathway. This work provides new insights into this pathway by showing a new property of PEX5. This chaperone characteristic defines an important new role to the cytosolic receptor.

Even more, this work elucidated the controversial subject of monomeric or oligomeric import, since it showed that even though oligomers might be imported, the monomers are the preferred substrate for the import machinery.

VII. REFERENCES

1. Rhodin, J., *Correlation of ultrastructural organization and function in normal and experimentally changed proximal convoluted tubule cells of the mouse kidney.* 1954, Karolinska Institutet: Aktiebolaget Godvil, Stockholm.
2. De Duve, C. and P. Baudhuin, *Peroxisomes (microbodies and related particles).* Physiol Rev, 1966. **46**(2): p. 323-57.
3. Lazarow, P.B. and Y. Fujiki, *Biogenesis of peroxisomes.* Annu Rev Cell Biol, 1985. **1**: p. 489-530.
4. Purdue, P.E. and P.B. Lazarow, *Peroxisome biogenesis.* Annu Rev Cell Dev Biol, 2001. **17**: p. 701-52.
5. Fahimi, H.D., et al., *Contributions of the immunogold technique to investigation of the biology of peroxisomes.* Histochem Cell Biol, 1996. **106**(1): p. 105-14.
6. Schrader, M., et al., *The importance of microtubules in determination of shape and intracellular distribution of peroxisomes.* Ann N Y Acad Sci, 1996. **804**: p. 669-71.
7. Schrader, M., et al., *Expression of PEX11beta mediates peroxisome proliferation in the absence of extracellular stimuli.* J Biol Chem, 1998. **273**(45): p. 29607-14.
8. Schrader, M., K. Krieglstein, and H.D. Fahimi, *Tubular peroxisomes in HepG2 cells: selective induction by growth factors and arachidonic acid.* Eur J Cell Biol, 1998. **75**(2): p. 87-96.
9. Schrader, M. and H.D. Fahimi, *Mammalian peroxisomes and reactive oxygen species.* Histochem Cell Biol, 2004. **122**(4): p. 383-93.
10. Chang, C.C., et al., *Metabolic control of peroxisome abundance.* J Cell Sci, 1999. **112 (Pt 10)**: p. 1579-90.
11. Wanders, R.J., et al., *Peroxisomal disorders in neurology.* J Neurol Sci, 1988. **88**(1-3): p. 1-39.
12. Lazarow, P.B. and C. De Duve, *A fatty acyl-CoA oxidizing system in rat liver peroxisomes; enhancement by clofibrate, a hypolipidemic drug.* Proc Natl Acad Sci U S A, 1976. **73**(6): p. 2043-6.
13. Wanders, R.J., et al., *Peroxisomal very long-chain fatty acid beta-oxidation in human skin fibroblasts: activity in Zellweger syndrome and other peroxisomal disorders.* Clin Chim Acta, 1987. **166**(2-3): p. 255-63.
14. Poirier, Y., et al., *Peroxisomal beta-oxidation--a metabolic pathway with multiple functions.* Biochim Biophys Acta, 2006. **1763**(12): p. 1413-26.
15. Biardi, L., et al., *Mevalonate kinase is predominantly localized in peroxisomes and is defective in patients with peroxisome deficiency disorders.* J Biol Chem, 1994. **269**(2): p. 1197-205.

16. Krisans, S.K., et al., *Farnesyl-diphosphate synthase is localized in peroxisomes.* J Biol Chem, 1994. **269**(19): p. 14165-9.
17. Brites, P., H.R. Waterham, and R.J. Wanders, *Functions and biosynthesis of plasmalogens in health and disease.* Biochim Biophys Acta, 2004. **1636**(2-3): p. 219-31.
18. Mannaerts, G.P. and P.P. Van Veldhoven, *Role of peroxisomes in mammalian metabolism.* Cell Biochem Funct, 1992. **10**(3): p. 141-51.
19. Sacksteder, K.A. and S.J. Gould, *The genetics of peroxisome biogenesis.* Annu Rev Genet, 2000. **34**: p. 623-652.
20. van den Bosch, H., et al., *Biochemistry of peroxisomes.* Annu Rev Biochem, 1992. **61**: p. 157-97.
21. Wanders, R.J. and H.R. Waterham, *Biochemistry of mammalian peroxisomes revisited.* Annu Rev Biochem, 2006. **75**: p. 295-332.
22. Tolbert, N.E., *Metabolic pathways in peroxisomes and glyoxysomes.* Annu Rev Biochem, 1981. **50**: p. 133-57.
23. Tolbert, N.E. and E. Essner, *Microbodies: peroxisomes and glyoxysomes.* J Cell Biol, 1981. **91**(3 Pt 2): p. 271s-283s.
24. Kamada, T., et al., *Functional differentiation of peroxisomes revealed by expression profiles of peroxisomal genes in Arabidopsis thaliana.* Plant Cell Physiol, 2003. **44**(12): p. 1275-89.
25. Reumann, S. and A.P. Weber, *Plant peroxisomes respire in the light: some gaps of the photorespiratory C2 cycle have become filled--others remain.* Biochim Biophys Acta, 2006. **1763**(12): p. 1496-510.
26. Michels, P.A., V. Hannaert, and F. Bringaud, *Metabolic aspects of glycosomes in trypanosomatidae - new data and views.* Parasitol Today, 2000. **16**(11): p. 482-9.
27. Parsons, M., *Glycosomes: parasites and the divergence of peroxisomal purpose.* Mol Microbiol, 2004. **53**(3): p. 717-24.
28. Opperdoes, F.R., *Compartmentation of carbohydrate metabolism in trypanosomes.* Annu Rev Microbiol, 1987. **41**: p. 127-51.
29. Jedd, G. and N.H. Chua, *A new self-assembled peroxisomal vesicle required for efficient resealing of the plasma membrane.* Nat Cell Biol, 2000. **2**(4): p. 226-31.
30. Wanders, R.J., *Metabolic and molecular basis of peroxisomal disorders: a review.* Am J Med Genet A, 2004. **126A**(4): p. 355-75.
31. Wanders, R.J., *Peroxisomes, lipid metabolism, and peroxisomal disorders.* Mol Genet Metab, 2004. **83**(1-2): p. 16-27.

32. Steinberg, S.J., et al., *Peroxisome biogenesis disorders.* Biochim Biophys Acta, 2006. **1763**(12): p. 1733-48.
33. Wanders, R.J. and H.R. Waterham, *Peroxisomal disorders: the single peroxisomal enzyme deficiencies.* Biochim Biophys Acta, 2006. **1763**(12): p. 1707-20.
34. Weller, S., S.J. Gould, and D. Valle, *Peroxisome biogenesis disorders.* Annu Rev Genomics Hum Genet, 2003. **4**: p. 165-211.
35. Ebberink, M.S., et al., *A novel defect of peroxisome division due to a homozygous non-sense mutation in the PEX11beta gene.* J Med Genet, 2012. **49**(5): p. 307-13.
36. Lazarow, P.B. and H.W. Moser, *Disorders of Peroxisome Biogenesis*, in *The Metabolic Basis of Inherited Disease*, C.R. Sriver, et al., Editors. 1995, McGraw-Hill: New York. p. 2287-2324.
37. Santos, M.J., et al., *Peroxisomal membrane ghosts in Zellweger syndrome--aberrant organelle assembly.* Science, 1988. **239**(4847): p. 1536-8.
38. Salomons, F.A., et al., *Peroxisomal remnant structures in Hansenula polymorpha Pex5 cells can develop into normal peroxisomes upon induction of the PTS2 protein amine oxidase.* J Biol Chem, 2001. **276**(6): p. 4190-8.
39. Yamasaki, M., et al., *Formation of peroxisomes from peroxisomal ghosts in a peroxisome-deficient mammalian cell mutant upon complementation by protein microinjection.* J Biol Chem, 1999. **274**(50): p. 35293-6.
40. Waterham, H.R. and M.S. Ebberink, *Genetics and molecular basis of human peroxisome biogenesis disorders.* Biochim Biophys Acta, 2012. **1822**(9): p. 1430-41.
41. Purdue, P.E., et al., *Rhizomelic chondrodysplasia punctata, a peroxisomal biogenesis disorder caused by defects in Pex7p, a peroxisomal protein import receptor: a minireview.* Neurochem Res, 1999. **24**(4): p. 581-6.
42. Fujiki, Y., R.A. Rachubinski, and P.B. Lazarow, *Synthesis of a major integral membrane polypeptide of rat liver peroxisomes on free polysomes.* Proc Natl Acad Sci U S A, 1984. **81**(22): p. 7127-31.
43. Suzuki, Y., et al., *Biosynthesis of membrane polypeptides of rat liver peroxisomes.* J Biochem, 1987. **101**(2): p. 491-6.
44. Eckert, J.H. and R. Erdmann, *Peroxisome biogenesis.* Rev Physiol Biochem Pharmacol, 2003. **147**: p. 75-121.
45. Elgersma, Y., et al., *An efficient positive selection procedure for the isolation of peroxisomal import and peroxisome assembly mutants of Saccharomyces cerevisiae.* Genetics, 1993. **135**(3): p. 731-40.

46. Erdmann, R., et al., *Isolation of peroxisome-deficient mutants of Saccharomyces cerevisiae.* Proc Natl Acad Sci U S A, 1989. **86**(14): p. 5419-23.
47. Gould, S.J., et al., *Development of the yeast Pichia pastoris as a model organism for a genetic and molecular analysis of peroxisome assembly.* Yeast, 1992. **8**(8): p. 613-28.
48. Kalish, J.E., et al., *Characterization of a novel component of the peroxisomal protein import apparatus using fluorescent peroxisomal proteins.* EMBO J, 1996. **15**(13): p. 3275-85.
49. Liu, H., et al., *An efficient screen for peroxisome-deficient mutants of Pichia pastoris.* J Bacteriol, 1992. **174**(15): p. 4943-51.
50. Nuttley, W.M., et al., *The PAH2 gene is required for peroxisome assembly in the methylotrophic yeast Hansenula polymorpha and encodes a member of the tetratricopeptide repeat family of proteins.* Gene, 1995. **160**(1): p. 33-9.
51. Dodt, G., et al., *From expressed sequence tags to peroxisome biogenesis disorder genes.* Ann N Y Acad Sci, 1996. **804**: p. 516-23.
52. Brown, L.A. and A. Baker, *Shuttles and cycles: transport of proteins into the peroxisome matrix (review).* Mol Membr Biol, 2008. **25**(5): p. 363-75.
53. Kiel, J.A., M. Veenhuis, and I.J. van der Klei, *PEX genes in fungal genomes: common, rare or redundant.* Traffic, 2006. **7**(10): p. 1291-303.
54. Schluter, A., et al., *The evolutionary origin of peroxisomes: an ER-peroxisome connection.* Mol Biol Evol, 2006. **23**(4): p. 838-45.
55. Lazarow, P.B., *Peroxisome biogenesis: advances and conundrums.* Curr Opin Cell Biol, 2003. **15**(4): p. 489-97.
56. Tabak, H.F., et al., *Formation of peroxisomes: present and past.* Biochim Biophys Acta, 2006. **1763**(12): p. 1647-54.
57. Koch, A., et al., *Peroxisome elongation and constriction but not fission can occur independently of dynamin-like protein 1.* J Cell Sci, 2004. **117**(Pt 17): p. 3995-4006.
58. Koch, A., et al., *Dynamin-like protein 1 is involved in peroxisomal fission.* J Biol Chem, 2003. **278**(10): p. 8597-605.
59. Motley, A.M. and E.H. Hettema, *Yeast peroxisomes multiply by growth and division.* J Cell Biol, 2007. **178**(3): p. 399-410.
60. Van Ael, E. and M. Fransen, *Targeting signals in peroxisomal membrane proteins.* Biochim Biophys Acta, 2006. **1763**(12): p. 1629-38.

61. Halbach, A., et al., *Targeting of the tail-anchored peroxisomal membrane proteins PEX26 and PEX15 occurs through C-terminal PEX19-binding sites.* J Cell Sci, 2006. **119**(Pt 12): p. 2508-17.
62. Fujiki, Y., et al., *Import of peroxisomal membrane proteins: the interplay of Pex3p- and Pex19p-mediated interactions.* Biochim Biophys Acta, 2006. **1763**(12): p. 1639-46.
63. Honsho, M., T. Hiroshige, and Y. Fujiki, *The membrane biogenesis peroxin Pex16p. Topogenesis and functional roles in peroxisomal membrane assembly.* J Biol Chem, 2002. **277**(46): p. 44513-24.
64. Pinto, M.P., et al., *The import competence of a peroxisomal membrane protein is determined by Pex19p before the docking step.* J Biol Chem, 2006. **281**(45): p. 34492-502.
65. Shibata, H., et al., *Domain architecture and activity of human Pex19p, a chaperone-like protein for intracellular trafficking of peroxisomal membrane proteins.* J Biol Chem, 2004. **279**(37): p. 38486-94.
66. Fransen, M., et al., *Human pex19p binds peroxisomal integral membrane proteins at regions distinct from their sorting sequences.* Mol Cell Biol, 2001. **21**(13): p. 4413-24.
67. Gloeckner, C.J., et al., *Human adrenoleukodystrophy protein and related peroxisomal ABC transporters interact with the peroxisomal assembly protein PEX19p.* Biochem Biophys Res Commun, 2000. **271**(1): p. 144-50.
68. Jones, J.M., J.C. Morrell, and S.J. Gould, *PEX19 is a predominantly cytosolic chaperone and import receptor for class 1 peroxisomal membrane proteins.* J Cell Biol, 2004. **164**(1): p. 57-67.
69. Matsuzono, Y., T. Matsuzaki, and Y. Fujiki, *Functional domain mapping of peroxin Pex19p: interaction with Pex3p is essential for function and translocation.* J Cell Sci, 2006. **119**(Pt 17): p. 3539-50.
70. Fang, Y., et al., *PEX3 functions as a PEX19 docking factor in the import of class I peroxisomal membrane proteins.* J Cell Biol, 2004. **164**(6): p. 863-75.
71. Muntau, A.C., et al., *The interaction between human PEX3 and PEX19 characterized by fluorescence resonance energy transfer (FRET) analysis.* Eur J Cell Biol, 2003. **82**(7): p. 333-42.
72. Matsuzono, Y. and Y. Fujiki, *In vitro transport of membrane proteins to peroxisomes by shuttling receptor Pex19p.* J Biol Chem, 2006. **281**(1): p. 36-42.
73. Fransen, M., et al., *Analysis of human Pex19p's domain structure by pentapeptide scanning mutagenesis.* J Mol Biol, 2005. **346**(5): p. 1275-86.

74. Kim, P.K., et al., *The origin and maintenance of mammalian peroxisomes involves a de novo PEX16-dependent pathway from the ER.* J Cell Biol, 2006. **173**(4): p. 521-32.
75. Matsuzaki, T. and Y. Fujiki, *The peroxisomal membrane protein import receptor Pex3p is directly transported to peroxisomes by a novel Pex19p- and Pex16p-dependent pathway.* J Cell Biol, 2008. **183**(7): p. 1275-86.
76. Schrader, M. and H.D. Fahimi, *Growth and division of peroxisomes.* Int Rev Cytol, 2006. **255**: p. 237-90.
77. Thoms, S. and R. Erdmann, *Dynamin-related proteins and Pex11 proteins in peroxisome division and proliferation.* FEBS J, 2005. **272**(20): p. 5169-81.
78. Abe, I. and Y. Fujiki, *cDNA cloning and characterization of a constitutively expressed isoform of the human peroxin Pex11p.* Biochem Biophys Res Commun, 1998. **252**(2): p. 529-33.
79. Tanaka, A., K. Okumoto, and Y. Fujiki, *cDNA cloning and characterization of the third isoform of human peroxin Pex11p.* Biochem Biophys Res Commun, 2003. **300**(4): p. 819-23.
80. Koch, J., et al., *PEX11 family members are membrane elongation factors that coordinate peroxisome proliferation and maintenance.* J Cell Sci, 2010. **123**(Pt 19): p. 3389-400.
81. Schrader, M., N.A. Bonekamp, and M. Islinger, *Fission and proliferation of peroxisomes.* Biochim Biophys Acta, 2012. **1822**(9): p. 1343-57.
82. Koch, A., et al., *A role for Fis1 in both mitochondrial and peroxisomal fission in mammalian cells.* Mol Biol Cell, 2005. **16**(11): p. 5077-86.
83. Schrader, M., *Shared components of mitochondrial and peroxisomal division.* Biochim Biophys Acta, 2006. **1763**(5-6): p. 531-41.
84. van der Klei, I.J. and M. Veenhuis, *PTS1-independent sorting of peroxisomal matrix proteins by Pex5p.* Biochim Biophys Acta, 2006. **1763**(12): p. 1794-800.
85. Elgersma, Y., et al., *Analysis of the carboxyl-terminal peroxisomal targeting signal 1 in a homologous context in Saccharomyces cerevisiae.* J Biol Chem, 1996. **271**(42): p. 26375-82.
86. Gould, S.J., et al., *A conserved tripeptide sorts proteins to peroxisomes.* J Cell Biol, 1989. **108**(5): p. 1657-64.
87. Lametschwandtner, G., et al., *The difference in recognition of terminal tripeptides as peroxisomal targeting signal 1 between yeast and human is due to different affinities of their receptor Pex5p to the cognate signal and to residues adjacent to it.* J Biol Chem, 1998. **273**(50): p. 33635-43.

88. Brocard, C. and A. Hartig, *Peroxisome targeting signal 1: is it really a simple tripeptide?* Biochim Biophys Acta, 2006. **1763**(12): p. 1565-73.

89. Klein, A.T., et al., *Recognition of peroxisomal targeting signal type 1 by the import receptor Pex5p.* J Biol Chem, 2001. **276**(18): p. 15034-41.

90. McCollum, D., E. Monosov, and S. Subramani, *The pas8 mutant of Pichia pastoris exhibits the peroxisomal protein import deficiencies of Zellweger syndrome cells--the PAS8 protein binds to the COOH-terminal tripeptide peroxisomal targeting signal, and is a member of the TPR protein family.* J Cell Biol, 1993. **121**(4): p. 761-74.

91. Fransen, M., et al., *Identification and characterization of the putative human peroxisomal C-terminal targeting signal import receptor.* J Biol Chem, 1995. **270**(13): p. 7731-6.

92. Wiemer, E.A., et al., *Human peroxisomal targeting signal-1 receptor restores peroxisomal protein import in cells from patients with fatal peroxisomal disorders.* J Cell Biol, 1995. **130**(1): p. 51-65.

93. Lazarow, P.B., *The import receptor Pex7p and the PTS2 targeting sequence.* Biochim Biophys Acta, 2006. **1763**(12): p. 1599-604.

94. Osumi, T., et al., *Amino-terminal presequence of the precursor of peroxisomal 3-ketoacyl-CoA thiolase is a cleavable signal peptide for peroxisomal targeting.* Biochem Biophys Res Commun, 1991. **181**(3): p. 947-54.

95. Swinkels, B.W., et al., *A novel, cleavable peroxisomal targeting signal at the amino-terminus of the rat 3-ketoacyl-CoA thiolase.* EMBO J, 1991. **10**(11): p. 3255-62.

96. Marzioch, M., et al., *PAS7 encodes a novel yeast member of the WD-40 protein family essential for import of 3-oxoacyl-CoA thiolase, a PTS2-containing protein, into peroxisomes.* EMBO J, 1994. **13**(20): p. 4908-18.

97. Rehling, P., et al., *The import receptor for the peroxisomal targeting signal 2 (PTS2) in Saccharomyces cerevisiae is encoded by the PAS7 gene.* EMBO J, 1996. **15**(12): p. 2901-13.

98. Schliebs, W. and W.H. Kunau, *PTS2 co-receptors: diverse proteins with common features.* Biochim Biophys Acta, 2006. **1763**(12): p. 1605-12.

99. Purdue, P.E., X. Yang, and P.B. Lazarow, *Pex18p and Pex21p, a novel pair of related peroxins essential for peroxisomal targeting by the PTS2 pathway.* J Cell Biol, 1998. **143**(7): p. 1859-69.

100. Sichting, M., et al., *Pex7p and Pex20p of Neurospora crassa function together in PTS2-dependent protein import into peroxisomes.* Mol Biol Cell, 2003. **14**(2): p. 810-21.

101. Titorenko, V.I., et al., *Pex20p of the yeast Yarrowia lipolytica is required for the oligomerization of thiolase in the cytosol and for its targeting to the peroxisome.* J Cell Biol, 1998. **142**(2): p. 403-20.

102. Matsumura, T., H. Otera, and Y. Fujiki, *Disruption of the interaction of the longer isoform of Pex5p, Pex5pL, with Pex7p abolishes peroxisome targeting signal type 2 protein import in mammals. Study with a novel Pex5-impaired Chinese hamster ovary cell mutant.* J Biol Chem, 2000. **275**(28): p. 21715-21.

103. Otera, H., et al., *The mammalian peroxin Pex5pL, the longer isoform of the mobile peroxisome targeting signal (PTS) type 1 transporter, translocates the Pex7p.PTS2 protein complex into peroxisomes via its initial docking site, Pex14p.* J Biol Chem, 2000. **275**(28): p. 21703-14.

104. Woodward, A.W. and B. Bartel, *The Arabidopsis peroxisomal targeting signal type 2 receptor PEX7 is necessary for peroxisome function and dependent on PEX5.* Mol Biol Cell, 2005. **16**(2): p. 573-83.

105. Braverman, N., et al., *An isoform of pex5p, the human PTS1 receptor, is required for the import of PTS2 proteins into peroxisomes.* Hum Mol Genet, 1998. **7**(8): p. 1195-205.

106. Otera, H., et al., *Peroxisome targeting signal type 1 (PTS1) receptor is involved in import of both PTS1 and PTS2: studies with PEX5-defective CHO cell mutants.* Mol Cell Biol, 1998. **18**(1): p. 388-99.

107. Dodt, G., et al., *Domain mapping of human PEX5 reveals functional and structural similarities to Saccharomyces cerevisiae Pex18p and Pex21p.* J Biol Chem, 2001. **276**(45): p. 41769-81.

108. Nito, K., M. Hayashi, and M. Nishimura, *Direct interaction and determination of binding domains among peroxisomal import factors in Arabidopsis thaliana.* Plant Cell Physiol, 2002. **43**(4): p. 355-66.

109. Carvalho, A.F., et al., *The N-terminal half of the peroxisomal cycling receptor Pex5p is a natively unfolded domain.* J Mol Biol, 2006. **356**(4): p. 864-75.

110. Costa-Rodrigues, J., et al., *Pex5p, the peroxisomal cycling receptor, is a monomeric non-globular protein.* J Biol Chem, 2005. **280**(26): p. 24404-11.

111. Uversky, V.N., *What does it mean to be natively unfolded?* Eur J Biochem, 2002. **269**(1): p. 2-12.

112. Otera, H., et al., *Peroxisomal targeting signal receptor Pex5p interacts with cargoes and import machinery components in a spatiotemporally differentiated manner: conserved Pex5p WXXXF/Y motifs are critical for matrix protein import.* Mol Cell Biol, 2002. **22**(6): p. 1639-55.

113. Saidowsky, J., et al., *The di-aromatic pentapeptide repeats of the human peroxisome import receptor PEX5 are separate high affinity binding sites for the peroxisomal membrane protein PEX14.* J Biol Chem, 2001. **276**(37): p. 34524-9.
114. Schliebs, W., et al., *Recombinant human peroxisomal targeting signal receptor PEX5. Structural basis for interaction of PEX5 with PEX14.* J Biol Chem, 1999. **274**(9): p. 5666-73.
115. Bottger, G., et al., *Saccharomyces cerevisiae PTS1 receptor Pex5p interacts with the SH3 domain of the peroxisomal membrane protein Pex13p in an unconventional, non-PXXP-related manner.* Mol Biol Cell, 2000. **11**(11): p. 3963-76.
116. Elgersma, Y., et al., *The SH3 domain of the Saccharomyces cerevisiae peroxisomal membrane protein Pex13p functions as a docking site for Pex5p, a mobile receptor for the import PTS1-containing proteins.* J Cell Biol, 1996. **135**(1): p. 97-109.
117. Erdmann, R. and G. Blobel, *Identification of Pex13p a peroxisomal membrane receptor for the PTS1 recognition factor.* J Cell Biol, 1996. **135**(1): p. 111-21.
118. Gould, S.J., et al., *Pex13p is an SH3 protein of the peroxisome membrane and a docking factor for the predominantly cytoplasmic PTs1 receptor.* J Cell Biol, 1996. **135**(1): p. 85-95.
119. Urquhart, A.J., et al., *Interaction of Pex5p, the type 1 peroxisome targeting signal receptor, with the peroxisomal membrane proteins Pex14p and Pex13p.* J Biol Chem, 2000. **275**(6): p. 4127-36.
120. Kragler, F., et al., *Two independent peroxisomal targeting signals in catalase A of Saccharomyces cerevisiae.* J Cell Biol, 1993. **120**(3): p. 665-73.
121. Oshima, Y., et al., *Plant catalase is imported into peroxisomes by Pex5p but is distinct from typical PTS1 import.* Plant Cell Physiol, 2008. **49**(4): p. 671-7.
122. Gatto, G.J., Jr., et al., *Peroxisomal targeting signal-1 recognition by the TPR domains of human PEX5.* Nat Struct Biol, 2000. **7**(12): p. 1091-5.
123. Stanley, W.A., et al., *Recognition of a functional peroxisome type 1 target by the dynamic import receptor pex5p.* Mol Cell, 2006. **24**(5): p. 653-63.
124. Dodt, G., et al., *Mutations in the PTS1 receptor gene, PXR1, define complementation group 2 of the peroxisome biogenesis disorders.* Nat Genet, 1995. **9**(2): p. 115-25.
125. Brocard, C., et al., *The tetratricopeptide repeat-domain of the PAS10 protein of Saccharomyces cerevisiae is essential for binding the peroxisomal targeting signal-SKL.* Biochem Biophys Res Commun, 1994. **204**(3): p. 1016-22.

126. Terlecky, S.R., et al., *The Pichia pastoris peroxisomal protein PAS8p is the receptor for the C-terminal tripeptide peroxisomal targeting signal.* EMBO J, 1995. **14**(15): p. 3627-34.

127. Dodt, G. and S.J. Gould, *Multiple PEX genes are required for proper subcellular distribution and stability of Pex5p, the PTS1 receptor: evidence that PTS1 protein import is mediated by a cycling receptor.* J Cell Biol, 1996. **135**(6 Pt 2): p. 1763-74.

128. Fransen, M., et al., *Analysis of mammalian peroxin interactions using a non-transcription-based bacterial two-hybrid assay.* Mol Cell Proteomics, 2002. **1**(3): p. 243-52.

129. Agne, B., et al., *Pex8p: an intraperoxisomal organizer of the peroxisomal import machinery.* Mol Cell, 2003. **11**(3): p. 635-46.

130. Reguenga, C., et al., *Characterization of the mammalian peroxisomal import machinery: Pex2p, Pex5p, Pex12p, and Pex14p are subunits of the same protein assembly.* J Biol Chem, 2001. **276**(32): p. 29935-42.

131. Gouveia, A.M., et al., *Characterization of peroxisomal Pex5p from rat liver. Pex5p in the Pex5p-Pex14p membrane complex is a transmembrane protein.* J Biol Chem, 2000. **275**(42): p. 32444-51.

132. Collins, C.S., et al., *The peroxisome biogenesis factors pex4p, pex22p, pex1p, and pex6p act in the terminal steps of peroxisomal matrix protein import.* Mol Cell Biol, 2000. **20**(20): p. 7516-26.

133. Matsumoto, N., S. Tamura, and Y. Fujiki, *The pathogenic peroxin Pex26p recruits the Pex1p-Pex6p AAA ATPase complexes to peroxisomes.* Nat Cell Biol, 2003. **5**(5): p. 454-60.

134. Platta, H.W., et al., *Functional role of the AAA peroxins in dislocation of the cycling PTS1 receptor back to the cytosol.* Nat Cell Biol, 2005. **7**(8): p. 817-22.

135. Palma, J.M., F.J. Corpas, and L.A. del Rio, *Proteome of plant peroxisomes: new perspectives on the role of these organelles in cell biology.* Proteomics, 2009. **9**(9): p. 2301-12.

136. Grou, C.P., et al., *The peroxisomal protein import machinery--a case report of transient ubiquitination with a new flavor.* Cell Mol Life Sci, 2009. **66**(2): p. 254-62.

137. Gouveia, A.M., et al., *Insertion of Pex5p into the peroxisomal membrane is cargo protein-dependent.* J Biol Chem, 2003. **278**(7): p. 4389-92.

138. Williams, C. and B. Distel, *Pex13p: docking or cargo handling protein?* Biochim Biophys Acta, 2006. **1763**(12): p. 1585-91.

139. Azevedo, J.E. and W. Schliebs, *Pex14p, more than just a docking protein.* Biochim Biophys Acta, 2006. **1763**(12): p. 1574-84.
140. Gouveia, A.M., et al., *Characterization of the peroxisomal cycling receptor, Pex5p, using a cell-free in vitro import system.* J Biol Chem, 2003. **278**(1): p. 226-32.
141. Oliveira, M.E., et al., *The energetics of Pex5p-mediated peroxisomal protein import.* J Biol Chem, 2003. **278**(41): p. 39483-8.
142. Costa-Rodrigues, J., et al., *The N terminus of the peroxisomal cycling receptor, Pex5p, is required for redirecting the peroxisome-associated peroxin back to the cytosol.* J Biol Chem, 2004. **279**(45): p. 46573-9.
143. Williams, C., et al., *A conserved cysteine is essential for Pex4p-dependent ubiquitination of the peroxisomal import receptor Pex5p.* J Biol Chem, 2007. **282**(31): p. 22534-43.
144. Carvalho, A.F., et al., *Ubiquitination of mammalian Pex5p, the peroxisomal import receptor.* J Biol Chem, 2007. **282**(43): p. 31267-72.
145. Carvalho, A.F., et al., *Functional characterization of two missense mutations in Pex5p - C11S and N526K.* Biochim Biophys Acta, 2007. **1773**(7): p. 1141-8.
146. Miyata, N. and Y. Fujiki, *Shuttling mechanism of peroxisome targeting signal type 1 receptor Pex5: ATP-independent import and ATP-dependent export.* Mol Cell Biol, 2005. **25**(24): p. 10822-32.
147. Grou, C.P., et al., *Properties of the ubiquitin-pex5p thiol ester conjugate.* J Biol Chem, 2009. **284**(16): p. 10504-13.
148. Debelyy, M.O., et al., *Ubp15p, a ubiquitin hydrolase associated with the peroxisomal export machinery.* J Biol Chem, 2011. **286**(32): p. 28223-34.
149. Grou, C.P., et al., *Identification of ubiquitin-specific protease 9X (USP9X) as a deubiquitinase acting on ubiquitin-peroxin 5 (PEX5) thioester conjugate.* J Biol Chem, 2012. **287**(16): p. 12815-27.
150. Alencastre, I.S., et al., *Mapping the cargo protein membrane translocation step into the PEX5 cycling pathway.* J Biol Chem, 2009. **284**(40): p. 27243-51.
151. Azevedo, J.E., et al., *Protein translocation across the peroxisomal membrane.* Cell Biochem Biophys, 2004. **41**(3): p. 451-68.
152. Lazarow, P.B. and C. de Duve, *The synthesis and turnover of rat liver of rat liver peroxisomes. IV. Biochemical pathway of catalase synthesis.* J Cell Biol, 1973. **59**(2 Pt 1): p. 491-506.
153. Lazarow, P.B. and C. de Duve, *The synthesis and turnover of rat liver peroxisomes. V. Intracellular pathway of catalase synthesis.* J Cell Biol, 1973. **59**(2 Pt 1): p. 507-24.

154. Kruse, C. and H. Kindl, *Malate synthase: aggregation, deaggregation, and binding of phospholipids.* Arch Biochem Biophys, 1983. **223**(2): p. 618-28.

155. Goodman, J.M., et al., *Alcohol oxidase assembles post-translationally into the peroxisome of Candida boidinii.* J Biol Chem, 1984. **259**(13): p. 8485-93.

156. Sulter, G.J., et al., *Occurrence of peroxisomal membrane proteins in methylotrophic yeasts grown under different conditions.* Yeast, 1990. **6**(1): p. 35-43.

157. van der Klei, I.J., W. Harder, and M. Veenhuis, *Biosynthesis and assembly of alcohol oxidase, a peroxisomal matrix protein in methylotrophic yeasts: a review.* Yeast, 1991. **7**(3): p. 195-209.

158. Glover, J.R., D.W. Andrews, and R.A. Rachubinski, *Saccharomyces cerevisiae peroxisomal thiolase is imported as a dimer.* Proc Natl Acad Sci U S A, 1994. **91**(22): p. 10541-5.

159. McNew, J.A. and J.M. Goodman, *An oligomeric protein is imported into peroxisomes in vivo.* J Cell Biol, 1994. **127**(5): p. 1245-57.

160. Lee, M.S., R.T. Mullen, and R.N. Trelease, *Oilseed isocitrate lyases lacking their essential type 1 peroxisomal targeting signal are piggybacked to glyoxysomes.* Plant Cell, 1997. **9**(2): p. 185-97.

161. Yang, X., P.E. Purdue, and P.B. Lazarow, *Eci1p uses a PTS1 to enter peroxisomes: either its own or that of a partner, Dci1p.* Eur J Cell Biol, 2001. **80**(2): p. 126-38.

162. Walton, P.A., P.E. Hill, and S. Subramani, *Import of stably folded proteins into peroxisomes.* Mol Biol Cell, 1995. **6**(6): p. 675-83.

163. Stewart, M.Q., et al., *Alcohol oxidase and dihydroxyacetone synthase, the abundant peroxisomal proteins of methylotrophic yeasts, assemble in different cellular compartments.* J Cell Sci, 2001. **114**(Pt 15): p. 2863-8.

164. Grou, C.P., et al., *Members of the E2D (UbcH5) family mediate the ubiquitination of the conserved cysteine of Pex5p, the peroxisomal import receptor.* J Biol Chem, 2008. **283**(21): p. 14190-7.

165. Sullivan, D.T., et al., *Glyceraldehyde-3-phosphate dehydrogenase from Drosophila melanogaster. Identification of two isozymic forms encoded by separate genes.* J Biol Chem, 1985. **260**(7): p. 4345-50.

166. Gouveia, A.M., et al., *Alkaline density gradient floatation of membranes: polypeptide composition of the mammalian peroxisomal membrane.* Anal Biochem, 1999. **274**(2): p. 270-7.

167. Palosaari, P.M. and J.K. Hiltunen, *Peroxisomal bifunctional protein from rat liver is a trifunctional enzyme possessing 2-enoyl-CoA hydratase, 3-hydroxyacyl-*

CoA dehydrogenase, and delta 3, delta 2-enoyl-CoA isomerase activities. J Biol Chem, 1990. **265**(5): p. 2446-9.

168. Hartl, F.U., et al., *Improved isolation and purification of rat liver peroxisomes by combined rate zonal and equilibrium density centrifugation.* Arch Biochem Biophys, 1985. **237**(1): p. 124-34.
169. Fujiki, Y., et al., *Polypeptide and phospholipid composition of the membrane of rat liver peroxisomes: comparison with endoplasmic reticulum and mitochondrial membranes.* J Cell Biol, 1982. **93**(1): p. 103-10.
170. Weibel, E.R., et al., *Correlated morphometric and biochemical studies on the liver cell. I. Morphometric model, stereologic methods, and normal morphometric data for rat liver.* J Cell Biol, 1969. **42**(1): p. 68-91.
171. Miyazawa, S., et al., *Complete nucleotide sequence of cDNA and predicted amino acid sequence of rat acyl-CoA oxidase.* J Biol Chem, 1987. **262**(17): p. 8131-7.
172. Leighton, F., et al., *The synthesis and turnover of rat liver peroxisomes. I. Fractionation of peroxisome proteins.* J Cell Biol, 1969. **41**(2): p. 521-35.
173. Leighton, F., L. Coloma, and C. Koenig, *Structure, composition, physical properties, and turnover of proliferated peroxisomes. A study of the trophic effects of Su-13437 on rat liver.* J Cell Biol, 1975. **67**(2PT.1): p. 281-309.
174. Poole, B., F. Leighton, and C. De Duve, *The synthesis and turnover of rat liver peroxisomes. II. Turnover of peroxisome proteins.* J Cell Biol, 1969. **41**(2): p. 536-46.
175. Lazarow, P.B., et al., *Biogenesis of peroxisomal proteins in vivo and in vitro.* Ann N Y Acad Sci, 1982. **386**: p. 285-300.
176. Mate, M.J., et al., *Structure of catalase-A from Saccharomyces cerevisiae.* J Mol Biol, 1999. **286**(1): p. 135-49.
177. Purdue, P.E., et al., *Targeting of human catalase to peroxisomes is dependent upon a novel C-terminal peroxisomal targeting sequence.* Ann N Y Acad Sci, 1996. **804**: p. 775-6.
178. Murthy, M.R., et al., *Structure of beef liver catalase.* J Mol Biol, 1981. **152**(2): p. 465-99.
179. Putnam, C.D., et al., *Active and inhibited human catalase structures: ligand and NADPH binding and catalytic mechanism.* J Mol Biol, 2000. **296**(1): p. 295-309.
180. Trelease, R.N., et al., *Rat liver catalase is sorted to peroxisomes by its C-terminal tripeptide Ala-Asn-Leu, not by the internal Ser-Lys-Leu motif.* Eur J Cell Biol, 1996. **71**(3): p. 248-58.

181. Tanaka, N., et al., *Molecular basis for peroxisomal localization of tetrameric carbonyl reductase.* Structure, 2008. **16**(3): p. 388-97.
182. Brul, S., et al., *Kinetics of the assembly of peroxisomes after fusion of complementary cell lines from patients with the cerebro-hepato-renal (Zellweger) syndrome and related disorders.* Biochem Biophys Res Commun, 1988. **152**(3): p. 1083-9.
183. Koepke, J.I., et al., *Restoration of peroxisomal catalase import in a model of human cellular aging.* Traffic, 2007. **8**(11): p. 1590-600.
184. Middelkoop, E., A. Strijland, and J.M. Tager, *Does aminotriazole inhibit import of catalase into peroxisomes by retarding unfolding?* FEBS Lett, 1991. **279**(1): p. 79-82.
185. Leon, S., J.M. Goodman, and S. Subramani, *Uniqueness of the mechanism of protein import into the peroxisome matrix: transport of folded, co-factor-bound and oligomeric proteins by shuttling receptors.* Biochim Biophys Acta, 2006. **1763**(12): p. 1552-64.
186. Wang, D., et al., *Physical interactions of the peroxisomal targeting signal 1 receptor pex5p, studied by fluorescence correlation spectroscopy.* J Biol Chem, 2003. **278**(44): p. 43340-5.
187. Oliveira, M.E., et al., *Mammalian Pex14p: membrane topology and characterisation of the Pex14p-Pex14p interaction.* Biochim Biophys Acta, 2002. **1567**(1-2): p. 13-22.
188. Will, G.K., et al., *Identification and characterization of the human orthologue of yeast Pex14p.* Mol Cell Biol, 1999. **19**(3): p. 2265-77.
189. Ghosh, D. and J.M. Berg, *A proteome-wide perspective on peroxisome targeting signal 1(PTS1)-Pex5p affinities.* J Am Chem Soc, 2010. **132**(11): p. 3973-9.
190. Nohammer, C., et al., *cDNA cloning and analysis of tissue-specific expression of mouse peroxisomal straight-chain acyl-CoA oxidase.* Eur J Biochem, 2000. **267**(4): p. 1254-60.
191. Pedersen, L. and A. Henriksen, *Acyl-CoA oxidase 1 from Arabidopsis thaliana. Structure of a key enzyme in plant lipid metabolism.* J Mol Biol, 2005. **345**(3): p. 487-500.
192. Zamocky, M. and F. Koller, *Understanding the structure and function of catalases: clues from molecular evolution and in vitro mutagenesis.* Prog Biophys Mol Biol, 1999. **72**(1): p. 19-66.
193. Mullen, R.T., M.S. Lee, and R.N. Trelease, *Identification of the peroxisomal targeting signal for cottonseed catalase.* Plant J, 1997. **12**(2): p. 313-22.

194. Titorenko, V.I., et al., *Acyl-CoA oxidase is imported as a heteropentameric, cofactor-containing complex into peroxisomes of Yarrowia lipolytica.* J Cell Biol, 2002. **156**(3): p. 481-94.
195. Danpure, C.J., *The molecular basis of alanine: glyoxylate aminotransferase mistargeting: the most common single cause of primary hyperoxaluria type 1.* J Nephrol, 1998. **11 Suppl 1**: p. 8-12.
196. Djordjevic, S., et al., *Structural implications of a G170R mutation of alanine:glyoxylate aminotransferase that is associated with peroxisome-to-mitochondrion mistargeting.* Acta Crystallogr Sect F Struct Biol Cryst Commun, 2010. **66**(Pt 3): p. 233-6.
197. Ple, S., et al., *Cochaperone interactions in export of the type III needle component PscF of Pseudomonas aeruginosa.* J Bacteriol, 2010. **192**(14): p. 3801-8.
198. Quinaud, M., et al., *Structure of the heterotrimeric complex that regulates type III secretion needle formation.* Proc Natl Acad Sci U S A, 2007. **104**(19): p. 7803-8.
199. Parsot, C., C. Hamiaux, and A.L. Page, *The various and varying roles of specific chaperones in type III secretion systems.* Curr Opin Microbiol, 2003. **6**(1): p. 7-14.
200. Ma, C., et al., *The peroxisomal matrix import of Pex8p requires only PTS receptors and Pex14p.* Mol Biol Cell, 2009. **20**(16): p. 3680-9.
201. Madrid, K.P., et al., *Modulation of the Leishmania donovani peroxin 5 quaternary structure by peroxisomal targeting signal 1 ligands.* Mol Cell Biol, 2004. **24**(17): p. 7331-44.
202. Niederhoff, K., et al., *Yeast Pex14p possesses two functionally distinct Pex5p and one Pex7p binding sites.* J Biol Chem, 2005. **280**(42): p. 35571-8.
203. Williams, C., M. van den Berg, and B. Distel, *Saccharomyces cerevisiae Pex14p contains two independent Pex5p binding sites, which are both essential for PTS1 protein import.* FEBS Lett, 2005. **579**(16): p. 3416-20.

VIII. PUBLICATIONS

THE JOURNAL OF BIOLOGICAL CHEMISTRY VOL. 286, NO. 47, pp. 40509–40519, November 25, 2011

PEX5 Protein Binds Monomeric Catalase Blocking Its Tetramerization and Releases It upon Binding the N-terminal Domain of PEX14*[S]

Received for publication, July 28, 2011, and in revised form, September 23, 2011 Published, JBC Papers in Press, October 5, 2011, DOI 10.1074/jbc.M111.287201

Marta O. Freitas[‡§1], Tânia Francisco[‡§1], Tony A. Rodrigues[‡§1], Inês S. Alencastre[‡§1], Manuel P. Pinto[‡1], Cláudia P. Grou[‡1], Andreia F. Carvalho[‡2], Marc Fransen[¶], Clara Sá-Miranda[‡], and Jorge E. Azevedo[‡§3]

From the [‡]Instituto de Biologia Molecular e Celular, Universidade do Porto, Rua do Campo Alegre, 823, 4150-180 Porto, Portugal, the [§]Instituto de Ciências Biomédicas Abel Salazar, Universidade do Porto, Largo Professor Abel Salazar, 2, 4009-003 Porto, Portugal, and the [¶]Departement Moleculaire Celbiologie, Katholieke Universiteit Leuven, Herestraat 49, B-3000 Leuven, Belgium

Background: PEX5 binds newly synthesized peroxisomal proteins in the cytosol and releases them in the organelle matrix.
Results: PEX5 binds monomeric catalase and releases it in the presence of PEX14.
Conclusion: PEX14 participates in the cargo release step.
Significance: Knowing how PEX5 interacts with cargo proteins and which factors disrupt this interaction are crucial for understanding this protein sorting pathway.

Newly synthesized peroxisomal matrix proteins are targeted to the organelle by PEX5. PEX5 has a dual role in this process. First, it acts as a soluble receptor recognizing these proteins in the cytosol. Subsequently, at the peroxisomal docking/translocation machinery, PEX5 promotes their translocation across the organelle membrane. Despite significant advances made in recent years, several aspects of this pathway remain unclear. Two important ones regard the formation and disruption of the PEX5-cargo protein interaction in the cytosol and at the docking/translocation machinery, respectively. Here, we provide data on the interaction of PEX5 with catalase, a homotetrameric enzyme in its native state. We found that PEX5 interacts with monomeric catalase yielding a stable protein complex; no such complex was detected with tetrameric catalase. Binding of PEX5 to monomeric catalase potently inhibits its tetramerization, a property that depends on domains present in both the N- and C-terminal halves of PEX5. Interestingly, the PEX5-catalase interaction is disrupted by the N-terminal domain of PEX14, a component of the docking/translocation machinery. One or two of the seven PEX14-binding diaromatic motifs present in the N-terminal half of PEX5 are probably involved in this phenomenon. These results suggest the following: 1) catalase domain(s) involved in the interaction with PEX5 are no longer accessible upon tetramerization of the enzyme; 2) the catalase-binding interface in PEX5 is not restricted to its C-terminal peroxisomal targeting sequence type 1-binding domain and also involves PEX5 N-terminal domain(s); and 3) PEX14 participates in the cargo protein release step.

Mammalian peroxisomal matrix proteins are synthesized on cytosolic ribosomes and post-translationally targeted to the organelle matrix by PEX5, the peroxisomal shuttle receptor (1–4). The vast majority of these proteins possess the so-called peroxisomal targeting signal type 1 (PTS1),[4] a C-terminal sequence frequently ending with the tripeptide SKL or a derivative of it (5). This PTS1 interacts directly with the C-terminal half of PEX5, a domain comprising seven tetratricopeptide repeats motifs arranged into a ring-like structure (6). A minor fraction of peroxisomal matrix proteins contains instead a PTS type 2 (PTS2), a degenerated nonapeptide near their N termini (7). The PTS2-PEX5 interaction is not direct but rather is mediated by the adaptor protein PEX7 (8).

According to current models (1–4), newly synthesized peroxisomal matrix proteins interact with PEX5 while still in the cytosol. These PEX5-cargo protein complexes then dock at the peroxisomal docking/translocation machinery (DTM), a multisubunit protein complex comprising the intrinsic membrane proteins PEX13, PEX14, and the RING finger peroxins PEX2, PEX10, and PEX12 (9, 10). By a still ill-defined process, this interaction ultimately leads to the insertion of PEX5 into the DTM with the concomitant translocation of the cargo protein into the peroxisomal matrix (11–13). In at least one case, that of the PTS2-containing protein thiolase, it is also at this stage that

* This work was supported in part by Fundação para a Ciência e Tecnologia, Portugal, and Fundo Europeu de Desenvolvimento Regional through COMPETE, Programa Operacional Factores de Competitividade in the context of QREN, Portugal, Grants PEst-C/SAU/LA0002/2011 and PTDC/BIA-BCM/64771/2006, and by the European Union VI Framework Program Grant LSHGCT-2004-512018, Peroxisomes in Health and Disease.
[S] The on-line version of this article (available at http://www.jbc.org) contains supplemental Fig. S1 and Table 1.
[1] Supported by Fundação para a Ciência e Tecnologia, Programa Operacional Potencial Humano do QREN, and Fundo Social Europeu.
[2] Supported by Programa Ciência, funded by Programa Operacional Potencial Humano do QREN, Tipologia 4.2, Promoção do Emprego Científico, by Fundo Social Europeu and by national funds from Ministério da Ciência, Tecnologia e Ensino Superior.
[3] To whom correspondence should be addressed: Instituto de Biologia Molecular e Celular, Universidade do Porto, Rua do Campo Alegre, 823, 4150-180 Porto, Portugal. Tel.: 351-226-074-900; Fax: 351-226-099-157; E-mail: jazevedo@ibmc.up.pt.

[4] The abbreviations used are: PTS1, peroxisomal targeting signal type 1; PTS2, peroxisomal targeting signal type 2; DTM, docking/translocation machinery; mCat, monomeric catalase; tCat, tetrameric catalase; SEC, size-exclusion chromatography; NDPEX14, N-terminal domain of PEX14; TPR, tetratricopeptide repeat.

PEX5 releases its cargo into the peroxisomal matrix (11). Interestingly, *in vitro* import experiments suggest that ATP hydrolysis is not needed at any of these steps, suggesting that the complete transport of a cargo protein from the cytosol into the peroxisomal matrix is driven by thermodynamically favored protein-protein interactions at the DTM (14–16). After these events, PEX5 is extracted from the DTM back into the cytosol. This involves monoubiquitination of PEX5 at a conserved cysteine residue (17–20) and the ATP-dependent extraction of the ubiquitin-PEX5 conjugate from the DTM by the mechanoenzymes PEX1 and PEX6, two members of the AAA family of ATPases (14–16). Finally, ubiquitin is removed from PEX5 probably by a combination of enzymatic and nonenzymatic processes (21, 22).

Despite all the advances made in recent years, there are still many aspects of this protein import pathway that remain unclear. A particularly important one regards the quaternary structure of the PEX5-cargo protein complex formed in the cytosol. In principle, a protein complex comprising a single PEX5 molecule and a cargo protein should be sufficient to ensure the correct targeting of that protein to the peroxisomal matrix. This is probably the case for all peroxisomal monomeric proteins (*e.g.* the sterol carrier protein 2 (23)), for some oligomeric enzymes in which the peroxisomal targeting signals become hidden upon oligomerization (24–27), and for natural or artificial heterodimers in which only one of the subunits contains peroxisomal targeting information (28–30). The situation for many other peroxisomal oligomeric proteins, however, is not that clear. Indeed, the observation that peroxisomes have the capacity to import some already oligomerized proteins, at least under conditions of high protein expression (28, 31–34), together with the fact that several peroxisomal oligomeric proteins may expose multiple PTS1 sequences at their surface, could suggest that these cargo proteins are transported to the organelle by more than one PEX5 molecule. Such a scenario was in fact the central premise of one hypothetical model proposed a few years ago aimed at describing the process of protein translocation across the peroxisomal membrane (35).

In an effort to understand how these proteins are sorted to the peroxisome, we started to characterize the interaction of their monomeric and oligomeric versions with PEX5. Here, we describe the results obtained with catalase, one of the most abundant peroxisomal matrix proteins and probably one of the most frequent clients of the DTM (36–38). Catalase is a heme-containing homo-tetrameric protein in its native state (four subunits of 60 kDa), with each subunit possessing a noncanonical PTS1 at its C terminus (KANL) (39–43). We selected catalase for this initial study because there are data suggesting that both its monomeric and tetrameric versions are substrates for the peroxisomal protein import machinery (27, 44–49). However, whether the peroxisomal import machinery, PEX5 in particular, displays any preference for monomeric or tetrameric catalase was unknown.

Here, we show that mammalian PEX5 binds monomeric catalase (hereafter referred to as mCat) in a much stronger manner than it binds tetrameric catalase (tCat). Actually, we were unable to detect stable PEX5-tCat complexes. Importantly, PEX5 binding to mCat blocks its tetramerization with an IC_{50} in the nanomolar range. The interaction of PEX5 with mCat was found to involve the PTS1-binding C-terminal half of PEX5 as well as a domain(s) present in its N-terminal half. Finally, we provide data suggesting that the PEX5-mCat interaction is disrupted by the N-terminal domain of PEX14, a central component of the DTM. The implications of these findings on the mechanism of protein translocation across the peroxisomal membrane are discussed.

EXPERIMENTAL PROCEDURES

Recombinant Proteins—The recombinant large isoform of human PEX5 (50, 51), hereafter referred to as PEX5 for simplicity, a protein comprising the first 324 amino acid residues of PEX5 (ΔC1PEX5), a protein containing amino acid residues 315–639 of PEX5 (TPRs), PEX5 containing the missense mutation N526K (PEX5N526K), a protein comprising the first 80 amino acid residues of human PEX14 (NDPEX14), and full-length PEX19 (PEX19) were obtained as described previously (18, 52–55). The following truncated versions of human PEX5 were also produced: PEX5ΔN110 (amino acid residues 111–639 of PEX5), PEX5ΔN147 (amino acid residues 148–639 of PEX5), PEX5ΔN196 (amino acid residues 197–639 of PEX5), PEX5ΔN267 (amino acid residues 268–639 of PEX5), and PEX5ΔN290 (amino acid residues 291–639 of PEX5). The cDNAs encoding these proteins were obtained by PCR using the primers listed in supplemental Table 1 and the pQE30-PEX5 construct as template. The amplified DNA fragments were then digested with NdeI and SalI and cloned into the NdeI/SalI digested pET-28c vector (Novagene). The QuikChange® site-directed mutagenesis kit (Stratagene) was used to replace tryptophan and phenylalanine/tyrosine residues in diaromatic motifs of PEX5 by alanines (see primers in supplemental Table 1). The three proteins obtained in this way are as follows: PEX5ΔN267-M7 and PEX5-M7, proteins with a mutated 7th diaromatic motif, and PEX5-M6,7, a protein possessing both the 6th and 7th diaromatic mutated. All plasmids were sequence-verified.

The cDNA encoding mouse PEX5 was amplified from a commercially available clone (clone MMM1013-7510385, Open Biosystems) using the primers listed in supplemental Table 1, digested with NdeI and SalI, and cloned into the NdeI/SalI digested pET-28c vector. Purification of all PEX5 proteins was done as described previously (54).

Synthesis of Radiolabeled Proteins—The cDNA encoding full-length human catalase (clone IMAGE ID 5551309, Open Biosystems) was amplified by PCR using the primers listed in supplemental Table 1. This DNA was digested with XbaI and KpnI and cloned into the XbaI/KpnI-digested pGEM-4 vector (Promega), originating pGEM-4-Cat. This plasmid was used as template to produce two other plasmids, one encoding a catalase lacking its four last C-terminal amino acid residues (CatΔKANL) and the other encoding a catalase in which these four residues were replaced by ED (CatED). These plasmids were obtained using the QuikChange® site-directed mutagenesis kit (Stratagene) and the primer pairs described in supplemental Table 1. ^{35}S-Labeled proteins were synthesized using the TNT® T7 QuickCoupled transcription/translation kit (Promega) in the presence of [^{35}S] methionine (specific activity

>1000 Ci/mmol; PerkinElmer Life Sciences) following the standard conditions of the manufacturer. Unless otherwise indicated, protein synthesis was allowed to proceed for 55 min and was then blocked with 0.5 mM of cycloheximide (final concentration). Chase incubations were done at 30 °C for the specified periods of time. Chase reactions performed in the presence of recombinant proteins typically contained 6 μl of the translation mixture in a final volume of 10 μl.

Native PAGE—Proteins were incubated in 10 μl of 50 mM Tris-HCl, pH 8.0, 2 mM DTT for 5 min at room temperature. After addition of 1 μl of 0.17% (w/v) bromphenol blue, 50% (w/v) sucrose, the samples were loaded into Tris nondenaturating discontinuous 8% polyacrylamide gels (56). The gels were run at 250 V at 4 °C for 1 h (unless indicated otherwise), blotted onto nitrocellulose membranes, stained with Ponceau S, and exposed to an x-ray film.

Size-exclusion Chromatography—^{35}S-Labeled proteins (50 μl of *in vitro* transcription/translation reactions) or mixtures containing recombinant proteins and ^{35}S-labeled proteins were diluted to 250 μl with 50 mM Tris-HCl, pH 7.5, 150 mM NaCl, 1 mM EDTA-NaOH, 1 mM DTT and injected into a Superose 12 10/300 GL column (GE Healthcare; loop volume 200 μl) running with the same buffer at 0.5 ml/min. The column was calibrated with the following globular proteins: ferritin (440 kDa), bovine serum albumin (66 kDa), and soybean trypsin inhibitor (21.5 kDa). Fractions of 500 μl were collected and subjected to trichloroacetic acid precipitation, and one-third of each sample was analyzed by SDS-PAGE. The gels were blotted onto nitrocellulose membranes, stained with Ponceau S, and exposed to an x-ray film. Soluble mouse liver peroxisomal matrix proteins were obtained by sonicating purified peroxisomes (prepared as in Ref. 57) in 50 mM Tris-HCl, pH 7.5, 150 mM NaCl, 1 mM EDTA-NaOH, 1 mM DTT, and 1:500 (v/v) mammalian protease inhibitor mixture (Sigma) and centrifuging for 30 min at 100,000 × *g*. Two hundred micrograms of soluble proteins, supplemented or not with 300 μg of recombinant mouse PEX5, were injected into the size-exclusion column, as above. Aliquots of 25 μl from each fraction were analyzed by SDS-PAGE/Western blotting with antibodies directed to catalase (catalog number RDI-CATALASEabr; Research Diagnostics, Inc) and L-bifunctional protein (58).

Miscellaneous—The concentration of PEX5 in rat liver cytosol (0.75 μM) was calculated from the following data: total amount of PEX5 in liver, 4 ng/μg of total peroxisomal protein; percentage of PEX5 in cytosol, 85% (59); peroxisomes, 2.5% (w/w) of total liver protein; protein content of liver, 260 mg/g (60); 1 g of liver corresponds to 0.94 ml of which 44.4% is cytosol (61).

The weighted average molecular mass of monomeric rat liver peroxisomal proteins was estimated from the densitometric analysis of a Coomassie-stained SDS gel loaded with a highly pure peroxisomal preparation (57). Peak areas were divided by the corresponding apparent molecular masses and expressed as percentage of total moles. The weighted average of these values is 49 kDa. For newly synthesized peroxisomal proteins, this value may be slightly underestimated because protein maturation processes that occur in the matrix of the organelle (*e.g.* the cleavage of the 75-kDa acyl-CoA oxidase into the 53- and 22-kDa subunits (62)) were not taken into account. Mole percentage for catalase (13 mol %) was calculated considering the mass percentage of the protein in rat liver peroxisomes, 15% (63), the weighted average molecular mass of rat liver peroxisomal proteins (49 kDa), the theoretical molecular mass of catalase (60 kDa), and the mass percentage of matrix proteins in total rat liver peroxisomes, 92% (57).

The amount of total peroxisomal matrix proteins in nanomoles/g of rat liver was calculated from the above referred data. A value of 122 nmol/g of liver was obtained. Because "all the major protein components of the peroxisome have the same rate of turnover" (half-life of 1.3–1.5 days (37, 38)), one can estimate the rate of total peroxisomal matrix protein synthesis (*k*) as 30 pmol/min/g of liver. The rate of synthesis for a particular protein is *k* times its mole fraction in the peroxisomal matrix. For catalase (0.13 mol fraction), this corresponds to 3.9 pmol/min/g of liver, a value similar to the one reported previously (3.87 pmol/min/g of liver (63)). The steady-state concentration of newly synthesized peroxisomal matrix proteins in the cytosol ($[P]_{cyt}$) can be estimated by the following expression: $[P]_{cyt} = k \times 1.443 \times t_{1/2}$, where $[P]_{cyt}$ is in pmol/g of liver; *k* is the rate of total peroxisomal matrix protein synthesis in pmol/min/g of liver, and $t_{1/2}$ is the cytosolic half-life of the protein in min (47). According to Lazarow and co-workers (46, 64), several peroxisomal proteins display cytosolic half-lives of about 7 min (see Fig. 5 in Ref. 64). Two outliers were noted by those authors as follows: one was catalase, a protein presenting a cytosolic half-life of 14 min; the other was urate oxidase, a protein that after 4 min of chase was already completely found in peroxisomes, an observation suggesting that its cytosolic half-life is 2 min or less. We assume that all peroxisomal matrix proteins present a similar kinetic behavior, *i.e.* that on average their cytosolic half-lives are 7–8 min. The total concentration of newly synthesized peroxisomal proteins in the cytosol is thus 0.73–0.83 μM, with mCat contributing with 0.19 μM.

RESULTS

The rabbit reticulocyte lysate-based *in vitro* transcription/translation system has been one of the most powerful tools for the characterization of the molecular mechanisms underlying protein sorting pathways. We reasoned that this system might also be of use to study the first step of the catalase peroxisomal import pathway, namely when and how catalase interacts with cytosolic PEX5.

Fig. 1*A* shows a native-PAGE analysis of a standard *in vitro* transcription/translation reaction programmed with a plasmid encoding human catalase (*lane 1*). Three populations of ^{35}S-labeled catalase are clearly seen in these gels. Notably, when catalase is synthesized in the presence of 1 μM human PEX5, the two slower migrating bands are no longer detected (Fig. 1*A*, *lane 2*). Apparently, some event(s) occurring in this system are blocked by PEX5.

To understand the nature of the three catalase populations detected in these experiments and thus the inhibitory effect of PEX5, we first performed a pulse-chase analysis. In the experiment shown in Fig. 1*B*, catalase was synthesized for 55 min; cycloheximide was added to stop further synthesis, and the reaction was then chased for 4 h. The autoradiograph reveals

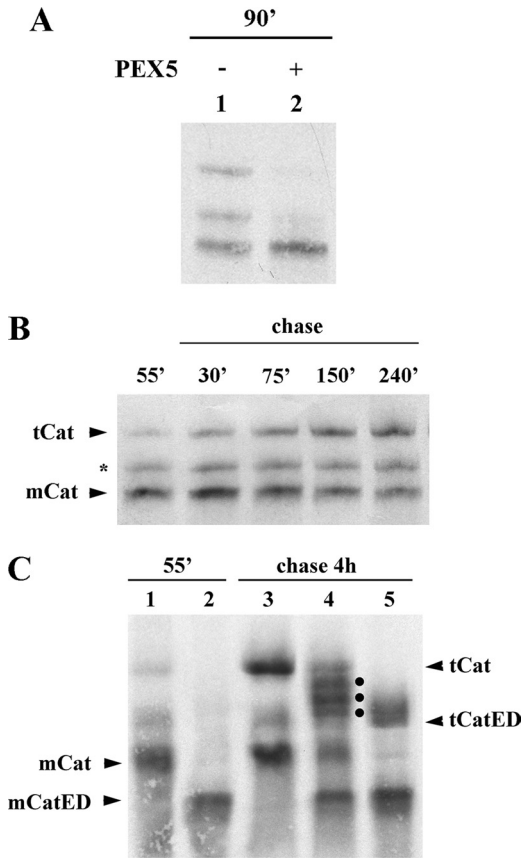

FIGURE 1. **^{35}S-Labeled catalase tetramerizes *in vitro*.** *A,* human catalase was synthesized *in vitro* in a rabbit reticulocyte lysate for 90 min at 30 °C in the absence or presence of 1 μM human PEX5, as indicated, and analyzed by native-PAGE/autoradiography. *B,* ^{35}S-labeled catalase was synthesized for 55 min. After adding cycloheximide, an aliquot was removed and frozen in liquid N_2 (*lane 55'*). The remainder of the reaction was then incubated at 30 °C, and aliquots were removed and frozen at the indicated time points. The samples were subjected to native-PAGE/autoradiography. The protein bands labeled with mCat and tCat correspond to the monomeric and tetrameric forms of catalase; the band labeled with an *asterisk* probably represents dimeric catalase (see text for details). *C,* catalase and a mutant version of it possessing two acidic amino acid residues at the C terminus (CatED) were synthesized *in vitro* for 55 min and supplemented with cycloheximide (*lanes 1* and *2*, respectively). Aliquots of each reaction were then combined and incubated for 4 h at 30 °C (*lane 4*) or incubated individually under the same conditions (*lanes 3* and *5* for catalase and CatED, respectively), and subjected to native PAGE/autoradiography. Note that this gel was run for 2.5 h to improve separation of tetramers. Longer electrophoretic runs also result in more diffuse bands. The *dots* in *lane 4* indicate the three expected heterotetramers. mCatED and tCatED indicate the monomeric and tetrameric forms of CatED, respectively.

that the faster migrating species (mCat; see below) is the main product after 55 min of synthesis. Its amount decreases during the chase period, with the concomitant increase of the slower migrating population (tCat). The protein band migrating between mCat and tCat (*asterisk* in Fig. 1*B*) remains fairly constant during the time course of these experiments. Its gel migration and kinetic behavior suggest that this population might be an oligomerization intermediate (probably a dimer), although further data are necessary to confirm this hypothesis.

Sedimentation analysis (data not shown) and size-exclusion chromatography (SEC; see below) of catalase before or after a 4-h chase incubation revealed that the faster migrating protein band corresponds to species displaying the hydrodynamic properties of a 60-kDa globular protein, whereas the protein in the slower migrating band behaves as a 200–250-kDa protein. Thus, the faster migrating band represents monomeric catalase, whereas the slower migrating band could be either the tetrameric enzyme or a protein complex containing catalase and some protein(s) from the *in vitro* protein synthesis system (*e.g.* a chaperone). To discriminate between these two possibilities, we adapted the strategy originally developed by Scandalios (65) to show that catalase is a tetrameric enzyme. For this purpose, we produced an acidic mutant version of catalase (CatED), which migrates faster than the normal enzyme in these gels, and we asked whether this protein is able to form heterotetramers with normal catalase upon a chase incubation of 4 h. If this is the case, then three heterotetramers containing 1, 2, or 3 molecules of the normal protein should be detected by native-PAGE; all these heterotetramers should migrate in these gels between the homotetramers of the parental molecules. If the slower migrating band corresponds to a complex containing catalase and some other protein(s), then the band pattern of the protein mixture should just correspond to the sum of the patterns obtained with each of the two catalase versions individually. The results presented in Fig. 1*C* indicate that the first possibility is the correct one.

We next asked whether PEX5 can bind mCat and tCat. Because of the fact that the PEX5-catalase interaction is not preserved upon native-PAGE (see below), we used SEC, a technique in which proteins can be separated in a more physiological buffer. Translation reactions containing mCat (55 min of synthesis) and a mixture of mCat and tCat (55 min of synthesis plus 4 h of chase) were first subjected to SEC to purify mCat and tCat, respectively. Each of these proteins was then incubated with PEX5 or buffer alone and subjected to a second SEC. The results obtained with mCat are presented in Fig. 2*A*. In the absence of PEX5, the radiolabeled protein present in fraction 24 of the first SEC (Fig. 2*A, panel 1*) still elutes as a monomeric protein in the second SEC (*panel 2*), indicating that no tetramerization of mCat occurs during this procedure. In contrast, in the presence of PEX5, the elution volume of mCat is reduced, and the radiolabeled protein elutes now together with recombinant PEX5 (Fig. 2*A, panels 3* and *4*). Thus, PEX5 interacts with mCat. A different result was obtained for tCat. As shown in Fig. 2*B*, the elution profiles of tCat in the presence or absence of PEX5 are almost identical (Fig. 2*B, panels 2* and *3*) suggesting that these two proteins may interact only weakly. (Note that a major fraction of tCat co-elutes with PEX5 (Fig. 2*B,* compare *panels 2* and *4*) implying that, contrary to the situation with mCat, the two proteins are kept under near-equilibrium conditions during chromatography. This should facilitate the detection of PEX5-tCat complexes.) We also did not find evidence for the existence of a PEX5-tCat protein complex when mouse liver peroxisomal matrix proteins preincubated with either recombinant mouse PEX5 or buffer alone were subjected to SEC. Indeed, the elution volume of mouse catalase remains basically the same regardless of the presence of PEX5 (Fig. 2*C, panels 1* and *2*). This behavior contrasts to the one displayed by the L-bifunctional protein, a monomeric 78-kDa protein in its native state (58), which elutes much earlier in the presence of PEX5 (Fig. 2*C, panels 4*) than in its absence (*panel 3*). We still tried to detect a PEX5-tCat interaction by subjecting ^{35}S-labeled tCat or mouse liver native catalase to ultracentrifugation

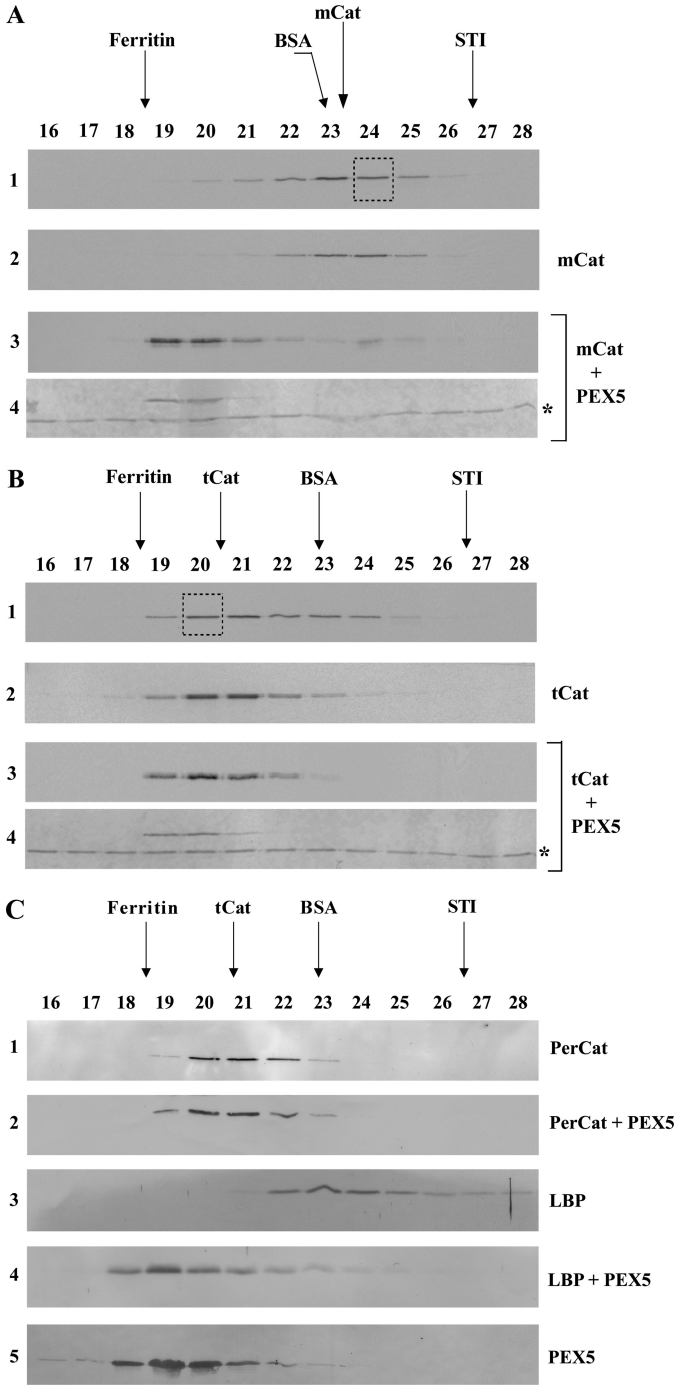

FIGURE 2. **PEX5 binds monomeric catalase.** *A,* ^{35}S-labeled catalase was synthesized *in vitro* for 55 min and subjected to SEC. Radiolabeled mCat eluting in fraction 24 of this chromatography (*panel 1, boxed lane*) was then subjected to a second SEC either alone (*panel 2*) or after receiving 1 μM recombinant PEX5 (*panels 3* and *4*). Fractions were collected and subjected to SDS-PAGE/Western blotting. Autoradiographs (*panels 1–3*) and the Ponceau S-stained membrane showing PEX5 (*panel 4*) are presented. No recombinant PEX5 or ^{35}S-labeled catalase were detected in the void volume of this column (fractions 14 and 15; not shown). The *asterisk* marks bovine serum albumin added to chromatography fractions before precipitation to control protein recoveries. *B,* ^{35}S-labeled catalase, synthesized *in vitro* for 55 min and incubated for 4 h at 30 °C in the presence of cycloheximide, was subjected to SEC. Radiolabeled tCat eluting in fraction 20 (*panel 1, boxed lane*) was then subjected to a second SEC either alone (*panel 2*) or after receiving 1 μM recombinant PEX5 (*panels 3* and *4*). Fractions were processed as described above. Autoradiographs (*panels 1–3*) and the Ponceau S-stained membrane (*panel 4*) are presented. *C,* soluble proteins from mouse liver peroxisomes were incubated either with recombinant PEX5 or buffer alone and subjected to SEC. Fractions were subjected to SDS-PAGE/Western blotting using antibodies directed to catalase (*PerCat*) or L-bifunctional protein. Immunoblots (*panels 1–4*) and a Ponceau S-stained membrane showing PEX5 (*panel 5*) are presented. Note that PEX5, a monomeric 70-kDa protein in solution, displays an abnormal behavior upon SEC because a major fraction of its polypeptide chain is natively unfolded (52).

through a solution containing 1 μM PEX5. Again, no evidence for a PEX5-tCat protein complex was obtained.[5] Thus, if tCat interacts with PEX5, the K_d value of the interaction is larger than 1 μM. We note that interactions between PEX5 and recombinant catalase have been described before, but no quantitative binding data were reported (45, 66). Regardless of these uncertainties, it is clear from our results that PEX5 binds stronger to mCat than to tCat. Considering that tCat, unlike mCat, contains four PTS1 sequences, a property that should increase the stability of a putative complex with PEX5 because of an avidity effect, this is an unexpected finding. Apparently, some domain of the catalase polypeptide chain involved in the interaction with PEX5 is no longer accessible when the protein tetramerizes.

The results presented above indicate that PEX5 binds mCat blocking its tetramerization. We explored this phenomenon to further characterize the PEX5-catalase interaction. In the experiments described below, *in vitro* synthesized catalase was chased for 4 h in the presence of several recombinant proteins and analyzed by native-PAGE. As shown in Fig. 3*A*, PEX5, at 1 μM in the chase incubation, completely blocked catalase tetramerization, as expected. The inhibitory effect of PEX5 is quite strong displaying an IC_{50} of about 100 nM (Fig. 3*B*). No such effect was observed with PEX5(N526K), a mutant PEX5 molecule possessing a single missense mutation in the PTS1-binding domain that abolishes its activity (Fig. 3*A*) (67, 68). A similar result was obtained when a mutant version of catalase lacking the PTS1 (CatΔKANL) was used in this assay; tetramerization of this species was no longer sensitive to the inhibitory action of PEX5 (Fig. 3*C*, compare *lane 3* with *6*). Thus, inhibition of catalase tetramerization by PEX5 requires the interaction of catalase PTS1 sequence with the C-terminal PTS1-binding domain of PEX5. Interestingly, however, this domain of PEX5 alone (referred to as TPRs) does not display this capacity when tested in this assay at a 1 μM concentration (Fig. 3*D*, *lane 5*), and the same is true for a recombinant protein comprising the N-terminal half of PEX5 (ΔC1PEX5; Fig. 3*D*, *lane 4*). Likewise, a mixture of these two domains of PEX5, both at 1 μM, does not interfere with catalase tetramerization (Fig. 3*D*, *lane 6*), suggesting that these two domains of PEX5 have to reside in the same molecule (*i.e.* they have to be in a *cis* configuration) to inhibit catalase tetramerization at this concentration.

A plausible explanation for this finding is that domains present in both halves of PEX5 contribute to the interaction with mCat. We tested this hypothesis by performing additional tetramerization assays but this time using 200-fold larger concentrations of TPRs and ΔC1PEX5 in the chase incubations. PEX19, a protein involved in a different aspect of peroxisomal biogenesis (reviewed in Ref. 69), was used as a negative control.

[5] M. O. Freitas and J. E. Azevedo, unpublished results.

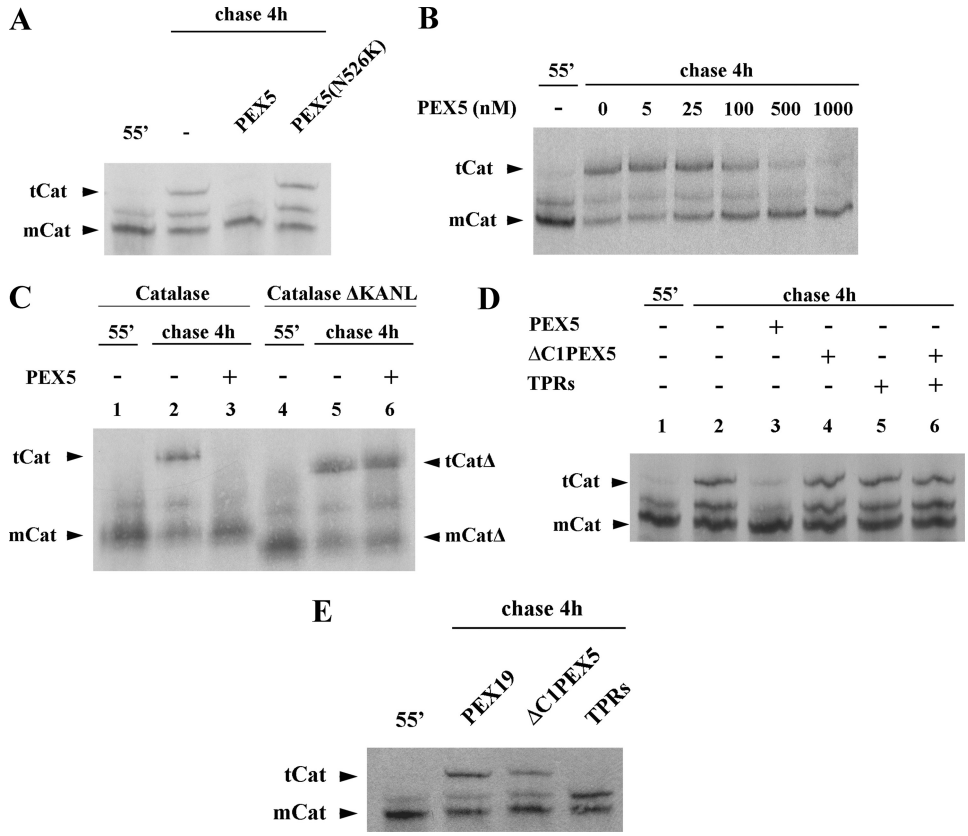

FIGURE 3. **PEX5 inhibits catalase tetramerization.** *A,* ^{35}S-labeled catalase was synthesized *in vitro* for 55 min (*lane 55'*) and chased for 4 h in the absence (*lane −*) or presence of 1 μM of the indicated recombinant proteins. *B,* same as in *A,* but using the indicated concentrations of PEX5. *C,* catalase (*lanes 1–3*) and a truncated version of it lacking the PTS1 signal (catalaseΔKANL; *lanes 4–6*) were synthesized for 55 min and chased in the absence (*lanes 2* and *5*) or presence of 1 μM PEX5 (*lanes 3* and *6*). *D,* ^{35}S-labeled catalase was synthesized *in vitro* for 55 min (*lane 1*) and chased in the absence (*lane 2*) or presence of 1 μM of the indicated recombinant proteins (*lanes 3–6*). ΔC1PEX5 and TPRs, recombinant proteins comprising the N- and C-terminal half of PEX5, respectively. *E,* same as in *A,* but using 200 μM of the indicated recombinant proteins. Samples were analyzed by native-PAGE/autoradiography. Note that the gel shown in *C* was run for 2.5 h. *mCat* and *tCat*, monomeric and tetrameric versions of catalase, respectively; *mCat*Δ and *tCat*Δ, monomeric and tetrameric forms of catalaseΔKANL, respectively.

These experiments revealed that ΔC1PEX5 displays a weak but reproducible ($n = 5$) inhibitory effect on catalase tetramerization (Fig. 3*E*). A complete inhibition of catalase tetramerization is observed in the presence of 200 μM TPRs (Fig. 3*E*). Interestingly, there is an increase in the intensity of the band migrating between mCat and tCat in the sample chased in the presence of TPRs. This observation could suggest that TPRs does not inhibit catalase dimerization, although further data will be necessary to corroborate this interpretation. In summary, these data suggest the PEX5-mCat interaction involves domains present in both halves of PEX5.

After binding a newly synthesized peroxisomal protein in the cytosol, PEX5 docks at the DTM and promotes the translocation of its cargo across the organelle membrane. At the end of this process, DTM-embedded PEX5 has to release its cargo into the organelle matrix. Previous work in yeast suggested that PEX8, an intraperoxisomal component of the DTM, performs this task (70). However, mammals and many other organisms lack a PEX8 ortholog (71), and so the triggering mechanism for this event remains unknown. If we assume that a similar mechanism also operates in mammals, *i.e.* a DTM component interacts with PEX5 triggering the release of cargo into the organelle matrix, as the presently available data suggest (see Introduction), then a good candidate to perform this task is PEX14. PEX14 is an intrinsic membrane protein possessing a single putative transmembrane domain. Its C-terminal two-thirds are exposed into the cytosol, whereas its N-terminal domain is either embedded in the peroxisomal membrane or even exposed into the matrix of the organelle (72, 73). The interaction of PEX5 with the N-terminal domain of PEX14 is well documented but still poorly understood in mechanistic terms. Indeed, it is known that this domain of PEX14 (hereafter referred to as NDPEX14) interacts strongly with seven diaromatic motifs located at the N-terminal half of PEX5, some of which are indispensable for the function of PEX5 (66, 74, 75), but the reason for this complex mode of binding is unknown.

Thus, we asked whether NDPEX14 affects the PEX5-mCat interaction. For this purpose, we purified ^{35}S-labeled mCat by SEC and incubated the radiolabeled protein with 1 μM recombinant PEX5 to generate the PEX5-mCat protein complex. This complex was then subjected to SEC either alone or after receiving 15 μM NDPEX14. As shown in Fig. 4, in the presence of NDPEX14, the elution volume of PEX5 is decreased (compare *panel 3* with *5*) indicating that a PEX5-NDPEX14 protein complex was formed. Importantly, under these conditions the vast majority of mCat elutes now as a monomeric protein (Fig. 4, compare *panel 2* with *4*). Thus, binding of NDPEX14 to PEX5 disrupts the PEX5-mCat interaction.

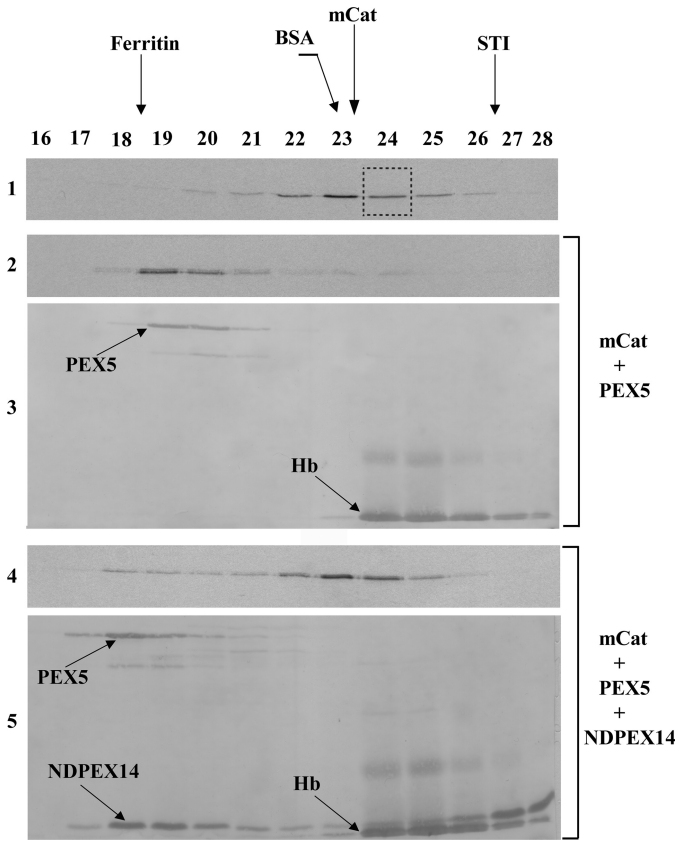

FIGURE 4. **N-terminal domain of PEX14 disrupts the mCat-PEX5 interaction.** ^{35}S-Labeled mCat was purified by SEC (*panel 1, fraction 24*), supplemented with 1 μM recombinant PEX5 and incubated for 30 min at room temperature to generate the PEX5-mCat protein complex. Half of this sample was analyzed directly by SEC (*panels 2* and *3*). The other half received recombinant NDPEX14 (15 μM) 30 min before chromatography (*panels 4* and *5*). Fractions were subjected to SDS-PAGE and blotted onto a nitrocellulose membrane. Autoradiographs (*panels 1, 2,* and *4*) and the Ponceau S-stained membranes (*panels 3* and *5*) are presented. *Hb*, hemoglobin from the reticulocyte lysate that co-purified with mCat in the first SEC.

To better understand how NDPEX14 affects the mCat binding activity of PEX5, we produced several truncated forms of recombinant PEX5 (see Fig. 5*A*), and after evaluating their monodispersity and capacity to interact with NDPEX14 by native-PAGE (see supplemental Fig. S1), we tested them in the *in vitro* catalase tetramerization assay in the absence or presence of NDPEX14. The aim of these experiments was to identify the smallest PEX5 truncated molecule that still retains the capacity to bind mCat at low concentrations (*i.e.* 1 μM), as assessed by its capacity to inhibit tetramerization of the enzyme, and to determine whether the PEX14-binding diaromatic motif(s) present in this molecule is(are) involved in the disruption of the PEX5-mCat interaction. As shown in Fig. 5*B* (*upper panel*), PEX5ΔN110, PEX5ΔN147 and PEX5ΔN196, proteins lacking the first 110, 147 or 196 amino acid residues of PEX5, respectively, are as potent as full-length PEX5 in this assay. As expected from the data presented in Fig. 4, neither full-length PEX5 nor any of these truncated proteins displays an inhibitory effect on catalase tetramerization in the presence of NDPEX14 (Fig. 5*B*, *lower panel*). PEX5ΔN267, a protein containing only the 7th diaromatic motif of PEX5, still inhibits catalase tetramerization, although in a less potent manner. Again, this inhibitory effect is abolished in the presence of NDPEX14 (Fig. 5*B, lower panel*). In contrast, PEX5ΔN290 displays no inhibitory activity (Fig. 5*B, upper panel*). Taken together, these results suggest that the region between amino acid residues 197 and 290 of PEX5 is involved in the mCat-PEX5 interaction and that binding of NDPEX14 to the single diaromatic motif present in PEX5ΔN267 is sufficient to disrupt that interaction.

Unexpectedly, substitution of the tryptophan and tyrosine residues in the diaromatic motif of PEX5ΔN267 by alanines, mutations that affect its PEX14 binding activity (66, 74), results in a protein, PEX5ΔN267-M7, that no longer inhibits catalase tetramerization (Fig. 5*C*), suggesting that these two aromatic residues are structurally important. Interestingly, when the same mutation was introduced in full-length PEX5, the resulting protein, PEX5-M7, was found to be as potent as the normal protein in inhibiting catalase tetramerization as well as in its response to NDPEX14 (Fig. 5*D*). This observation suggests, on one hand, that other regions of PEX5 compensate for the alterations associated with the mutation at 7th diaromatic motif, and, on the other hand, that at least one of the remaining six diaromatic motifs present in PEX5-M7 is involved in the NDPEX14-induced disruption of the mCat-PEX5 interaction. Data suggesting that the 6th diaromatic motif of PEX5 plays a major role in the NDPEX14-induced disruption of the mCat-PEX5 interaction were obtained when recombinant PEX5-M6,7, a PEX5 protein mutated at both the 6th and 7th diaromatic motifs, was tested in the catalase tetramerization assay. As shown in Fig. 5*D*, PEX5-M6,7 displays an inhibitory activity in this assay, although in a less potent manner than PEX5. This finding again suggests that the structure/function of this region of PEX5 required for the interaction with mCat is not fully preserved upon mutation of the diaromatic motifs. Importantly, the inhibitory activity of PEX5-M6,7 is no longer significantly neutralized by NDPEX14. These results suggest that binding of NDPEX14 to the 6th diaromatic motif of PEX5 and probably also to the 7th motif (as inferred from the PEX5ΔN267 data) disrupts the mCat-PEX5 interaction.

DISCUSSION

The proposed mechanism for the catalase assembly pathway consists of three steps as follows: 1) apo-monomers + heme → holomonomers; 2) holomonomers → holodimers; and 3) holodimers → homotetramers (reviewed in Ref. 76). The step at which PEX5 binds and transports catalase to the peroxisome, however, has remained a controversial issue. In this work, we used an *in vitro* system to characterize the PEX5-catalase interaction. Our results suggest that in the presence of PEX5 step 3 no longer occurs, but whether the inhibitory effect of PEX5 is exerted at step 1 and/or 2 remains unknown. Nevertheless, it is interesting to note that the mCat species is a soluble and monodisperse protein suggesting that it already possesses a near-native conformation.

Unexpectedly, a qualitative assessment of the binding affinities of mCat and tCat for PEX5 revealed that PEX5 has a bias toward binding the former, suggesting that some domain of the catalase polypeptide chain is no longer available to interact with PEX5 when the protein tetramerizes. If we exclude catalase

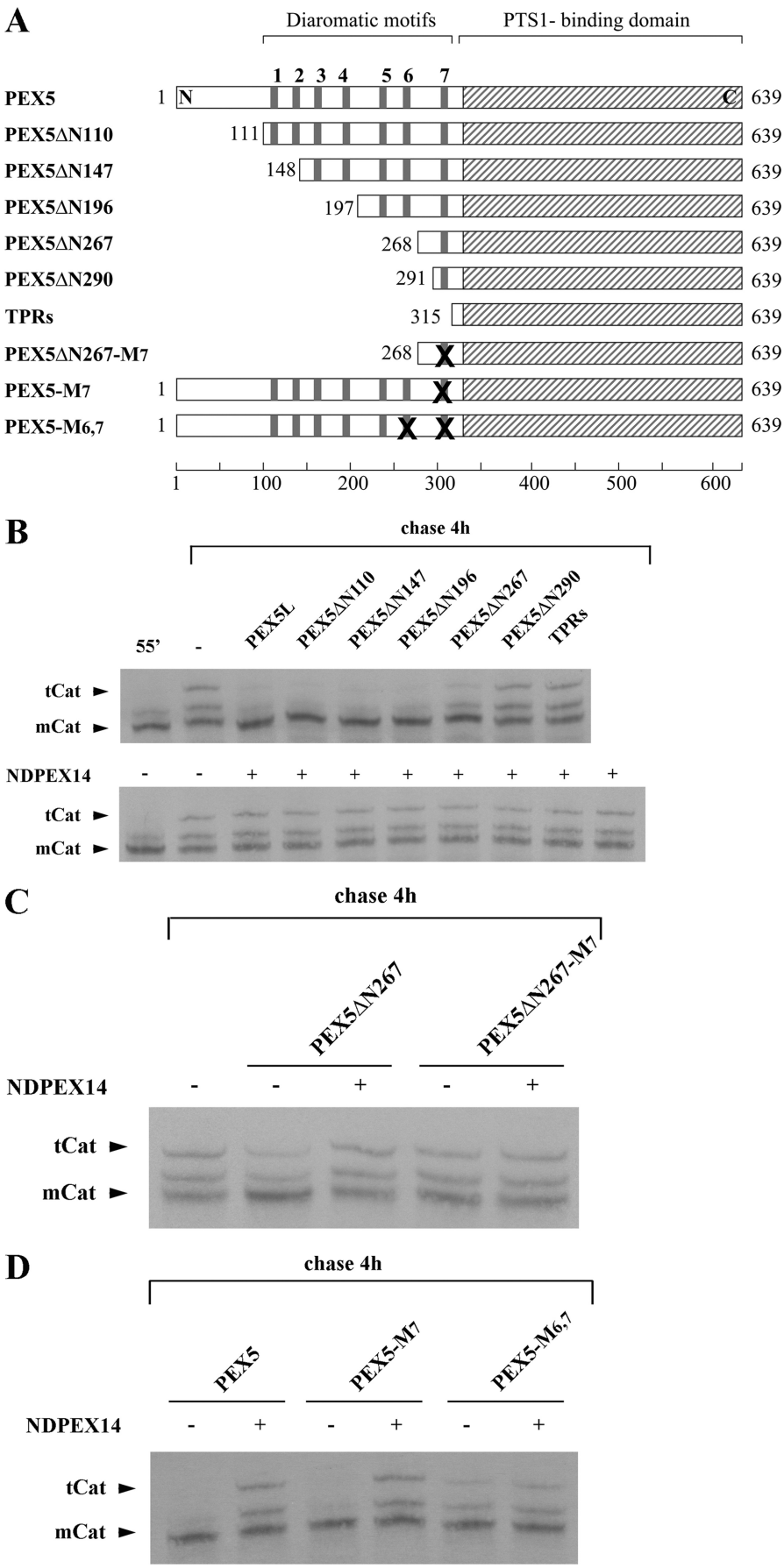

PTS1 from this reasoning, as the crystal structures of catalase might suggest (39, 40, 42), it is reasonable to assume that another domain of the mCat protein is involved in this phenomenon. Data supporting this possibility were obtained when we focused our attention on PEX5. Indeed, we found that the PTS1-binding domain of PEX5 is required for the mCat-PEX5 interaction, as expected, but evidence for the participation of an N-terminal domain of PEX5 in this interaction was also obtained. Each of these two PEX5 domains alone (*i.e.* in *trans*) can bind mCat inhibiting its tetramerization, but this effect is dramatically increased when these domains reside in the same molecule. Thus, they most likely bind mCat simultaneously.

The conclusion that the catalase-binding interface in PEX5 encompasses more than its PTS1-binding domain is probably also valid for other organisms. Indeed, as shown previously, yeast catalase possesses peroxisomal targeting information in two different regions of its polypeptide chain, one at the C terminus (the PTS1 sequence) and the other located in its N-terminal third (77), an observation that would be compatible with the existence of two different catalase-binding domains in yeast PEX5. Likewise, the observation that pumpkin catalase interacts with the N-terminal half of PEX5 in the yeast two-hybrid system (78), together with data on cottonseed catalase showing that its last four residues (which are conserved in pumpkin catalase) are sufficient to target a reporter protein to the peroxisome (79), could suggest that plant PEX5 possesses more than one catalase-interacting domain.

As already mentioned, binding of PEX5 to mCat inhibits its tetramerization in a potent manner. This previously unknown capacity of PEX5 evokes the properties of a family of bacterial chaperones functioning in type III secretion systems. These chaperones, some of which also contain tetratricopeptide repeats, bind proteins to be secreted in the cytoplasm preventing premature or incorrect interactions and participate in the secretion step itself (Ref. 80 and reviewed in Ref. 81). Although additional data will be necessary to reinforce the functional similarities between PEX5 and these chaperones, it is interesting to note that we have recently observed the same phenomenon when studying another oligomeric peroxisomal protein.[5]

Regardless of the mechanistic reasons behind the inhibitory activity of PEX5 on peroxisomal protein oligomerization, it is evident that such a property may be biologically relevant only if the amount of cytosolic PEX5 in a cell is sufficient to sequester mCat and all the other newly synthesized peroxisomal proteins that are en route to the organelle. The data available for rat liver suggest that this may well be the case. Indeed, we estimated that the cytosolic concentration of PEX5 is 0.75 μM, whereas the concentration of newly synthesized peroxisomal proteins is 0.73–0.83 μM, with mCat occupying a major fraction of this pool (0.19 μM; see under "Experimental Procedures" for details). Thus, even if we assume that newly synthesized peroxisomal proteins become available to bind PEX5 immediately after their synthesis (*i.e.* their folding process is not incompatible with PEX5 binding), we still reach the conclusion that there is a sufficient amount of PEX5 to bind a significant fraction of mCat.

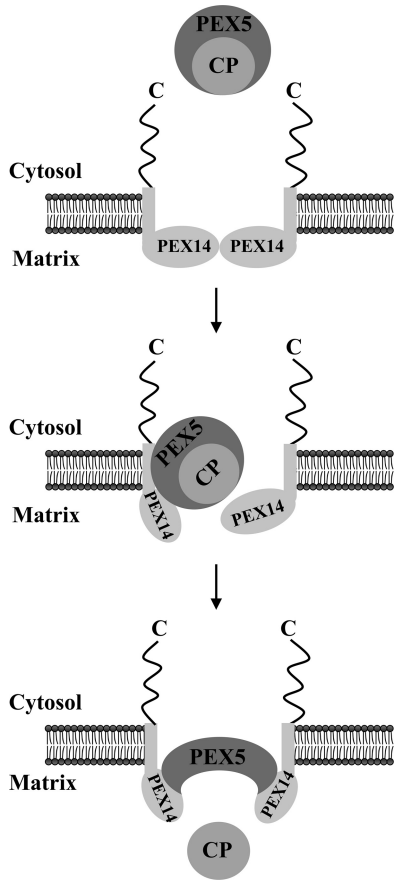

FIGURE 6. **Role of PEX14 in the release of cargo proteins into the peroxisomal matrix.** A newly synthesized cargo protein (*CP*) is recognized by PEX5 in the cytosol. This protein complex then docks at and becomes inserted into the peroxisomal DTM of which only PEX14 is shown for simplicity. The DTM component(s) providing the docking site for the PEX5-cargo protein complex have not been unambiguously identified yet. As discussed elsewhere, two strong candidates for this role are PEX13 (86) and PEX14 itself (87, 88). Note that PEX13 may also participate in the cargo-release step (66). The multiple interactions of PEX5 with the N-terminal domain of the several PEX14 molecules present in the DTM ultimately trigger the release of the cargo into the peroxisomal matrix.

The results presented here thus corroborate and extend the pioneering observations of Lazarow and de Duve (46, 47) suggesting that rat liver catalase arrives at the peroxisome still in its monomeric state. However, they also seem to collide with the idea that catalase is imported into the organelle only after tetramerization (49). This is not completely so. Indeed, as discussed above, the crucial factor determining whether or not catalase tetramerizes before import may well be the amount of PEX5 present in the cytosol. If a cell contains a stoichiometric excess of PEX5 over newly synthesized peroxisomal proteins,

FIGURE 5. **PEX5 diaromatic motifs involved in the NDPEX14-induced disruption of the mCat-PEX5 interaction.** *A,* schematic representation of recombinant PEX5 proteins. The diaromatic motifs in the N-terminal half of PEX5 are numbered *1–7*. Replacement of tryptophan and phenylalanine/tyrosine residues by alanines in these motifs is indicated by *X*. *B–D,* ^{35}S-labeled catalase was synthesized *in vitro* for 55 min (*lane 55′*) and chased for 4 h in the absence (*lane −*) or presence of 1 μM of the indicated recombinant PEX5 proteins alone or together with NDPEX14 (30 μM). Samples were analyzed by native-PAGE/autoradiography.

then it is likely that catalase remains monomeric and is imported as such; if not, a fraction of it will tetramerize before import. Although speculative, this possibility would explain why different results are obtained in different experimental systems (see Ref. 49 and references therein).

PEX14, a central component of the DTM, was regarded for many years as a protein involved solely in the docking of the receptor at the peroxisomal membrane (82). However, several observations have challenged this concept, and it is now clear that this protein also participates in the translocation of cargoes across the peroxisomal membrane (83, 84). The finding that the N-terminal domain of human PEX14 disrupts the PEX5-mCat interaction together with data reported earlier for *Leishmania donovani* PEX5 showing that its affinity for a PTS1 protein is decreased in the presence of PEX14 (85) suggest still another function for this membrane protein, a role in the release of cargoes from DTM-embedded PEX5 into the peroxisomal matrix.

Interestingly, from the seven diaromatic motifs present in human PEX5, only one or two play a major role in the NDPEX14-induced disruption of the mCat-PEX5 interaction. This finding together with previous data showing that diaromatic motifs 2–4 of PEX5 are required for catalase import *in vivo* (66) suggests that the multiple interactions that are probably established between the N-terminal domain of peroxisomal PEX14 and the diaromatic motifs present in PEX5 occur in a sequential manner and may serve two different purposes. According to this hypothetical model (see Fig. 6), the first set of interactions may contribute to the docking/insertion of the PEX5-cargo protein complex into the DTM; subsequently, binding of additional PEX14 molecules to the 6th (and probably 7th) diaromatic motif(s) of PEX5 would trigger the release of the cargo protein into the peroxisomal matrix.

Acknowledgment—We thank Kalervo Hiltunen (University of Oulu, Finland) for the kind gift of the L-bifunctional antibody.

REFERENCES

1. Grou, C. P., Carvalho, A. F., Pinto, M. P., Alencastre, I. S., Rodrigues, T. A., Freitas, M. O., Francisco, T., Sá-Miranda, C., and Azevedo, J. E. (2009) *Cell. Mol. Life Sci.* **66,** 254–262
2. Lanyon-Hogg, T., Warriner, S. L., and Baker, A. (2010) *Biol. Cell* **102,** 245–263
3. Ma, C., and Subramani, S. (2009) *IUBMB Life* **61,** 713–722
4. Wolf, J., Schliebs, W., and Erdmann, R. (2010) *FEBS J.* **277,** 3268–3278
5. Brocard, C., and Hartig, A. (2006) *Biochim. Biophys. Acta* **1763,** 1565–1573
6. Stanley, W. A., and Wilmanns, M. (2006) *Biochim. Biophys. Acta* **1763,** 1592–1598
7. Lazarow, P. B. (2006) *Biochim. Biophys. Acta* **1763,** 1599–1604
8. Schliebs, W., and Kunau, W. H. (2006) *Biochim. Biophys. Acta* **1763,** 1605–1612
9. Agne, B., Meindl, N. M., Niederhoff, K., Einwächter, H., Rehling, P., Sickmann, A., Meyer, H. E., Girzalsky, W., and Kunau, W. H. (2003) *Mol. Cell* **11,** 635–646
10. Reguenga, C., Oliveira, M. E., Gouveia, A. M., Sá-Miranda, C., and Azevedo, J. E. (2001) *J. Biol. Chem.* **276,** 29935–29942
11. Alencastre, I. S., Rodrigues, T. A., Grou, C. P., Fransen, M., Sá-Miranda, C., and Azevedo, J. E. (2009) *J. Biol. Chem.* **284,** 27243–27251
12. Gouveia, A. M., Guimaraes, C. P., Oliveira, M. E., Reguenga, C., Sa-Miranda, C., and Azevedo, J. E. (2003) *J. Biol. Chem.* **278,** 226–232
13. Gouveia, A. M., Guimarães, C. P., Oliveira, M. E., Sá-Miranda, C., and Azevedo, J. E. (2003) *J. Biol. Chem.* **278,** 4389–4392
14. Miyata, N., and Fujiki, Y. (2005) *Mol. Cell. Biol.* **25,** 10822–10832
15. Oliveira, M. E., Gouveia, A. M., Pinto, R. A., Sá-Miranda, C., and Azevedo, J. E. (2003) *J. Biol. Chem.* **278,** 39483–39488
16. Platta, H. W., Grunau, S., Rosenkranz, K., Girzalsky, W., and Erdmann, R. (2005) *Nat. Cell Biol.* **7,** 817–822
17. Carvalho, A. F., Pinto, M. P., Grou, C. P., Alencastre, I. S., Fransen, M., Sá-Miranda, C., and Azevedo, J. E. (2007) *J. Biol. Chem.* **282,** 31267–31272
18. Grou, C. P., Carvalho, A. F., Pinto, M. P., Wiese, S., Piechura, H., Meyer, H. E., Warscheid, B., Sá-Miranda, C., and Azevedo, J. E. (2008) *J. Biol. Chem.* **283,** 14190–14197
19. Okumoto, K., Misono, S., Miyata, N., Matsumoto, Y., Mukai, S., and Fujiki, Y. (2011) *Traffic* **12,** 1067–1083
20. Williams, C., van den Berg, M., Sprenger, R. R., and Distel, B. (2007) *J. Biol. Chem.* **282,** 22534–22543
21. Debelyy, M. O., Platta, H. W., Saffian, D., Hensel, A., Thoms, S., Meyer, H. E., Warscheid, B., Girzalsky, W., and Erdmann, R. (2011) *J. Biol. Chem.* **286,** 28223–28234
22. Grou, C. P., Carvalho, A. F., Pinto, M. P., Huybrechts, S. J., Sá-Miranda, C., Fransen, M., and Azevedo, J. E. (2009) *J. Biol. Chem.* **284,** 10504–10513
23. Shiozawa, K., Konarev, P. V., Neufeld, C., Wilmanns, M., and Svergun, D. I. (2009) *J. Biol. Chem.* **284,** 25334–25342
24. Faber, K. N., van Dijk, R., Keizer-Gunnink, I., Koek, A., van der Klei, I. J., and Veenhuis, M. (2002) *Biochim. Biophys. Acta* **1591,** 157–162
25. Luo, B., Norris, C., Bolstad, E. S., Knecht, D. A., and Grant, D. F. (2008) *J. Mol. Biol.* **380,** 31–41
26. Stewart, M. Q., Esposito, R. D., Gowani, J., and Goodman, J. M. (2001) *J. Cell Sci.* **114,** 2863–2868
27. Tanaka, N., Aoki, K., Ishikura, S., Nagano, M., Imamura, Y., Hara, A., and Nakamura, K. T. (2008) *Structure* **16,** 388–397
28. Elgersma, Y., Vos, A., van den Berg, M., van Roermund, C. W., van der Sluijs, P., Distel, B., and Tabak, H. F. (1996) *J. Biol. Chem.* **271,** 26375–26382
29. Islinger, M., Li, K. W., Seitz, J., Völkl, A., and Lüers, G. H. (2009) *Traffic* **10,** 1711–1721
30. Nilsen, T., Slagsvold, T., Skjerpen, C. S., Brech, A., Stenmark, H., and Olsnes, S. (2004) *J. Biol. Chem.* **279,** 4794–4801
31. Glover, J. R., Andrews, D. W., and Rachubinski, R. A. (1994) *Proc. Natl. Acad. Sci. U.S.A.* **91,** 10541–10545
32. Lee, M. S., Mullen, R. T., and Trelease, R. N. (1997) *Plant Cell* **9,** 185–197
33. Leiper, J. M., Oatey, P. B., and Danpure, C. J. (1996) *J. Cell Biol.* **135,** 939–951
34. McNew, J. A., and Goodman, J. M. (1994) *J. Cell Biol.* **127,** 1245–1257
35. Gould, S. J., and Collins, C. S. (2002) *Nat. Rev. Mol. Cell Biol.* **3,** 382–389
36. Ghosh, D., and Berg, J. M. (2010) *J. Am. Chem. Soc.* **132,** 3973–3979
37. Leighton, F., Coloma, L., and Koenig, C. (1975) *J. Cell Biol.* **67,** 281–309
38. Poole, B., Leighton, F., and De Duve, C. (1969) *J. Cell Biol.* **41,** 536–546
39. Maté, M. J., Zamocky, M., Nykyri, L. M., Herzog, C., Alzari, P. M., Betzel, C., Koller, F., and Fita, I. (1999) *J. Mol. Biol.* **286,** 135–149
40. Murthy, M. R., Reid, T. J., 3rd, Sicignano, A., Tanaka, N., and Rossmann, M. G. (1981) *J. Mol. Biol.* **152,** 465–499
41. Purdue, P. E., Castro, S. M., Protopopov, V., and Lazarow, P. B. (1996) *Ann. N.Y. Acad. Sci.* **804,** 775–776
42. Putnam, C. D., Arvai, A. S., Bourne, Y., and Tainer, J. A. (2000) *J. Mol. Biol.* **296,** 295–309
43. Trelease, R. N., Xie, W., Lee, M. S., and Mullen, R. T. (1996) *Eur. J. Cell Biol.* **71,** 248–258
44. Brul, S., Wiemer, E. A., Westerveld, A., Strijland, A., Wanders, R. J., Schram, A. W., Heymans, H. S., Schutgens, R. B., Van den Bosch, H., and Tager, J. M. (1988) *Biochem. Biophys. Res. Commun.* **152,** 1083–1089
45. Koepke, J. I., Nakrieko, K. A., Wood, C. S., Boucher, K. K., Terlecky, L. J., Walton, P. A., and Terlecky, S. R. (2007) *Traffic* **8,** 1590–1600
46. Lazarow, P. B., and de Duve, C. (1973) *J. Cell Biol.* **59,** 507–524
47. Lazarow, P. B., and de Duve, C. (1973) *J. Cell Biol.* **59,** 491–506
48. Middelkoop, E., Strijland, A., and Tager, J. M. (1991) *FEBS Lett.* **279,** 79–82

49. Léon, S., Goodman, J. M., and Subramani, S. (2006) *Biochim. Biophys. Acta* **1763,** 1552–1564
50. Braverman, N., Dodt, G., Gould, S. J., and Valle, D. (1998) *Hum. Mol. Genet.* **7,** 1195–1205
51. Fransen, M., Brees, C., Baumgart, E., Vanhooren, J. C., Baes, M., Mannaerts, G. P., and Van Veldhoven, P. P. (1995) *J. Biol. Chem.* **270,** 7731–7736
52. Carvalho, A. F., Costa-Rodrigues, J., Correia, I., Costa Pessoa, J., Faria, T. Q., Martins, C. L., Fransen, M., Sá-Miranda, C., and Azevedo, J. E. (2006) *J. Mol. Biol.* **356,** 864–875
53. Carvalho, A. F., Grou, C. P., Pinto, M. P., Alencastre, I. S., Costa-Rodrigues, J., Fransen, M., Sá-Miranda, C., and Azevedo, J. E. (2007) *Biochim. Biophys. Acta* **1773,** 1141–1148
54. Costa-Rodrigues, J., Carvalho, A. F., Fransen, M., Hambruch, E., Schliebs, W., Sá-Miranda, C., and Azevedo, J. E. (2005) *J. Biol. Chem.* **280,** 24404–24411
55. Pinto, M. P., Grou, C. P., Alencastre, I. S., Oliveira, M. E., Sá-Miranda, C., Fransen, M., and Azevedo, J. E. (2006) *J. Biol. Chem.* **281,** 34492–34502
56. Sullivan, D. T., Carroll, W. T., Kanik-Ennulat, C. L., Hitti, Y. S., Lovett, J. A., and Von Kalm, L. (1985) *J. Biol. Chem.* **260,** 4345–4350
57. Gouveia, A. M., Reguenga, C., Oliveira, M. E., Eckerskorn, C., Sá-Miranda, C., and Azevedo, J. E. (1999) *Anal. Biochem.* **274,** 270–277
58. Palosaari, P. M., and Hiltunen, J. K. (1990) *J. Biol. Chem.* **265,** 2446–2449
59. Gouveia, A. M., Reguenga, C., Oliveira, M. E., Sa-Miranda, C., and Azevedo, J. E. (2000) *J. Biol. Chem.* **275,** 32444–32451
60. Fujiki, Y., Fowler, S., Shio, H., Hubbard, A. L., and Lazarow, P. B. (1982) *J. Cell Biol.* **93,** 103–110
61. Weibel, E. R., Stäubli, W., Gnägi, H. R., and Hess, F. A. (1969) *J. Cell Biol.* **42,** 68–91
62. Miyazawa, S., Hayashi, H., Hijikata, M., Ishii, N., Furuta, S., Kagamiyama, H., Osumi, T., and Hashimoto, T. (1987) *J. Biol. Chem.* **262,** 8131–8137
63. Leighton, F., Poole, B., Lazarow, P. B., and De Duve, C. (1969) *J. Cell Biol.* **41,** 521–535
64. Lazarow, P. B., Robbi, M., Fujiki, Y., and Wong, L. (1982) *Ann. N.Y. Acad. Sci.* **386,** 285–300
65. Scandalios, J. G. (1965) *Proc. Natl. Acad. Sci. U.S.A.* **53,** 1035–1040
66. Otera, H., Setoguchi, K., Hamasaki, M., Kumashiro, T., Shimizu, N., and Fujiki, Y. (2002) *Mol. Cell. Biol.* **22,** 1639–1655
67. Dodt, G., Braverman, N., Wong, C., Moser, A., Moser, H. W., Watkins, P., Valle, D., and Gould, S. J. (1995) *Nat. Genet.* **9,** 115–125
68. Gatto, G. J., Jr., Geisbrecht, B. V., Gould, S. J., and Berg, J. M. (2000) *Nat. Struct. Biol.* **7,** 1091–1095
69. Fujiki, Y., Matsuzono, Y., Matsuzaki, T., and Fransen, M. (2006) *Biochim. Biophys. Acta* **1763,** 1639–1646
70. Wang, D., Visser, N. V., Veenhuis, M., and van der Klei, I. J. (2003) *J. Biol. Chem.* **278,** 43340–43345
71. Schlüter, A., Fourcade, S., Ripp, R., Mandel, J. L., Poch, O., and Pujol, A. (2006) *Mol. Biol. Evol.* **23,** 838–845
72. Oliveira, M. E., Reguenga, C., Gouveia, A. M., Guimarães, C. P., Schliebs, W., Kunau, W. H., Silva, M. T., Sá-Miranda, C., and Azevedo, J. E. (2002) *Biochim. Biophys. Acta* **1567,** 13–22
73. Will, G. K., Soukupova, M., Hong, X., Erdmann, K. S., Kiel, J. A., Dodt, G., Kunau, W. H., and Erdmann, R. (1999) *Mol. Cell. Biol.* **19,** 2265–2277
74. Saidowsky, J., Dodt, G., Kirchberg, K., Wegner, A., Nastainczyk, W., Kunau, W. H., and Schliebs, W. (2001) *J. Biol. Chem.* **276,** 34524–34529
75. Schliebs, W., Saidowsky, J., Agianian, B., Dodt, G., Herberg, F. W., and Kunau, W. H. (1999) *J. Biol. Chem.* **274,** 5666–5673
76. Zámocký, M., and Koller, F. (1999) *Prog. Biophys. Mol. Biol.* **72,** 19–66
77. Kragler, F., Langeder, A., Raupachova, J., Binder, M., and Hartig, A. (1993) *J. Cell Biol.* **120,** 665–673
78. Oshima, Y., Kamigaki, A., Nakamori, C., Mano, S., Hayashi, M., Nishimura, M., and Esaka, M. (2008) *Plant Cell Physiol.* **49,** 671–677
79. Mullen, R. T., Lee, M. S., and Trelease, R. N. (1997) *Plant J.* **12,** 313–322
80. Plé, S., Job, V., Dessen, A., and Attree, I. (2010) *J. Bacteriol.* **192,** 3801–3808
81. Parsot, C., Hamiaux, C., and Page, A. L. (2003) *Curr. Opin. Microbiol.* **6,** 7–14
82. Sacksteder, K. A., and Gould, S. J. (2000) *Annu. Rev. Genet.* **34,** 623–652
83. Azevedo, J. E., and Schliebs, W. (2006) *Biochim. Biophys. Acta* **1763,** 1574–1584
84. Ma, C., Schumann, U., Rayapuram, N., and Subramani, S. (2009) *Mol. Biol. Cell* **20,** 3680–3689
85. Madrid, K. P., De Crescenzo, G., Wang, S., and Jardim, A. (2004) *Mol. Cell. Biol.* **24,** 7331–7344
86. Williams, C., and Distel, B. (2006) *Biochim. Biophys. Acta* **1763,** 1585–1591
87. Niederhoff, K., Meindl-Beinker, N. M., Kerssen, D., Perband, U., Schäfer, A., Schliebs, W., and Kunau, W. H. (2005) *J. Biol. Chem.* **280,** 35571–35578
88. Williams, C., van den Berg, M., and Distel, B. (2005) *FEBS Lett.* **579,** 3416–3420